All Polymer Micropump

Hansen, Thomas Steen

Publication date:
2008

Document Version
Publisher's PDF, also known as Version of record

All Polymer Micropump

Thomas Steen Hansen

Ph.D. Thesis
September 30, 2007

Department of Chemical Engineering
Technical University of Denmark

ISBN 978-87-91435-72-2
Printed by Frydenberg a/s, Copenhagen, Denmark

Preface

This thesis presents the results of my Ph.D. project "All Polymer Micropump", carried out at the Danish Polymer Centre, Department of Chemical Engineering, The Technical University of Denmark and the The Danish Polymer Centre, Risø National Laboratory, The Technical University of Denmark. The work was performed during the period from October 2004 to October 2007, and was financed by the Graduate School of Polymer Science, Risø National Laboratory, and The Technical University of Denmark.

I would like to thank Professor Ole Hassager and Professor Niels B. Larsen for supervising the project. Thanks to Ole Hassager for giving me opportunity to carry out this study at the Department of Chemical Engineering. A very special thanks to Niels B. Larsen for his always optimistic approach to challenges during the project. I am very grateful for the inspiring guidance, the great discussions and the insistence on maintaining a good methodical approach to the scientific work.

I would like to thank the former head of program Keld West for many interesting discussions, for his patient explanations of electrochemical processes, and his always helpfulness in overcoming the encountered obstacles. Also thanks to the staff affiliated with CleaR, the Clean Room facility at Risoe, Ina Blom and Esben Højrup for keeping the equipment running.

Also, I would like to thank Dr. Bjørn Winther-Jensen who introduced me to the field of conductive polymers, and from whom I have learned a lot. He has always been ready with good advices and ideas, when I needed help. A special thanks to Dr. Noel Clark and all the people at Ensis-papro at CSIRO, Melbourne for their hospitality during my stay "Down Under". Thanks to Priya Subramanian for her help and introduction to their lab facilities.

Contents

Abstract

In this thesis an all polymer micropump, and the fabrication method required to fabricate this, are examined. Polymer microfluidic devices are of major scientific interest because they can combine complicated chemical and biological analysis in cheap and disposable devices. The electrode system in the micropump is based on the conducting polymer poly(3,4 ethylenedioxythiophene) (PEDOT). The majority of the work conducted was therefore aimed at developing methods for patterning and processing PEDOT. First a method was developed, where the conducting polymer PEDOT can be integrated into non-conductive substrates like polymethylmethacrylate (PMMA), polystyrene (PS), and cyclic olefin copolymer (COC). The integration is done after the polymerisation, in a washing step where the residual salt from the polymerisation is removed. By using a washing solvent that both removes the salt and dissolves the top layer of the substrate, the PEDOT is integrated into the non-conductive polymer. The result is a material that retains the good conductivity of PEDOT, but gains the mechanical stability of the substrate. The best results were obtained for PEDOT/PMMA.
The new mechanically stable PEDOT/PMMA was micro-patterned using clean room techniques. The conductive blend was coated with a layer of photoresist, exposed and developed. The resulting pattern was etched in a reactive ion etcher, yielding a well defined patterned with a resolution of approximately 2 μm. This technique was utilised to fabricate an ac electroosmotic (ACEO) micropump. The ACEO pump consists of an array of interdigitated small and large PEDOT/PMMA encapsulated in a polyurethane (PUR) channel system. The pumping velocity was detected using fluorescent microspheres and a confocal microscope. The pump characteristics resembled those of pumps based on metal electrodes as reported in literature. There was, however, an indication that the PEDOT electrodes were easier damaged than metal electrodes, but the damage could be prevented by applying a thin layer of protective non-conductive polymer on top of the electrodes.
A new stretchable conductive polymer was developed by mixing polyurethane in to the solution from which the PEDOT was cast. The resulting PEDOT/PUR material showed good conductivity. The film was elongated 50 % ten times and apart from a small irreversible increase in resistance during the first elongation, the film resistance was stable during the rest of the elongations. Another set of films was stretched 200% four times. At approximately 100 % elongation, a significant decrease in conductivity was observed, but the films still remained fairly conductive during the following elongations. The aging of the films was examined at 21°C and 60°C and a logarithmic decay in conductivity with time was observed at both temperatures. The expected lifetime was found to be several years if stored at room temperature.
Next, a new method for patterning conducting polymers is described. A photoresist master, with a bas-relief pattern, is fabricated using classical clean room techniques. On top of the master a hot agarose solution is cast. When cooled the agarose solidifies and forms a high water content gel with good mechanical stability. The cooled agarose stamp, with the inverse bas-relief pattern, is peeled off the master

and impregnated with a deactivation agent. When placed on a conducting polymer film the deactivation agent diffuses from the stamp to the conducting polymer in the areas of contact, hence the film is deactivated in a pattern spatially defined by the relief pattern of the stamp. A resolution of approximately $2\mu m$ was achieved. Finally, the PEDOT/PUR material was patterned using an inkjet printer. The inkjet printing was done on a scientific inkjet printer, where the nozzles can be observed by a video camera and the drop expelling force and frequency can be controlled. To achieve proper printing it was required to synthesise a new short chained polyurethane. The resolution of the inkjet printer was in the order of 200 μm. The inkjet printed pattern is compared with the agarose stamping technique in a setup where the conductivity perpendicular to the stretching direction is measured on two electrodes fabricated by the two methods.

Dansk Resumé

I denne afhandling undersøges egenskaberne af en polymer mikropumpe, og de metoder som kræves for at fremstille en sådan. Elektroderne i mikropumpen er fremstillet af den elektrisk ledende polymer poly(3,4-ethylendioxythiophen) (PEDOT). En metode blev udviklet, hvormed man kan integrere PEDOT i ikke-ledende polymersubstrater, såsom polymethylmethacrylat (PMMA), polystyren (PS), og cyclisk olefin copolymer (COC). Integrationen foregår efter polymeriseringen af PEDOT i et vasketrin, hvor overskudssalt fjernes fra filmen. Ved at bruge et opløsnings-middel, som både fjerner saltet og opløser den øverste del af substratet, bliver PEDOT integreret ned i den ikke-ledende polymer. Resultatet er et materiale, som ikke kun bibeholder PEDOT's gode ledningsevne, men også har substratets gode mekaniske egenskaber. De bedste resultater blev opnået med PEDOT/PMMA.

Det mekanisk stabile PEDOT/PMMA blev mikromønstret vha. klassisk rentrumsteknik. Det ledende materiale blev dækket med fotoresist, eksponeret og fremkaldt. Prøven blev ætset i en reaktiv ion-ætser, hvilket resulterede i et veldefineret mønster med en opløsning omkring 2 μm. Denne metode blev brugt til at fremstille en AC elektroosmotisk (ACEO) mikropumpe. ACEO pumpen blev indkapslet i et polyurethan (PUR) kanalsystem, og pumpehastigheden blev målt vha. fluorescerende mikrokugler og et konfokalt mikroskop. Polymerpumpens egenskaber mindede om lignende pumper, der er fremstillet i metal, og som er beskrevet i literaturen. Der var dog en tendens til at PEDOT-elektroderne blev lettere skadet en metal-elektroderne, men dette kunne undgås, hvis elektrodernr blev dækket med et tyndt lag isolerende polymer.

En ny strækbar ledende polymerblanding blev fremstillet ved at blande polyurethan i den opløsning, hvorfra PEDOT blev polymeriseret. En PEDOT/PUR film blev forlænget 50 % 10 gange, og udover et lille fald i ledningsevne under den første forlængelse, var ledningsevnen konstant under de resterende forlængelser. Et andet sæt film blev forlænget 200 % 4 gange. Ved ca. 100 % forlængelse var der et signifikant fald i ledningsevne. Filmene forblev dog relativt elektrisk ledende under de næste 4 forlængelser. Filmenes ældning blev undersøgt ved 21°C og 60°C, og ved begge temperaturer blev et logaritmisk fald i ledningsevne observeret over tid. Levetiden blev estimeret til adskillige år, hvis prøverne opbevares ved stuetemperatur.

Derefter beskrives en ny mønstringsmetode. En reliefmaske fremstilles vha. fotoresist og almindelig rentrumsteknik. Ovenpå bliver en varm agarose-opløsning påført. Ved nedkøling stivner agarosen til en mekanisk stabil gel med højt vandindhold. Det afkølede agarose-stempel, nu med et reliefmønster, tages af masken, og imprægneres med en deaktiveringsagent. Herefter placeres den på en ledende polymerfilm, hvor

deaktiveringsagenten vil diffundere ned til filmen i de områder, hvor der er kontakt. Filmen bliver altså deaktiveret i et mønster defineret af den reliefstruktur, som agarose-stemplet har. En opløsning på omkring 2 μm blev opnået.
Det nyudviklede PEDOT/PUR materiale blev mønstret vha. af inkjet printning. En inkjet printer specialt udviklet til forskningsformål blev benyttet. Det gjorde det muligt at kontrollere dråbehastigheden, og overvåge dyserne igennem et videokamera. For at opnå et ordentligt resultat var det nødvendigt at syntetisere en kortkædet polyurethan. Opløsningen med inkjet printeren var i størrelsesordenen 200 μm. Både inkjet printeren og agarosestemplingen blev brugt til at fremstille et setup, hvor ledningsevnen på tværs af forlængelsesretningen kan måles.

Notation and Abbrevations

A	Area
d	distance
f	force
F_{el}	Electrostatic Force
h	height
L	Length
p	Pressure
p_{el}	Electrostatic Pressure
S	Siemens
t	time
V	Volume
v	Velocity
V_{rms}	Volts Root Mean Square
Z	Impedance
ϵ	Permittivity
ρ	Density
μ	viscosity
ω	angular frequency
Ω	Ohm
Ω/sq	Ohm per Square
ac	alternating current
ACEO	ac electroosmotic
AFM	Atomic Force Microscopy
COC	Cyclic Olefin Copolymer
CP	Conductive polymer
CV	Cyclic voltammogram
EDOT	3,4-ethylenedioxythiophene
HMDS	Hexamethyldisilazane
PEDOT	Poly(3,4-ethylenedioxythiophene)
PDMS	Polydimethylsiloxane
PET	Polyethylene terephthalate
PMMA	Polymethylmethacrylate
PS	Polystyrene
PUR	Polyurethane
PVDF	Polyvinylidene fluoride
Re	Reynolds number
RIE	Reactive Ion Etcher
SCM	Strectable Conductive Material
SEBS	Poly(styrene-ethylene-co-butylene-styrene)
SEM	Scanning Electron Microscopy
TEOS	tetraethoxysilane
THF	Tetrahydrofuran
Tos	para-toluenesulfonic acid/Tosylate
VPP	Vapour Phase Polymerisation

List of Publications

This thesis is based on the following papers:

Integration of conducting polymer network in non-conductive polymer substrates, TS Hansen, K West, O Hassager, NB Larsen, **Synthetic Metals**, 2006, 156, 1203-1207

An All-polymer micropump based on the conductive polymer PEDOT, TS Hansen, K West, O Hassager, NB Larsen, **J. Micromechanics & Microengineering**, 2007, 17, 860-866

Highly Stretcable and Conductive Polymer Material Made from PEDOT and Polyurethane Elastomers, TS Hansen, K West, O Hassager, NB Larsen, **Advanced Functional Materials**, In Press

Direct Fast Patterning of Conductive Polymers Using Agarose Stamping, TS Hansen, K West, O Hassager, NB Larsen, **Advanced Materials**, In Press

Micropatterning of a Stretchable Conductive Polymer using Inkjet printing and Agarose Stamping, TS Hansen, O Hassager, NB Larsen and NB Clark, Accepted by **Synthetic Metals**

Papers not included in the current thesis:

Reliability of Poly (3,4-ethylenedioxythiophene) strain gauge, R Mateiu, M Lillemose, TS Hansen, A Boisen, O Geschke, **Microelectronic Engineering**, 2007, 84, 1270-1273

Chapter 1

Introduction

The field of microfluidics has the potential of completely changing the way we utilise chemistry and biology. Like the miniaturisation of electronic components has meant a revolution in the computer industry, the miniaturisation of the lab could revolutionise the way we conduct chemical measurements. By downscaling the dimensions and time of measurements, the through-put is increased and thousands of parallel measuremens can be employed easing eg. screening of drugs and analysing of samples. The techniques used in microfluidics have traditionally been borrowed from the field of microelectronics; hence the materials used in the early years of microfluidics were mainly silicon, noble metals and glass. Recently focus has also been directed to the use of polymers because they are cheap and disposable and they possess properties that differ from the classical materials. In continuation of this trend, the current project is introducing conductive polymer to the field of microfluidics by construction of an all-polymer micropump in which the electrical part of the device is constructed from conductive polymer.

1.1 Conductive polymers

The simplest of all conductive polymers is the polyacetylene. Using a Ziegler-Natta catalyst, polyacetylene was produced as a metallic film by Hideki Shirakawa and co-workers in 1974. Although looking metallic, polyacetylene films exhibited no conductivity of significance until 1977, when Alan J. Heeger, Alan G. MacDiarmid and Hideki Shirakawa exposed the film to halogen gas. They found that oxidation/doping with chlorine, bromine or iodine vapour increased the conductivity of polyacetylene with a factor of 10^9 [2, 3]. This discovery led to the Nobel prize in chemistry in 2000 to Alan J. Heeger,

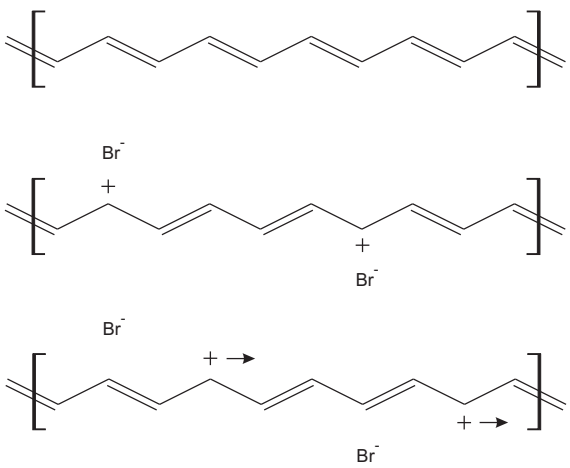

Figure 1.1: Polyacetylene in its undoped form (top) exhibits low electrical conductivity. Positive charge carriers are introduced on the polymer backbone by doping the polyacetylene with eg. bromine (middle). The positive charge carriers or electron holes can move along the backbone (bottom) causing the electrical conductivity to increase with a factor of 10^9 compared with the undoped state.

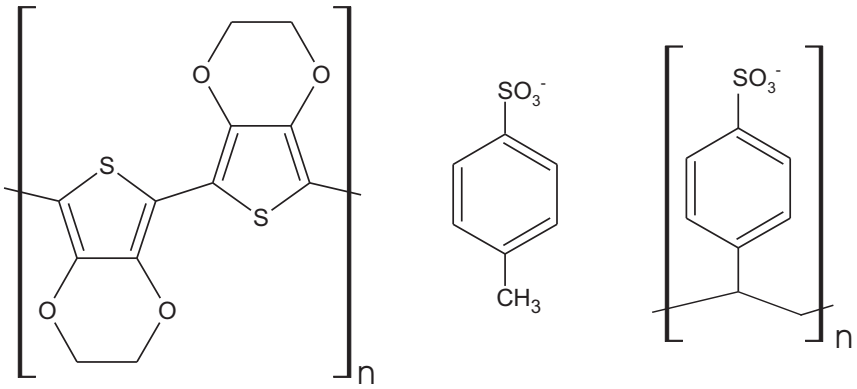

Figure 1.2: The PEDOT polymer (left) and two types of dopants: Tosylate (centre) and Polystyrenesulfonic acid (right)

Alan G. MacDiarmid and Hideki Shirakawa. Polyacetylene in its undoped and doped form is presented in figure 1.1. The conductivity arises from the

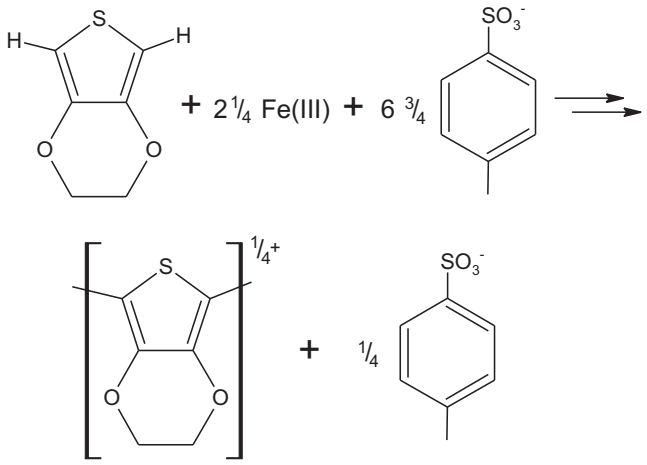

Figure 1.3: The in situ polymerisation of PEDOT reaction scheme normalised to one unit of EDOT [1]. The removal of the residual salt ($6^1/_4$ Fe(II)Tos + 2 HTos) is not shown.

movement of the positive charge along conjugated double bonds. Polyacetylene itself has little practical use because it reacts with oxygen in the air and degrades. Several other stable conductive polymers have since been found and thoroughly examined. The most described are polyaniline, polypyrrole, polythiophene and derivatives of these. Poly(3,4-ethylenedioxythiophene), or PEDOT for short, is a polythiophene showing good conductivity and exceptionally long time stability [4]. In addition PEDOT is relatively transparent and has the advantage that homogenous films can be cast from a single solution. PEDOT was therefore chosen to be the optimal conductive polymer for microfluidics applications. Just like polyacetylene, PEDOT requires a dopant to be conductive. The most used dopants are the salts of para-toluenesulfonic acid (tosylate or Tos) and Polystyrenesulfonic acid (PSS) [4]. PEDOT and Tosylate are shown in figure 1.2. The dopant is often added as a counterion to the oxidant used to polymerise the PEDOT, e.g., Fe(III)Tos added to the monomer EDOT yields PEDOT:Tos. Both prepolymerised PEDOT:PSS and the reactants for polymerising PEDOT:Tos directly in situ are commercially available. Prepolymerised PEDOT:PSS offers an easy way of applying conductive polymers, but the conductivity is significantly lower than in situ polymerised PEDOT:Tos [4]. In situ polymerisation also gives opportunities of adding or blending non-conductive components into the conductive polymer matrix [5, 6] and thereby improve

its mechanical properties. This method was extensively exploited in the current PhD project. The reaction scheme [1] for the in situ polymerisation is presented in figure 1.3. The fabrication of PEDOT films is done by heating a solution containing the monomer, oxidant, and a pH-regulator until the solvent has evaporated, the polymerisation initiates, and a film is formed. Approximately 90 percent of the film is oxidants from the polymerisation reaction, which are removed by washing the film in an appropriate solvent. Non-conductive polymers can be added in the washing step (chapter 3) or in the initial casting solution (chapter 5) depending on the properties of the added polymer.

Material	Conductivity
Copper [7]	600000 S/cm
Indium Tin Oxide [8]	5000 S/cm
Graphite [9]	500-1500 S/cm
PEDOT:Tos [10]	500-1000 S/cm
PEDOT:PSS [4]	1-10 S/cm
Silicon [11]	$\sim 10^{-4}$ S/cm
Glass [12]	10^{-8}-10^{-10} S/cm

Table 1.1: Conductivity of various materials

The conductivity of in situ polymerised PEDOT:Tos and prepolymerised PEDOT:PSS is around 700 S/cm and 2-3 S/cm respectively. The conductivity of various other conductors and non-conducters is presented in table 1.1 for comparison.

1.2 Micropumps

The two most essential characteristics of a micropump are the maximum flow rate and maximum pressure, but also operating voltage, restrictions on pumping fluid and dimensions are important when a pump is evaluated. Which characteristics that are preferred depend on the application of the pump. In the following, the most common micropump techniques will be reviewed and examples of pump performances reported in literature will be given. The overview of the pumps is mostly based on review articles [13], [14] and [15].

1.2.1 Displacement pumps

Physical displacement of fluid is the most examined micropump type. The principle is simple, but the fabrication is often complex due to the multi-

layer structures involved. The principle of a displacement pump is sketched in figure 1.4. The volume of a pumping champer is altenated by an actuation mechanism and one or two valves ensures that the volume flow is one-directional. As a driver for the volume change, one can use a Piezoeletric material, external air pressure, heat generating internal air pressure, electromagnetism, or electrostatic attraction between two electrodes. Some of the most common valves are flap valves, ball valves, or nozzle valves. In table 1.2 some of the results from literature are summarised.

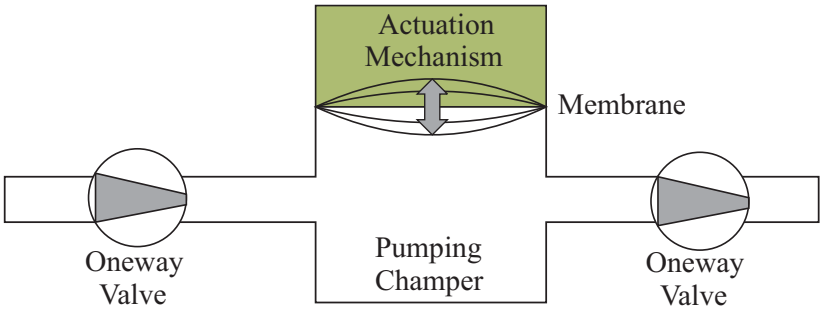

Figure 1.4: A schematic view of a displacement pump. The volume of a pumping chamber is alternated by an actuator mechanism attached to a membrane. One or two one way valves ensure that the flow is led in one direction.

1.2.2 Dynamic pumps

Dynamic micropumps define a variety of different pump types including electrohydrodynamic, magnetic hydrodynamic and electroosmotic pumps. Dynamic micropumps are based on electric or magnetic interaction between stationary electrodes and movable ions in the pumping fluid. The absence of movable parts in dynamic micropumps is the main advantage compared to displacement pumps. The eletric/magnetic field applies a force on the ions, and the force is transferred to the fluid through friction between the moving ions and the fluid molecules. The working principle of the DC electroosmotic micropump is sketched in figure 1.5, as an example of a dynamic pump. The negatively charged channel walls attract positive ions in the fluid and an external electric field causes the positive ions and fluid to move. The disadvantage of the dynamic pumps is requirements to the pumping fluid e.g. electroosmotic micropumps require water with ion concentration in a certain range and electrohydrodynamic pumps require a dielectric pumping fluid. A

more detailed description of dynamic pumps is given in [13] and a description of the AC electroosmotic pump used in this project is presented in section 3.2. Typical properties of a number of dynamic pumps are presented in table 1.3

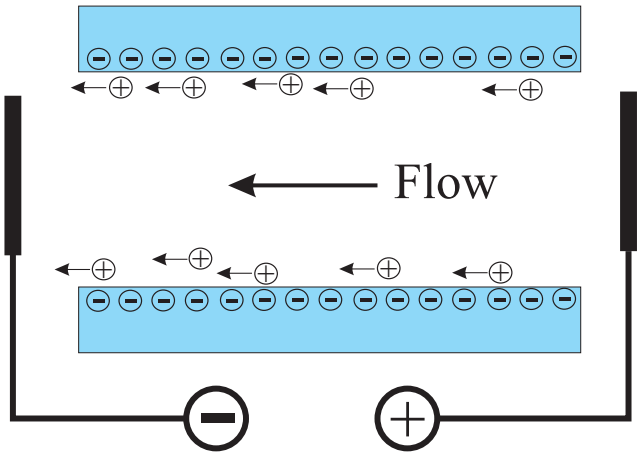

Figure 1.5: The principle of a simple Electroosmotic micropump. The negatively charged walls attract positive ions. An external electric field applies a force to the positive ions that through friction with the fluid generate the flow

Author	Actuation mechanism	Valve	Voltage (V)	Maximum pressure (mbar)	Maximum flowrate (ml/min)
Olsson et al [16]	Piezo	Nozzle	200	740	1.1
Carrozza et al [17]	Piezo	Ball	300	250	2.7
Zengerle et al [18]	Electrostatic	Flap	200	290	0.16
Grover et al [19]	Pneumatic	Flap	-	300	0.0028
Guo et al [20]	Solenoid	Flap	12	0.12	1

Table 1.2: Examples of displacement pumps

Author	Pump type	Voltage (V)	Maximum pressure (mbar)	Maximum flow rate (μl/min)	Restrictions on fluid
Ahn et al [21]	Hydrodynamic	120	2.50	50	Organic (Tested on Ethanol)
Studer et al [22]	AC electroosmotic	10	-	0.06	Saline (Conc: $10^{-5} - 10^{-3}$ M)
Brask et al [23]	DC electroosmotic	30	5000	3	Saline (Conc: $10^{-3} - 10^{-1}$ M)

Table 1.3: Examples of dynamic pumps

1.3 Fluid behaviour on micrometer length scale

Fluid flow on the micrometer length scale has some fundamental differences from fluid flow on the centimetre to metre scale. This is mainly attributed to the low Reynolds number associated with microsystems ($Re = \frac{l_0 v_0 \rho}{\mu}$). Typical values of a microfluidic system are presented in tabel 1.4 (based on the values given in table 1.2 and 1.3 and the values used for the device described in chapter 4). The fluid flow is governed by the Navier-Stokes

Parameter	Typical value
Length scale (l_0)	$10 - 1000 \mu m$
Velocity (v_0)	$10 - 1000 \mu m/s$
Fluid density (ρ) (water)	$1000 kg/m^3$
Fluid viscosity (μ) (water)	$8.9 \cdot 10^{-4} Pa \cdot s$
Pressure (p)	$1 - 100000 Pa$
Reynolds number ($Re = \frac{l_0 v_0 \rho}{\mu}$)	$10^{-4} - 1$

Table 1.4: Typical physical properties of a microfluidic system

equation when the Reynolds number is below 2000 [24] (assuming that the fluid is incompressible):

$$\rho \left(\frac{\partial \mathbf{v}}{\partial t} + \mathbf{v} \cdot \nabla \mathbf{v} \right) = -\nabla p + \mu \nabla^2 \mathbf{v} + f \tag{1.1}$$

where $\mathbf{v}$ is the velocity, p is the pressure, μ is the viscosity, ρ is the density and f is a force acting on the fluid e.g. gravity. Using the values in table 1.4, an order of magnitude analysis can be made on the terms in the Navier-Stokes equation. These are presented in table 1.5. The order of magnitude

Expression	Order of magnitude analysis	Order of Magnitude value
Unsteady acceleration	$\rho \frac{\partial \mathbf{v}}{\partial t} \approx \rho \frac{\Delta \mathbf{v}}{\Delta t} \approx \rho \frac{\mathbf{v}_0}{\Delta t}$	$\frac{0.01-1}{\Delta t} N/m^3$
Convective acceleration	$\rho \mathbf{v} \cdot \nabla \mathbf{v} \approx \rho \mathbf{v}_0 \frac{\Delta \mathbf{v}}{\Delta x} \approx \rho \mathbf{v}_0 \frac{\mathbf{v}_0}{l_0}$	$10^{-4} - 10^{2} N/m^3$
Pressure gradient	$\nabla p \approx \frac{\Delta p}{\Delta x} \approx \frac{p_0}{l_0}$	$10^{4} - 10^{9} N/m^3$
Viscosity contribution	$\mu \nabla^2 \mathbf{v} \approx \mu \frac{\Delta \mathbf{v}}{(\Delta x)^2} \approx \mu \frac{\mathbf{v}_0}{l_0^2}$	$10^{4} - 10^{10} N/m^3$

Table 1.5: Order of magnitude analysis of fluid flow on the microscale

analysis shows that the convective acceleration term ($\rho \mathbf{v} \cdot \nabla \mathbf{v}$) is insignificant. Without the convective acceleration, the flow is defined as creeping flow, characterised by no eddies [24]. The other term on the left hand side is the unsteady acceleration $\rho \frac{\partial \mathbf{v}}{\partial t} \approx \frac{0.1}{\Delta t} N/m^3$. This term is insignificant for time scales above $10^{-4} s$ showing that the flow in a microfluidic system reaches

steady-state within milliseconds. Both of the nonlinear terms on the left hand side of Navier-Stokes are usually neglected in micro flow problems [25]. One should however be aware that oscillating flows like the AC electroosmotic pump described in chapter 3 and nozzles on inkjet printers operate with frequencies in the kHz range and that the timescale therefore is sufficiently low for the unsteady acceleration to have significance.

1.4 Fabrication of polymer devices

Several techniques for micropatterning of ordinary non-conductive polymers have been developed. Some of the techniques, like soft lithography, have been specifically developed for microfluidic applications whereas e.g. injection molding is a technique borrowed from other industrial areas. The subject has been treated in several excellent review papers [26–29]. The most applied techniques will shortly be described in the following.

1.4.1 Hot embossing

Hot embossing is a simple method for generating structures in thermoplastic polymers. A master stamp with a bas-relief is made in either silicon or metal using classical clean room techniques. The master is placed against a sheet of thermoplast, heated to near or above Tg, and a pressure is applied. The method is fast and simple once the master has been produced and the resolution is well below 1 μm [27], but obviously depending on the resolution of the stamp. Fabrication of the master can be time consuming and the method is therefore not always suited for fast prototyping.

1.4.2 Injection molding

Injection molding is mainly known from industrial applications where it is used to fabricate everyday objects in plastic, but injection molding can also be utilised for manufacturing microfluidic devices. The method resembles hot embossing, but instead of using a polymer sheet, a polymer melt is injected into a chamber where the master is located. The melt is cooled, the chamber opened and the replica removed. Fabrication of the master is time consuming, as for hot embossing, but also polymer temperature, cooling time and injection pressure requires optimisation. When optimised and running, injection molding has a very high output, but due to the long run-in time, the process is mostly used to produce microfluidic devices that already have been tested and optimised.

1.4.3 PDMS casting

PDMS casting is a method developed to introduce poly(dimethylsiloxane), PDMS, devices in microfluidics. A curable elastomer is poured on to a bas-relief master yielding an inverse bas-relief of the photoresist master [30]. PDMS casting involves lower temperatures and less stress on the master relief, compared to hot embossing and injection molding, and the master structure can therefore be constructed directly in photoresist. The easy master and replica fabrication have made PDMS casting a very popular tool for making prototype devices.

1.4.4 Laser ablation

In laser ablation a powerful laser is used to remove material in designated areas [29]. The strong laser heats up the polymer which decomposes and evaporates. The resolution of laser ablation depends on the wavelength of the laser, the optics used, and the properties of the polymer, but it is often in the range of 50-200 μm [31, 32]. One can use lasers with wavelength ranging from UV (F_2: 157 nm, ArF:193 nm, KrF:248) to deep infrared like CO_2-lasers (10.6 μm) depending on the absorption spectrum of the relevant polymer. Cross-section of the indentation produced by laser ablation is approximately gaussian due to the nature of the patterning mechanism, hence the method is not suited if a well defined squared channel is needed. The surface of the polymer is altered by the ablation and it has been reported that channels produced by laser ablation have higher surface charge than channels made with less harsh patterning techniques like embossing [29]. The method is ideal for fast prototyping of microstructures because no masters are required and the patterns can be generated directly through a software interface.

1.5 Thesis outline

In **chapter 2** the blending of PEDOT with a number of non-conductive polymers is examined. The blending is required to increase the mechanical properties of the PEDOT, which in its pristine form is fragile and exhibits poor adhesion to hydrophilic substrates. It is found that the PEDOT can be integrated into a polymer substrate by using a solvent, which dissolves both the substrate and removes the used oxidants. The main focus is on PEDOT integrated into Polymethylmethacrylate (PMMA) which can be done by washing with a mixture of butanol and anisole. Several other combinations of conducting polymers and none-conductive polymer substrates are

examined

Chapter 3 describes how the integrated PEDOT/PMMA is patterned, using clean room techniques, to form an AC electroosmotic (ACEO) micropump. In addition, a new kind of polyurethane channel system is tested and an all polymer micropump is constructed in PEDOT/PMMA and polyurethane. The characteristics of the pump are examined using fluorescent microspheres in the fluid observed in a confocal microscope, and processed by image analysis tools.

The topic of **Chapter 4** is a material made of PEDOT and polyurethane (PUR), which both exhibits good conductivity and is highly stretchable and elastic. Conductive polymers have been considered non-stretchable because of their conjugated backbone, which is true for most pristine conductive polymers. By adding polyurethane during the in situ polymerisation a material is made, which can be stretched 200 percent and still remains fairly conductive. The material was developed with the intent to use it as a movable electrode in an all polymer displacement pump.

In **Chapter 5** a new technique for patterning conductive polymers is presented. Using a 3D structured agarose stamp, a deactivation agent can be delivered to a uniform conductive polymer film in well defined areas. The diffusion of the deactivation agent from the stamp to the film is spatially confined to the areas of intimate contact. The deactivation agent will eliminate the electric conductivity, while the areas of no contact remain conductive. Feature sizes down to 2 μm can be constructed, but the resolution is highly depending on the thickness of the conducting polymer.

Chapter 6 compares the agarose stamping technique with inkjet printing. The two methods are used to pattern the stretchable conductive polymer. A setup is constructed in which the resistance perpendicular to the stretching direction can be measured. It is found that the agarose stamping itself affects the conductivity of the sample during elongation, but not significantly. Furthermore it is concluded that the stretchable conductive polymer can be ink-jet printed if the molecular weight of the polyurethane is sufficiently low.

Finally, in **chapter 7** the results of the Ph.D. is summarised and in **Appendices A & B** non-published and less successful results obtained are described.

References

[1] K. E. Aasmundtveit, E. J. Samuelsen, L. A. A. Pettersson, O. Inganäs, T. Johansson, and R. Feidenhans'l. Structure of thin films of poly(3,4-ethylenedioxythiophene). *Synthetic Metals*, 101:561–564, 1999.

[2] C. K. Chiang, C. R. Fincher, Y. W. Park, A. J. Heeger, H. Shirakawa, E. J. Louis, S. C. Gau, and Alan G. MacDiarmid. Electrical conductivity in doped polyacetylene. *Physical Review Letters*, 39:1–4, 1977.

[3] H. Shirakawa, EJ Louis, AG Macdiarmid, CK Chiang, and AJ Heeger. Synthesis of electrically conducting organic polymers - halogen derivatives of polyacetylene, (ch)x. *Journal of the Chemical Communications-Chemical Communications*, 16:578–580, 1977.

[4] L. Groenendaal, Friedrich Jonas, Dieter Freitag, Harald Pielartzik, and John R. Reynolds. Poly(3,4-ethylenedioxythiophene) and its derivatives: Past, present and future. *Lab on a Chip*, 12:481–494, 2000.

[5] Bjørn Winther-Jensen, Jun Chen, Keld West, and Gordon Wallace. Stuffed conductive polymer. *Polymer*, 46:4664–4669, 2005.

[6] Thomas Steen Hansen, Keld West, Ole Hassager, and Niels B. Larsen. Integration of conducting polymer network in non-conductive polymer substrates. *Synthetic Metals*, 156:1203–1207, 2006.

[7] David R. Lide. *Handbook of Chemistry and Physics*. CRC, 84 edition, 2003.

[8] Radhouane Bel Hadj Tahar, Takayuki Ban, Yutaka Ohya, and Yasutaka Takahashi. Tin doped indium oxide thin films: Electrical properties. *Journal of Applied physics*, 83:2631–2645, 1998.

[9] N. Deprez and D. S. McLachlan. The analysis of the electrical conductivity of graphite conductivity of graphite powders during compaction. *Journal of Physics D: Applied Physics*, 21:101–107, 1988.

[10] Bjørn Winther-Jensen, Dag W. Breiby, and Keld West. Base inhibited oxidative polymerization of 3,4-ethylenedioxythiophene with iron(iii)tosylate. *Synthetic Metals*, 152:1–4, 2005.

[11] M. Khardani, M. Bouaïcha, W. Dimassi, M. Zribi, S. Aouida, and B. Bessaïs. Electrical conductivity of free-standing mesoporous silicon thin films. *Thin Solid Films*, 495:243–245, 2006.

[12] P. L. Kirby. Electrical conduction in glass. *British Journal of Applied Physics*, 1:193–202, 1950.

[13] D. J. Laser and J. G. Santiago. A review of micropumps. *Journal of Micromechanics and Microengineering*, 14:R35–R64, 2004.

[14] N. T. Nguyen, X. Huang, and T. K. Chuan. Mems-micropumps: A review. *Journal of Fluids Engineering, Transactions of the ASME*, 124:384–392, 2002.

[15] Peter Woias. Micropumps - past, progress and future prospects. *Sensors and Actuators B*, 105:28–38, 2005.

[16] A. Olsson, P. Enoksson, G. Stemme, and E. Stemme. Micromachined flat-walled valveless diffuser pumps. *Journal of Microelectromechanical Systems*, 6:161, 1997.

[17] M. C. Carrozza, N. Croce, B. Magnani, and P. Dario. A piezoelectric-driven stereolithography-fabricated micropump. *Journal of Micromechanics and Microengineering*, 5:177–179, 1995.

[18] R. Zengerle, J. Ulrich, S. Kluge, M. Richter, and A. Richter. A bidirectional silicon micropump. *Sensors and Actuators A*, 50:81–86, 1995.

[19] W. H. Grover, A. M. Skelley, C. N. Liu, E. T. Lagally, and R. A. Mathies. Monolithic membrane valves and diaphragm pumps for practical large-scale integration into glass microfluidic devices. *Sensors and Actuators B*, 89:315–323, 2003.

[20] Shuxiang Guo, Jian Wang, and Jian Guo. A novel type of micropump using solenoid actuator for biomedical applications. *2007 IEEE International Conference on Robotics and Automation*, 1:654–659, 2007.

[21] Si-Hong Ahn and Yong-Kweon Kim. Sensors and actuators a. *Science*, 70:1–5, 1998.

[22] Vincent Studer, Anne Pépin, Yong Chen, and Armand Ajdari. Fast and tunable intergrated ac electrokinetic pumping in a microdfluidic loop. *Y. Chen. Analyst*, 129:944–949, 2004.

[23] Anders Brask, Jörg P. Kutter, and Henrik Bruus. Long-term stable electroosmotic pump with ion exchange membranes. *Lab on a Chip*, 5:730–738, 2005.

[24] R. Byron Bird, Warren E. Stewart, and Edwin N. Lightfoot. *Transport phenomena*. Wiley, 2 edition, 2002.

[25] George Em Karniadakis and Ali Beskok. *Micro Flow - Fundamentals and Simulation*. Springer, 1 edition, 2002.

[26] M. Heckele and W. K. Schomburg. Review on micro molding of thermoplastic polymers. *Journal of micromechanics and microengineering*, 14:R1–R14, 2004.

[27] Holger Becker and Claudia Gärtner. Polymer microfabrication methods for microfluidic analytical applications. *Electrophoresis*, 21:12–26, 2000.

[28] Holger Becker and Laurie E. Locascio. Polymer microfluidic devices. *Talanta*, 56:267–287, 2002.

[29] Gina S. Fiorini and Daniel T. Chiu. Disposable microfluidic devicec: fabrication, function, and application. *Biotechniques*, 38:429–446, 2005.

[30] J. Cooper McDonald, David C. Duffy, Janelle R. Anderson, Daniel T. Chiu, Hongkai Wu, Olivier J. A. Schueller, and George M. Whitesides. Fabrication of microfluidic systems in poly(dimethylsiloxane). *Electrophoresis*, 21:27–40, 2000.

[31] Chantal G. Khan Malek. Laser processing for bio-microfluidic applications (part i). *Analytical and Bioanalytical Chemistry*, 385, 2006.

[32] Chantal G. Khan Malek. Laser processing for bio-microfluidic applications (part ii). *Analytical and Bioanalytical Chemistry*, 385, 2006.

Chapter 2

Integration of conducting polymer network in non-conductive polymer substrates

2.1 Introduction

Recent research has shown that it is possible to produce highly conducting polymer films of poly(3,4-ethylenedioxythiophene) (PEDOT) on large areas [1] and with a high stability [2]. This has let to an increasing interest in making all-polymer micro sensors based on PEDOT. One of the major problems in utilising the reported films is the often poor adhesion of the conducting polymers to glass and non-conducting polymer substrates. Aqueous environment, as required for bio analytical applications, pose particular problems: The adhesion may be so weak that the PEDOT layer sometimes delaminates from the substrate upon immersion in water. A commercial product is available from AGFA (Agfa-Gevaert group, Mortsel Belgium) [3], which can be applied to various substrates by spin coating. However, the surface conductivity of films resulting from this product is significantly lower than films produced by in situ polymerisation. The method presented here permits facile application of a PEDOT layer onto most non-conductive polymer substrates and is also demonstrated to be applicable to other conducting

[1] This chapter is based on an article published in **Synthetic Metals**, 2006, vol. 156, p. 1203-1207

polymers. Winther-Jensen et al. [4] has shown that PEDOT can be anchored to silicon using plasma treatment which permits micro structuring by classical lithographic and lift-off techniques. Furthermore, it has been shown that PEDOT and polypyrrole can be polymerised in polyurethane foam [5] [6] by vapour phase polymerisation resulting in conductivities of $10^{-3} - 10^{-1}$ S/cm. The method presented here does not require any vacuum techniques and still yields high conductivity. The conducting polymer is washed into a non-conducting polymer substrate and integrated into the top layer of the substrate structure. The resulting hybrid material acquires some of the mechanical properties of the substrate, while still remaining as conductive as a pristine layer of PEDOT. In this chapter we demonstrate the integration of PEDOT into poly(methyl methacrylate) (PMMA), polycarbonate (PC), cyclic olefin copolymer (COC), poly(ethylene terephtalate) (PET) and polystyrene (PS) with the best results observed on PMMA, PC, or COC. The investigation of the integration of conducting polymers into non-conducting polymer substrates is focussed on the PEDOT/PMMA system, but many of the properties can most likely be extended to other combinations of conducting polymers and substrates. PEDOT polymer coatings were fabricated using in situ polymerization of EDOT with Fe(III) tosylate as oxidation agent [7] and with pyridine as inhibitor [8]. This yields a highly conducting polymer coating with conductivity between 500 S/cm and 1000 S/cm. After polymerisation the polymer layer contains a large amount of residual and spent oxidant from the oxidation. The salt can be removed by washing, usually using water or alcohol, resulting in shrinkage of the polymer structure to 5% of its original thickness [9, 10]. Aben et al. [9] demonstrated trapping of tetraethoxysilane (TEOS) in the shrunken conducting polymer layer by using a TEOS containing washing solution. Later, it has also been shown that a number of conducting polymers can be loaded with macromolecules and other polymers during the washing step [10]. In the present paper, the ability to load the conducting polymer is used to integrate it into the surface of a non-conducting polymer substrate. A layer of the conducting polymer is polymerised onto a non-conductive polymer, followed by washing with a solvent that partially dissolves the substrate. The top part of the substrate is washed into the conducting polymer layer during the shrinkage, and due to entanglement of the polymer chains the conducting polymer layer is effectively integrated into the substrate. Furthermore mechanical and chemical properties of the conducting polymer/substrate surface resemble the substrate surface. This is an advantage because the mechanical strength of conducting polymers can be quite poor. In order to integrate the conducting polymer into a substrate it is required that a solvent exists which is capable

of dissolving both the substrate and the residual salt.

2.2 Experimental

The EDOT monomer (Baytron M) and Fe(III) tosylate (40 % in butanol, Baytron C) were purchased from Bayer AG (Leverkusen, Germany). The PMMA substrates were purchased from Nordisk Plast A/S (Auning, Denmark). Other polymer substrates employed were prepared by injection molding of polycarbonate (DP1-1265, BASF, Ludwigshafen, Germany) or polystyrene (Polystyrol 154, Bayer, Leverkusen, Germany), hot pressing of COC (Topas 8007, Ticona, Frankfurt, Germany), or curing of poly(dimethylsiloxane) (Sylgard 184, Dow Chemicals, Midland, Michigan, U.S.A.). All other chemicals were purchased from Sigma-Aldrich (Taufkirchen, Germany). All chemicals were used as received. Ultra-pure water with a resistivity of $>$18.2 MΩcm was used. The polymerisation was conducted from a solution containing 6.5 ml Baytron C, 2.0 ml water, 0.22 ml EDOT and 0.15 ml pyridine. The water is added to decrease the viscosity and prolong the pot life of the solution. The solution was applied onto 50 x 50 x 1.5 mm PMMA sheets by spin coating using a Delta 10TT (Süss Microtec, Munich, Germany) spin coater. Spinning speeds of 250 to 4000 rpm for 30 seconds were employed. Afterwards the substrates were baked at 65°C for 10 minutes on a hotplate to evaporate any remaining solvent and initiate the polymerisation. The substrates were subsequently washed by applying 3 ml of a 1:1 mixture of butanol and anisole to the conducting polymer coated substrate surface while spinning at 1000 rpm for 20 sec. The washing solvent was added in the middle of the sample in a steady flow during the first 10 seconds of the spinning. The washed substrates were further dried for 5 minutes at 65°C on a hot plate. The other combinations of conducting polymers and substrates were produced in similar ways, using other washing solvents as summarised in table 2.3.

2.3 Results and discussion

The overall conductance of a PEDOT layer has been shown to be roughly invariant when the layer is diluted with an amount of non-conducting material up to a fractional loading of approximately 75% [9]. We hypothesised that integration of the substrate polymer into the conducting polymer layer would likewise cause minimal, if any, decrease in the surface conductivity. Two PEDOT series were produced to test this hypothesis. Series A was pro-

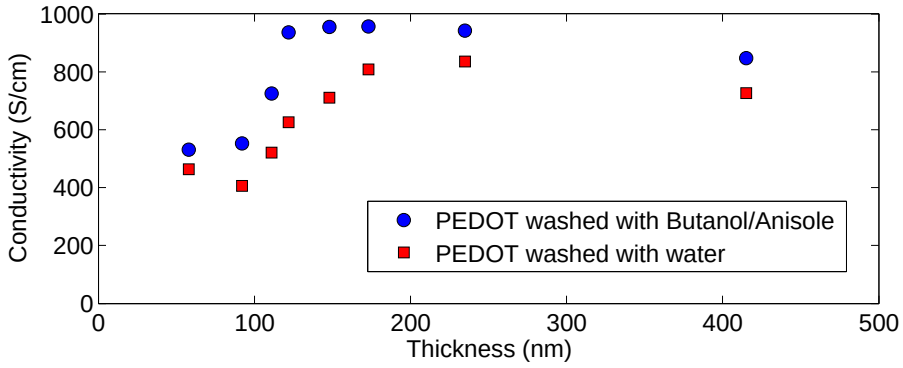

Figure 2.1: The conductivity of the integrated (washed with butanol/anisole) and non-integrated PEDOT (washed with water) versus the nominal PEDOT film thickness.

duced with spinning velocities of 250, 500, 750, 1000, 1500, 2000, 3000 and 4000 rpm, respectively, and subsequently washed with a butanol anisole mixture. Series B was prepared using an equal set of parameters but washed by immersion in water instead of washing with butanol/anisole. The thickness of the PEDOT layers of the B series was measured using an Ambios XP-2 profilometer (Ambios Technology, Inc., Santa Cruz, US) using a stylus force of 1 mg. The layer thickness in the A series samples was not measured as the PEDOT is fully integrated into the PMMA structure. However, we expect the same mass of conducting polymer per area to be present on samples of the two series produced at equal spinning velocity, as only the subsequent washing step differs between the samples. The effective thickness of the PEDOT layer of the A series samples is therefore assumed to be equal to that of the B series, permitting an effective conductivity of PEDOT in the A series to be calculated as if the thickness were that of B series samples. In reality the conducting PEDOT-PMMA blend is thicker than the conducting PEDOT layer in the B series, and consequently the real conductivity of this layer is lower than the calculated value. Measurements of the surface conductance were conducted using a four-point probe (Jandel Engineering Ltd, Linslade, UK) connected to a Keithley 2400 SourceMeter (Keithley, Cleveland, US). These values were recalculated as conductivities as explained above and are shown in figure 2.1 as function of the effective PEDOT thickness. The values correspond to conductivities reported earlier [8]. The effective conductivity

of PEDOT washed into PMMA is approximately 10-30 percent higher than that of PEDOT washed with water. Both types of conducting layers show a lower measured conductivity for nominal thicknesses less than 150 nm. This may be due inhibition of the electron transfer between conducting domains as the layer thickness becomes comparable to the size of the conducting domains in PEDOT. This fits with the transition to the lower conductivity occurring at a smaller PEDOT loading for the A series, as the shrinkage of the PEDOT layer is smaller in this case where PMMA takes up some of the void created when the oxidant is washed out of the conducting polymer layer. The effective conductivity is generally not negatively affected by the integration of the PEDOT into PMMA, although a small dependence on the washing solution is observed, which has also been reported previously [11]. The washing mixtures reported here are based on optimisation of two parameters in the washing step; the composition and the amount of the washing solvent. The amount of washing fluid is crucial because a certain amount is required to remove the residual salt, but too much washing solvent will dissolve the substrate, causing delamination of the PEDOT layer during spinning. The composition of the solvent determines how much of the substrate that is dissolved and therefore the degree of integration.

Material	Force required for damage
Standard wet	$<$0.08 N
Standard dry	0.15-0.43 N
Integrated wet	1.90-2.60 N
Integrated dry	1.90-2.60 N

Table 2.1: The force required to visually damage the PEDOT layer for the integrated PEDOT/PMMA and the standard PEDOT on PMMA materials using the wear test setup of figure 2.1

2.3.1 Adhesion and mechanical properties

The adhesion of the PEDOT layer to the PMMA substrate was tested using the tape test (Tesa 4024, Charlotte, US). Whereas the PEDOT layer was easily removed from the B series, it was not possible to remove the PEDOT from the A series using this method. It was actually only possible to remove the PEDOT layer from the A series by abrasion of the PMMA as well. The adhesion of the PEDOT layer was examined using the setup shown in Figure 2.2. A steel pin was attached to a PMMA lever resting on an aluminium block and, through the pin, on the PEDOT/PMMA sample. The steel pin was 3 mm in diameter and had a rounded tip (se inset on Figure 2.2). The force

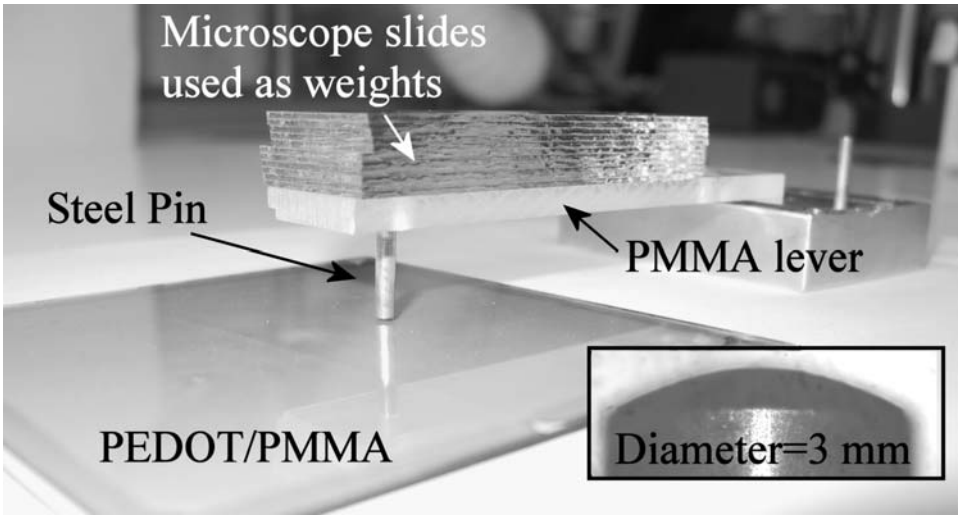

Figure 2.2: The figure shows the device used to compare the wear resistance of integrated PEDOT and pure PEDOT surfaces. Although not giving quantitative results, the device revealed better wear resistance of the PEDOT/PMMA than pure PEDOT on PMMA.

applied to the sample surface was controlled by the number of microscope slides on top of the lever.

The PEDOT/PMMA sample was then gently pulled out by hand and it was observed by visual inspection whether the steel pin had done any damage to the PEDOT. Although the method does not give a quantitative measure for the strength of the PEDOT layer, it gives an estimate of the relative difference in wear resistance between the integrated and the standard PEDOT layers. Both the standard and the integrated PEDOT layers were tested under dry and wet conditions. During the wet test the PEDOT/PMMA was soaked in water. The results of the wear tests are presented in table 2.1. The adhesion of PEDOT layers is especially poor in wet conditions, which also often results in damage to the PEDOT layer during washing. However, even in dry conditions the wear resistance of the integrated PEDOT is much higher than of a coated PEDOT layer. Such high wear resistance and adhesion under wet conditions is necessary if the PEDOT is to be used for micro patterning or as electrodes in sensors. The depth of the integrated PEDOT layer was examined by gradual removal of the surface layer while monitoring

its optical and electrical properties. An integrated PEDOT/PMMA sample was made by the production method presented above with a spinning velocity of 500 rpm, which would result in a PEDOT layer with a thickness of 235 nm if washed in water. The sample was placed in a Plasmatherm 740 Reactive Ion Etcher (RIE) (Unaxis, St. Petersburg, FL) and partially covered with a glass microscope slide leaving 1/5 of the sample uncovered. The sample was then etched with 50 sccm O_2 at 50 mbar and a power of 150 watts at 13.56 MHz for 5 seconds. The glass slide was moved to leave 2/5 of the sample uncovered, which was etched again. This procedure was repeated 4 times in all resulting in five different parts which in total had been etched 20, 15, 10, 5 and 0 seconds, respectively. The etching depth of each part was measured by profilometry and is presented in table 2.2. The edges between the steps were not as well defined as if the regions had been defined by photolithography. The accuracy of the step heights is approximately $\pm$ 10 nm. Assuming that all parts of the PEDOT layer contributes equally to the conductance, it is possible to calculate how the PEDOT is distributed in the PMMA. The surface resistance of each layer was measured using the four point probe described above, and based on comparison with the undiluted thickness from the B series, we can estimate the degree to which PEDOT is diluted by the substrate polymer. The amount of PEDOT in the remaining layers was also determined from visible light absorption at 700 nm using Lambert-Beer's law. Based on the conductivity and absorption measurements the amount of PEDOT in the PMMA was determined as a function of etch depth - see table 2.2. It should be noted that the ion bombardment participating in the etching process could potentially cause selective implanting of different atoms. However, the degree of implantation of the two purely organic molecular species EDOT and MMA is not expected to differ significantly. There is a fairly good correlation between the distributions determined by resistivity and absorption (Table 2.2), showing that the top layer of the substrate contains approximately 30-40% PEDOT. The examination also reveals that the PEDOT is present at substantial depths in the PMMA substrate, with 25-30% of the conducting polymer at depths greater than 500 nm, although the pure PEDOT layer is only 235 nm thick. The integration of the PEDOT into the PMMA substrate matrix must be considered the main reason for the superior mechanical properties of the conductive layer compared to a surface adlayer.

Etching time (s)	Depth (nm)	Step size (nm)	Surface resistance (Ω/sq)	PEDOT remaining based on conductance	Percent PEDOT in layer based on conductance	Absorbance at 700 nm	PEDOT remaining based on absorbance	Percent PEDOT in layer based on absorbance
0	0	-	75.07	100%	40%	0.365	100 %	32 %
5	150	150	100.47	75%	33%	0.291	79 %	28 %
10	290	140	135.60	55%	30%	0.230	63 %	36 %
15	400	110	184.20	41%	39%	0.168	46 %	36 %
20	500	100	309.10	24%	-	0.112	31 %	- %

Table 2.2: Results from the O_2 etching of the PEDOT/BA sample. The PEDOT content was determined using both surface resistivity and optical absorption (700 nm). The result shows that the top 500 nm of the PMMA sample consist of app. 30-40 % PEDOT

Conductive polymer	Substrate	Washing solvent	Comment
PEDOT	PMMA	Butanol/Anisole	Good integration with excellent and uniform film properties
Polypyrrole	PMMA	Butanol/Anisole	Good integration but poor transparency
PEDOT	Polycarbonate	Butanol/THF	Good integration with excellent and uniform film properties
PEDOT	Polystyrene	THF	Good integration but uneven surface
PEDOT	PET (foil)	Chloroform	Slightly integrated with very rough surface
PEDOT	COC	Toluene/THF	Good integration and uniform film properties
PEDOT	PDMS	Many types	No adhesion at all

Table 2.3: Results from washing PEDOT into different kinds of substrates. The best results were obtained with PEDOT on PMMA, PC and COC

2.3.2 Surface analysis

If the material is to be used in a microfluidic system, the surface properties are of great importance, as they influence a number of properties such as double layer capacitance and adhesion. It has been reported that the surface of PEDOT washed in water is smooth on the sub-μm scale [8] in contrary to the non-washed PEDOT/Fe(II)Tos surface, which is quite rough. A non-washed PEDOT/ Fe(II)Tos film and a PEDOT film washed in butanol/anisole, both spun at a speed of 500 rpm, were examined using a XE 150 Atomic Force Microscope (PSIA, Santa Clara, US) operating in intermittent contact mode and using BudgetSensors BS-tap300 cantilevers. AFM topography scans of the PEDOT/Fe(II)Tos surface are shown in Figure 2.3 (top). The surface is covered with particles or "'hills"' with a diameter of 0.5-1 μm and a height of 200-400 nm (50x50 μm^2 image). Between the larger particles the surface has a flaky appearance (2x2 μm^2 image). Corresponding topography scans on the PEDOT sample washed with butanol/anisole is presented in figure 2.3 (bottom). The surface is much smoother than the PEDOT/Fe(II)Tos and the height variations are less than 10 nm over distances of 10-20 μm (50x50 μm^2 image), except for a very low density of particles of heights of 20-40 nm (not shown). The latter particles could be residual salt which has not been completely removed in the washing process. On the sub-micron length scale, small protrusions are observed, with a height of 1-3 nm and a diameter of 10-50nm. This could be remains of the flakes from the PEDOT/Fe(II)Tos state or they could be crystalline areas in the PEDOT structure. The AFM images revealed that the surface of the PEDOT/PMMA blend is smooth on the sub-μm scale and therefore resembles pure PEDOT washed with water.

2.3.3 Integration in other polymer substrates

The method for PEDOT integration was tested with other polymer substrates and for polypyrrole on PMMA. The polypyrrole was polymerised using vapour phase polymerisation as reported in [8] on a PMMA substrate and washed in the same manner as described above. The film was absorbed into the PMMA substrate, and showed much better mechanical properties than a polypyrrole adlayer on PMMA washed with water. Furthermore, several other kinds of substrates were tested. The results of the examination are presented in table 2.3. The integration of PEDOT was most successful on PMMA, PC and COC, whereas no integration was obtained in cross-linked PDMS. This is in accordance with our understanding of the integration process. Since PDMS is cross linked, and therefore insoluble, transport

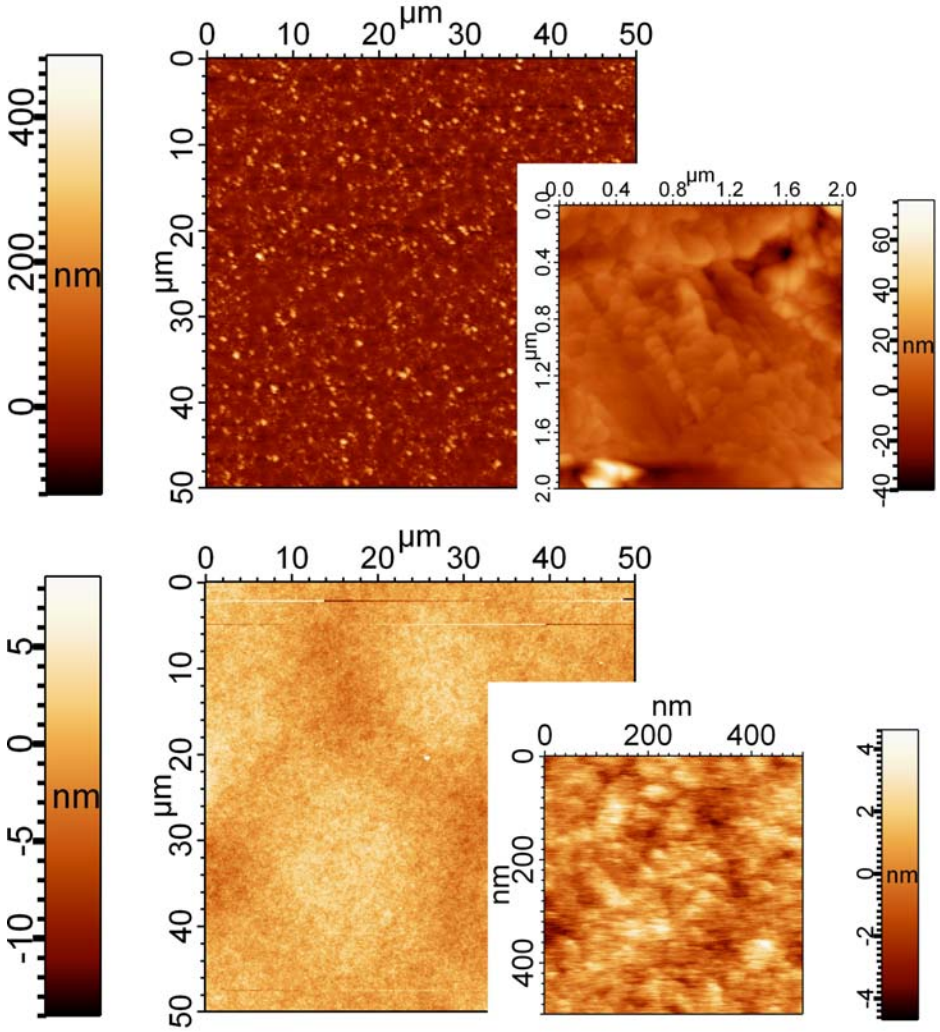

Figure 2.3: AFM images of the PEDOT/Fe(II)Tos (top) and PEDOT/PMMA (bottom). The PEDOT/Fe(II)Tos surface is rough and covered with particles. The PEDOT/PMMA is very smooth with small 2-4 nm elevations

of polymer material from the substrate into the likewise insoluble PEDOT phase is prohibited. The integration of PEDOT into PET was quite poor because of the poor solubility of PET in the applied solvents. Integration

was, however, demonstrated using chloroform, but the resulting surface layer was milky in appearance. It is quite remarkable that the charged hydrophilic polymer PEDOT can be integrated with the very hydrophobic polymer COC. This indicates that more than ordinary blending plays a significant role in the integration of conductive polymers. All of the integrated samples showed conductivity of the same order of magnitude as pure PEDOT.

2.4 Conclusion

The conducting polymers PEDOT and polypyrrole were integrated into various non conductive polymer substrates. Special attention was paid to PEDOT on PMMA, which yielded uniform and transparent films with the same or lower surface resistance than that of a corresponding non-integrated adlayer of PEDOT on PMMA. Reactive ion etching in combination with electrical conductivity and light absorption measurements showed that the top part of the network consisted of 30-40 vol% PEDOT and 60-70 vol% PMMA. This explains the good mechanical properties of the surface. No quantitative measure of the wear resistance was performed but it was determined that the integrated PEDOT surface had a much higher strength than non integrated PEDOT. This was particularly pronounced in aqueous environments. Polypyrrole could be integrated into PMMA in a similar way, although the film was not as smooth and transparent as integrated PEDOT layers. This is a characteristic property of polypyrrole, rather than of the integration into the PMMA. PEDOT was also successfully integrated into PC, COC, PET and PS with varying roughness of the resulting surfaces.

2.5 References

[1] Winther-Jensen B, West K, *Macromolecules* **2004**; 37; 4538-4543

[2] Winther-Jensen B, West K, *Reactive & Functional Pol.* **2006**; 66; 479-483

[3] Tehrani P et al, *Smart Mater. Struct.* **2005**; 14 N21-N25

[4] Winther-Jensen B, Norrman K, Kingshott P, West K, *Plasma Proc & Pol* **2005**; 2; 319-327

[5] Shenoy SL, Kaya I, Erkey C, Weiss RA, *Synthetic metals 2001*; 123; 509-514

[6] Fu Y, Weiss RA, Gan, PP, Bessette MD, *Polym. Engn. & Sci.* **1998**; 38; 857-862

[7] Winther-Jensen B, Chen J, West K, Wallace G, *Macromolecules* **2004**; 37; 5930-5935

[8] Winther-Jensen B, Breiby DW, West K, *Synthetic Metals* **2005**; 152; 1-4

[9] Aben GVA, Somers MJM, Hanssen PHC, Schrooten LM, *SID 98 DIGEST* **1998**, P-21; 528-531

[10] Winther-Jensen B, Chen J, West K, Wallace G, *Polymer* **2005**; 46; 4664-4669

[11] Kim JY, Jung JH, Lee DE, Joo J, *Synthetic Metals* **2002**; 126; 311-316

Chapter 3

All-polymer micropump based on the conductive polymer poly (3,4-ethylenedioxythiophene) and a polyurethane channel system

3.1 Introduction

Microfluidic systems are of major scientific and application oriented interest due to their potential for integrating and simplifying complex analytical procedures in a resource efficient, inexpensive device. Most microfluidic systems require or would benefit from integrated micropumps to unleash their true integrative potential. Micropumps have therefore been a topic of extensive research as presented in several recent excellent reviews [1-4]. The underlying microengineering required for integratable pump fabrication has mostly relied on existing clean room based micromachining processes. Devices have thus mainly been made in silicon, glass and selected polymers such as PMMA and PDMS for microchannels and for mechanical pumping elements. Electrically active components and connectors have been made in patterned metal, typically chemically inert gold or platinum. Micropumps made in such materials benefit from the ease of making high precision geome-

[2]This chapter is based on an article published in **J. Micromechanics & Microengineering**, 2007, vol. 17,p. 860-866

tries and from the long-term stability of the resulting devices [3]. A recent type of pump design is the ac electroosmotic (ACEO) pump. The ACEO pump was first suggested by Ajdari [5], and has later been described both experimentally [6-11] and theoretically [5, 6, 12]. The ACEO pump consists of two interdigitated arrays of electrodes of unequal width in a channel, with an ac potential applied between the electrode arrays. The advantages of this pump design are its simple construction, the absence of moveable parts and a low operating voltage (1-5 V). A disadvantage is its inability to pump liquids with ion strengths below 10^{-5} M or above 10^{-2} M. ACEO pumps have been fabricated and tested by several groups, including Studer et al [10] who used a glass substrate with patterned titanium/platinum electrodes and a channel system of PDMS. The processing of the latter materials is well established, but both processing and materials costs are often prohibitively high for making these pumps widely applied in inexpensive disposable devices. All-polymer devices may offer just those benefits of low cost through ease of manufacture and inexpensive materials. The main focus in the current work is on the introduction and validation of new materials, conducting polymers and elastomers, into the field of microfluidics, thereby broadening the choice of materials available for disposable active devices. The conductivity and stability of conductive polymers have been greatly improved in recent years [13], thereby making them increasingly competitive to inorganic conductors. One of the most widely employed conductive polymers is poly(3,4- ethylenedioxythiophene) (PEDOT) due to its high conductivity, high stability and ease of application to surfaces. Former work [14] presented a way of blending PEDOT with poly(methyl methacrylate) (PMMA), which gives excellent mechanical properties combined with high conductivity. The PEDOT is easy to micropattern and is therefore well suited for making sensors and other electronic features in microfluidic devices. This new blend is in the present work utilized as the active component of an all-polymer micropump, where the conductive polymer is used as electrode material in an ACEO pump. In addition, flexible thermoplastic polyurethanes (PUR) are explored as an alternative to polydimethylsiloxane (PDMS) for sealable polymer microflow channels. Combining PEDOT blended with PMMA and the thermoplastic PUR Tecoflex EG-80A yields a fully functional all-polymer microfluidic system. This system can be constructed without the use of expensive materials such as noble metals. Polyurethane has recently been introduced as a material for membranes in microfluidics [15], and in the current work a new methodology for patterning is presented. The pumping characteristics of the ACEO pump presented in this paper resemble those reported by Studer et al [10]

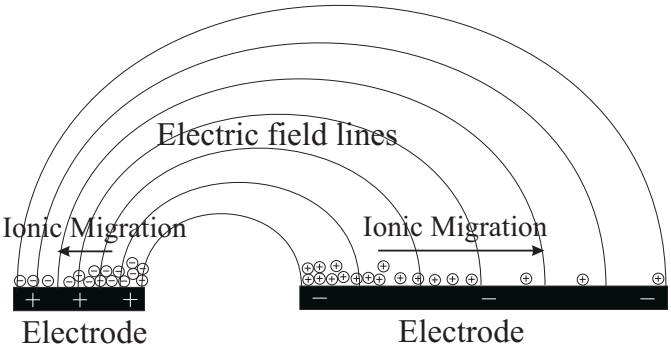

Figure 3.1: A sketch of the pumping principle of the ACEO pump. The electric field lines between the electrodes are shortest closest to gap resulting in the highest electric field strength at these points. The screening layer is therefore charged faster near the gap and causes an ion gradient along the electrode surface. The gradient causes ion migration and thereby fluid motion.

3.2 Theory of ACEO pumps

The pumping effect in ACEO pumps stems from the migration of ions in the screening layer on the electrodes and the friction caused by the moving ions on the surrounding fluid [5]. Ions migrate during each potential cycle to screen the electrodes as the potential increases. The parts closest to the gap between the electrodes are screened at a faster rate due to the higher electric field at these points. This implies that the ion concentration in the screening layer decreases with increasing distance from the gap, thereby generating a concentration gradient that makes the ions migrate along the electrode surface away from the gap. Since the electrodes are asymmetric, the migration and the fluid flow become asymmetric, as sketched in figure 3.1. The applied frequency and potential, as well as the ionic strength, are essential parameters for reaching conditions where the electrodes are not completely screened or unscreened. Brown et al [7] developed a simple model describing the correlation between potential, frequency, ion concentration and electrode geometry for the system. However, the approximations used in this model are only valid for potentials smaller than 0.025 V. At higher potentials the physical processes become highly nonlinear and very complex to describe analytically. Some general trends can still be predicted: the velocity of the fluid will be proportional to the inverse of the overall system size, and the

optimum frequency will scale with the square root of the ionic strength. Flow reversal at certain frequencies and potentials has been reported [11], which is not predicted by any of the existing models. Furthermore, it is unclear how the ratio between electrode widths affects the pump characteristics. Models describing the ACEO system more accurately at high potentials are thus much needed.

3.3 Chemicals and Instruments

The EDT monomer (Baytron M) and Fe(III) tosylate (40% in butanol, Baytron C) were purchased from Bayer AG (Leverkusen, Germany). The 2 mm thick PMMA substrates were purchased from Nordisk Plast A/S (Auning, Denmark). The polyurethane (Tecoflex EG-80A) was purchased from Noveon (Cleveland, USA). The photoresist Microposit S1813 was purchased from Shipley (Marlborough, USA). The photoresist SU-8 2025 was purchased from Microchem (Massachusetts, USA). All other chemicals were purchased from Sigma-Aldrich (Taufkirchen, Germany). All chemicals were used as received. Ultra-pure water with a resistivity of >18.2 (MΩ cm) was used. The conductivity was measured with a four-point probe (Jandel Engineering Ltd, Linslade, UK) connected to a four-point source meter (Keithley 2400, Cleveland, US). Step heights were measured with an Ambios XP-2 (Ambios Technology, Inc., Santa Cruz, US) profilometer using a stylus force of 1 mg. A Karl Süss MA4 mask aligner (Munich, Germany) was used to expose the photoresist. A Plasmatherm (Unaxis, St Petersburg, FL) 740 reactive ion etcher (RIE) was used for etching. HMDS treatment was performed in a YES 6112 oven (Yield Engineering Systems, San Jose, US). Contact angles were measured using an OCA 15+ from Dataphysics (Filderstadt, Germany). Motion detection was done on a Zeiss LSM 5 confocal laser scanning microscope (Carl Zeiss, Oberkochen, Germany) using 488 nm excitation light. The microspheres used for tracking were 500 nm fluorescent labelled polystyrene spheres (Molecular Probe, Carlsbad, US).

3.4 Fabrication

PEDOT on PMMA samples were produced as described previously [14], with a thickness of 250 nm, a conductivity of 500-700 S cm^{-1} and an optical transmission in the visible range (400-700 nm) of 50-70%. The integrated PEDOT in PMMA samples were coated by Microposit S1813 photoresist using spin coating at 2000 rpm for 30 s, and prebaked at 85 °C for 20 min

in a convection oven. The samples were exposed in the mask aligner (365 nm illumination) at a dose of 200 mJ cm^{-2} and developed in 15% MF-351 developer for 60 s. The samples were then etched in the RIE for 3 min at 300 W and 7 Pa O_2. The remaining photoresist was removed by immersing the sample in ethanol for a few minutes. All fabrication steps took place in a class 10 clean room (CleaR, Risø National Laboratory). A test series of conducting lines of decreasing width was constructed in PEDOT to test the resolution of the lithographic techniques applied to the PEDOT/PMMA samples. The electrodes had a length of 500 μm and widths of 20, 15, 12, 10, 6, 4 and 2 μm, respectively. Each of the conducting lines was connected at their ends to two large 15 mm $\times$ 50 mm rectangles of conducting polymer, functioning as electrical contact pads. Four-point probe measurement of the resistance of the lines as function of the nominal line width was performed by applying two of the four probes to each of the contact pads. The result of the resolution test showed that electrodes down to 4 μm in width could easily be constructed, whereas electrodes of 2 μm width showed a relative large decrease in conductance. Interpolation of the conductance measurements showed an edge effect of approximately 500 nm, i.e., the outermost 500 nm along the edge of each line had a markedly lower conductance than the rest of the line. The edge effects probably originate from the exposure in the mask aligner: the substrate consists of extruded PMMA that has been spin coated and heated three times [14] before being exposed. It is therefore difficult to achieve a completely planar surface, which may lead to a small separation between the mask and the substrate, and an associated exposure of edge regions of the masked areas. The outcome of the resolution test was that 4 μm structures with high conductivity can be fabricated with fairly good precision and the smallest features were therefore chosen to be 4 μm.

The conductivity of the PEDOT after patterning was found to be 500-700 S cm^{-1}. The RIE removed approximately 600 nm of PEDOT/PMMA as measured by profilometry. The conductivity in the etched areas was lower than 1×10^{-4} S cm^{-1} (detection limit). An optical microscope image of the final PEDOT pattern is shown in figure 3.2. The channel part of the pump was constructed in a flexible thermoplastic PUR, which in many ways has properties resembling PDMS. PDMS has been used in many microfluidic applications because of ease of fabrication, flexibility and high transparency [16]. The PUR chosen for our work shares the same properties, but in addition PUR is a thermoplastic polymer, which may be injection molded, embossed or extruded. This is a major advantage over PDMS, which cannot be processed with ordinary mass production equipment due to its cross-linking. Furthermore, PMMA and polyurethane are partially mixable [17-19]. This

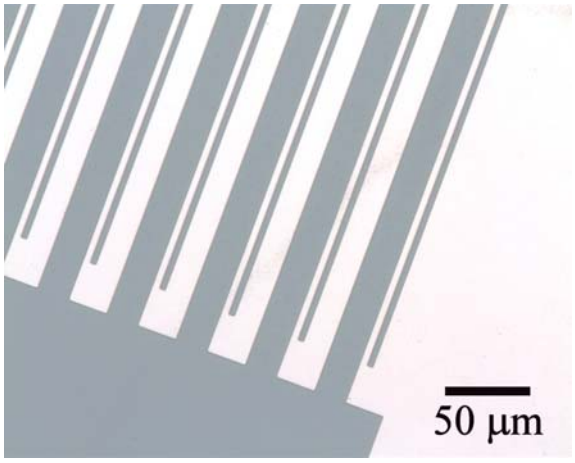

Figure 3.2: The PEDOT pump electrode array. The narrow and wide electrodes have widths of 4 μm and 20 μm, respectively.

makes it possible to bond the PMMA to PUR by heating the substrates to near the PUR glass transition temperature. PUR is slightly hydrophilic showing a water contact angle of 81°-82°. This implies that no further treatment is required for bonding or surface wetting. In contrast, the surface of PDMS must be oxidized both for bonding and for reducing the contact angle of 108°- 109° to below 90° [20-22]. Furthermore, PDMS loses its hydrophilicity after a period of time in air, giving PDMS-based devices a limited shelf-life. None of these problems occur with PUR. PUR can be heat-bonded to a range of polymers, such as PMMA, polycarbonate and polystyrene but not to glass or silicon. The fabrication of the PUR channels was done using embossing dies made from SU-8 photoresist. SU-8 2025 was spun at 1500 rpm for 60 s on a clean silicon wafer yielding a 25 μm thick layer. The sample was prebaked at 65°C for 2 min and at 95°C for 2 min with a temperature ramp to avoid cracking of the structure. The SU-8 was exposed in the mask aligner (365 nm illumination) at a dose of 480 mJ cm^{-2}, followed by post-baking at 65 °C for 2 min and at 95 °C for 2 min with a temperature ramp. The post-baked layer was developed in SU-8 developer for 180 s. The SU-8 was then plasma treated in the RIE in 5.5 Pa argon at 50 W for 15 s to activate the surface. It was subsequently treated in the HMDS oven at 150 °C. After treatment with HMDS the finished SU-8 structure was used as die for the PUR structure. The RIE/HMDS treatment is not mandatory, but it

prolongs the lifetime of the die and eases release of the polyurethane. Approximately 25 g of Tecoflex EG-80A pellets were compressed in a hydraulic press at 120 °C and 50 kN (3- 4 MPa) to melt the pellets into a uniform air-bubble free disc with a thickness of 2 mm. The disc was folded and placed in the press between the SU-8 die and an aluminium foil covered steel plate. The press was kept at 120 °C and a pressure of 20 kN (approximately 2.0 MPa) was applied for 2 min. The patterned PUR sample was cooled and peeled off the SU-8 die, and washed with NDG soap (AIS, Rochester, UK) and water. Holes for the inlet and outlet were punched with a needle. Small metal tubes with a diameter of 0.5 mm were placed in the punched holes during bonding. The PUR channel system was placed on top of the PEDOT/PMMA pump structure and bonded at 90 °C for 1 h in a convection oven without any applied pressure. After bonding, the metal pins were replaced by polyethylene tubes with a diameter of 1 mm in the outlet/inlet holes. Due to the difference in diameter of the holes and tubes, the channels were effectively sealed. The homogeneity and quality of the bonding were investigated by reflected light confocal microscopy, which highlights large changes in refractive index like a polymer/air interface. No reflections from polymer/air interfaces outside the channel area were observed. This is in agreement with tight sealing of the bonded regions. The height resolution of the confocal microscope configuration employed is approximately 2 μm. At this resolution, no deformation or sagging of the channel structure itself could be observed. This is an important structural verification as the PUR structure might deform during release from the SU-8 die. This is not found to be a problem if the PUR is peeled off slowly. A schematic view and an image of the final device are presented in figures 3.3 to 3.5.

3.5 Testing

The channel system consists of a loop with a total length of 30 mm and with an entrance and exit channel (figure 3.5). The height of the channel is 25 μm and the width 200 μm. The height of the channel is important for the pumping characteristics of the pump as the fluid propulsion occurs at the wall. This means that increasing the channel height would increase the flow volume but decrease the generated pressure difference. As a certain pressure drop is expected in the non-pumping part of the channel, the height is a compromise between volume flow and pressure drop. A correlation between the pressure drop and velocity in the channel can be reached if the channel is treated as a slit, which is a fairly good approximation considering the large

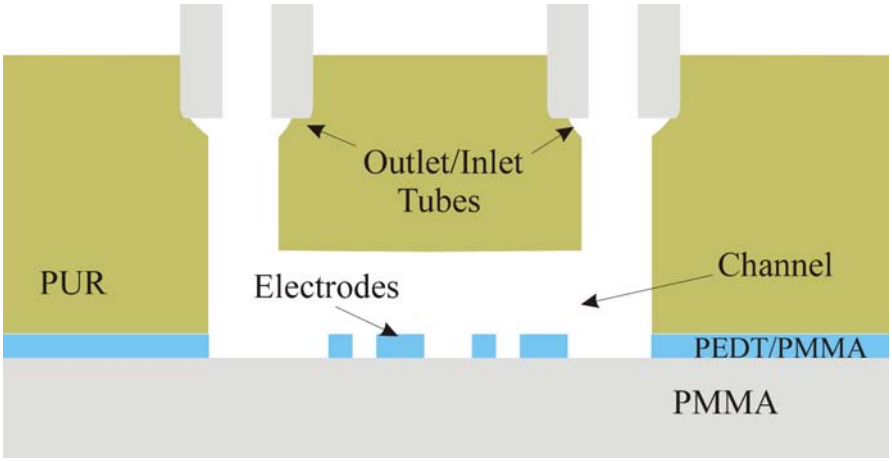

Figure 3.3: A schematic cross section of the pump structure perpendicular to the electrode lines.

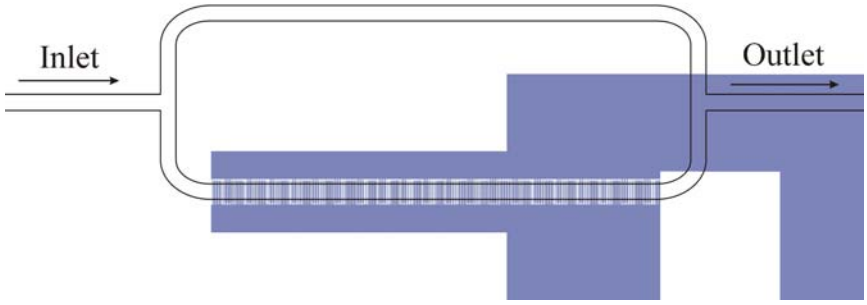

Figure 3.4: An image of the assembled pump seen from above. The inlet and outlet channels are used for purging the system, but are sealed when pumping. The fluid velocity is measured on the channel on the opposite site of the arrays.

width-to-height ratio. It is then known [23] that the pressure drop (Δp) can be found from equation (1):

$$\Delta p = 12 \mathbf{v}_{ave} \frac{\mu L}{h^2} \tag{3.1}$$

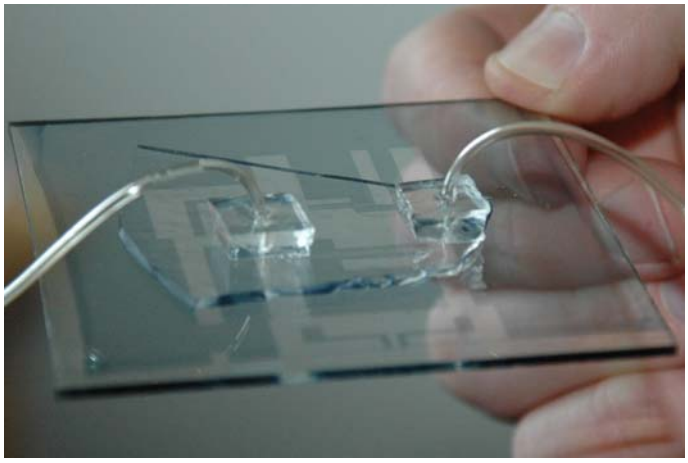

Figure 3.5: Photograph of the completed device.

v_{ave} is the average velocity, μ the viscosity of the fluid, L the channel length and h the channel height. The pressure drop over the contour length of the fabricated loop is approximately 4 $\times 10^4$ Pa/v_{ave} if water at room temperature is used as pumping fluid. This yields a pressure drop of 4 Pa at an average velocity of 100 $\mu m/s$, setting a lower limit on the required pressure generation of the pump. The corresponding volume flow at 100 μm/s is 0.03 μL/min, which could be increased by increasing the height of the channel. Each segment of the electrode array consists of a narrow electrode of width 4 μm, a gap of 4 μm, a wide electrode of width 20 μm and a large gap of 16 μm, giving a total segment width of 44 μm. This is repeated 200 times with a resulting array length of 8800 μm. The ratio between the electrodes and the gaps is based on numerical optimization of the geometry presented in a previous publication [24]. The length of the electrodes is 500 μm and the fluid channel of width 200 μm does therefore only cover a part of the electrodes. The pump was tested using a 10^{-4} M KCl solution with 2 ppm (by weight) microspheres in suspension. The channel system was flushed with pumping fluid between each test. Confocal laser scanning microscopy was employed for visualizing the motion of the fluorescent spheres. The particle motion was recorded in the loop lane without pumping electrodes to avoid confounding local motion patterns in the vicinity of the electrodes. The microscope system was capable of scanning an area of approximately 500 μm $\times$ 500 μm at 10 Hz, yielding a suitable image quality for particle tracking analysis. The spheres were tracked using a dedicated particle image velocimetry program

running under MatLab (Mathworks, Natick, Massachusetts, US). Particle velocities were measured at a range of driving potentials for three different frequencies: 10 kHz, 20 kHz and 40 kHz. The results of the analysis are presented in figure 3.6. Positive velocities are defined as fluid (particle) motion from the wide towards the narrow electrode within an electrode segment (opposite to the definition used in some other publications). The properties of the pump such as velocity and pumping direction correspond with those described in the literature [6, 9, 10]. The pump is capable of pumping in both directions, although at the highest velocities in the positive direction with the tested parameters. The pump requires a few seconds before reaching a constant velocity. This is most likely due to elasticity or bubbles in the channel system needing some time to adjust to the changed pressure/flow field. The limits of driving potential and frequency were also examined. The limits were similar to those observed by Studer et al [10] for a corresponding electrode system made from platinum/titanium on glass, except for our system having a slightly higher susceptibility to electrode damage for voltages above 5 V at frequencies below 10 kHz. This is also the reason why the point at 10 kHz and 5.6 Vrms is not included in figure 3.6. Two types of damage behaviour were observed. In the first type, the electrodes turn dark blue. This is a well-known phenomenon when PEDOT is reduced and the positive charge carriers are eliminated. This causes a decrease in conductivity and therefore in pumping efficiency, but the conductivity can be restored by re-oxidizing the electrodes. This phenomenon was observed for low frequencies and intermediate potentials. The second type of damage is the removal of the PEDOT electrode material. The removal is probably caused by the same phenomenon that damages the platinum electrodes used by other authors [10]. This behaviour was observed at high potentials and intermediate frequencies. Another problem that arises from the use of conductive polymers as electrode material is the release of ions from the PEDOT. The conductive polymer consists of a positive charged PEDOT backbone and negatively charged tosylate ions. The PEDOT is integrated into the PMMA, but it still cannot be excluded that other anions migrate into the PEDOT, or that the tosylate anions may migrate out of the polymer and contaminate the solution being pumped. Both damage to the electrodes and ion migration can be avoided if the electrodes are coated with an insulating encapsulating layer. This was explored using either 100 nm thick PMMA or 200 nm thick cyclic olefin copolymer (Topas 8007, Ticona, Frankfurt, Germany). The damage to the electrodes is reduced, but so is the pumping efficiency. None of the coated pumps were capable of pumping at a velocity higher than 40 $\mu m/s$. The pumps were however very stable and the PMMA covered pump were

capable of pumping at 20 $\mu m/s$ for 40 min at 5.6 Vrms and a frequency 15 kHz without a decrease in velocity and without visible electrode damage.

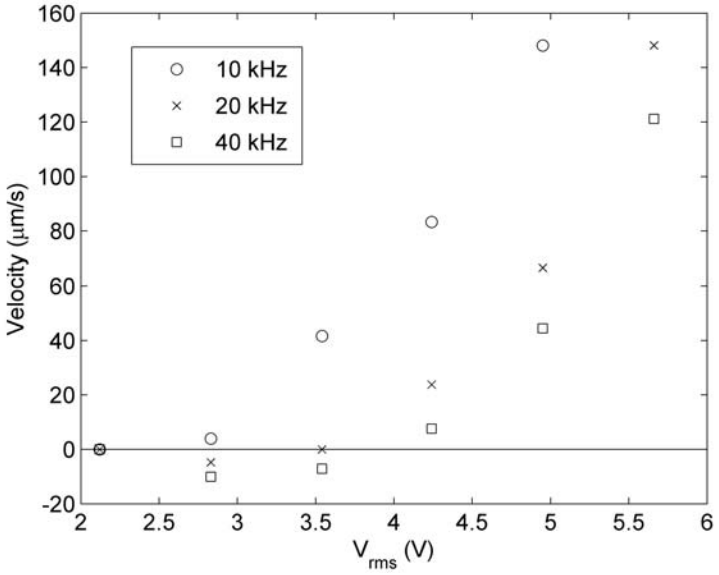

Figure 3.6: The velocity in the loop against the potential at three different frequencies. The reverse pumping is not significant at the measured frequencies and potential

3.6 Electrochemical and Electrical Analysis of the PEDOT/PMMA electrodes

As mentioned above, PEDOT is able to interact electrochemically with the electrolyte even though it is embedded in the PMMA matrix. To investigate the extent and kinetics of this reaction, a 6 mm (diameter) disc of PEDOT in PMMA was cycled electrochemically in a 1 M NaCl solution between its fully reduced state (-0.95 V versus a silver/silver chloride reference electrode) and an oxidized state at 0.5 V versus Ag/AgCl. The cyclic voltammograms (CVs) are shown in figure 3.7 (left). In this graph the current is normalized as capacitance by division with the sweep rate to facilitate comparison of CVs of widely different sweep rates. It is seen that this electrode has a capacitance above 5 mF cm^{-2} over a large voltage range, which is approximately two orders of magnitude larger than of a neat platinum electrode.

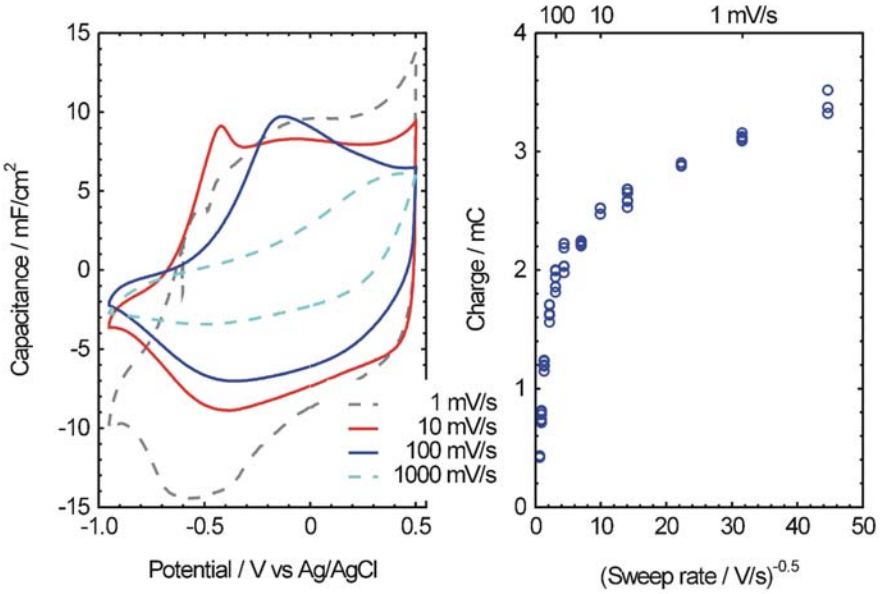

Figure 3.7: Left: cyclic voltammograms of a PEDOT/PMMA electrode in 1 M NaCl. The currents are normalized as capacitances to facilitate the direct comparison of CVs at widely differing sweep rates. At low sweep rates reduction of traces of oxygen in the electrolyte offsets the voltammogram at negative electrode potentials. Right: the charge involved in one electrochemical cycle at different sweep rates (between 0.5 mV s^{-1} and 5 V s^{-1}).

This shows that the PEDOT/PMMA electrode is able to pass a relatively large amount of charge into the electrolyte without excessive polarization. A rough estimate of the diffusion time constant in the PEDOT layer can be obtained by plotting the charge involved in a full cycle versus the sweep rate to the power of -$\frac{1}{2}$ [25]. In this diagram, the transition from semi-infinite diffusion to diffusion in a bounded region will show up as a transition from a straight line through the origin to a range where the charge becomes independent on the sweep rate. As seen in figure 3.7 (right), a transition can be observed, but even at the very lowest sweep rates tested, the accumulated charge increases slowly. Although most of the charge in the PEDOT/PMMA composite can be accessed relatively fast (with a corresponding diffusion time constant between 10 and 20 s), a small part of the charge is only available at much longer time scales. This is a general phenomenon for conjugated

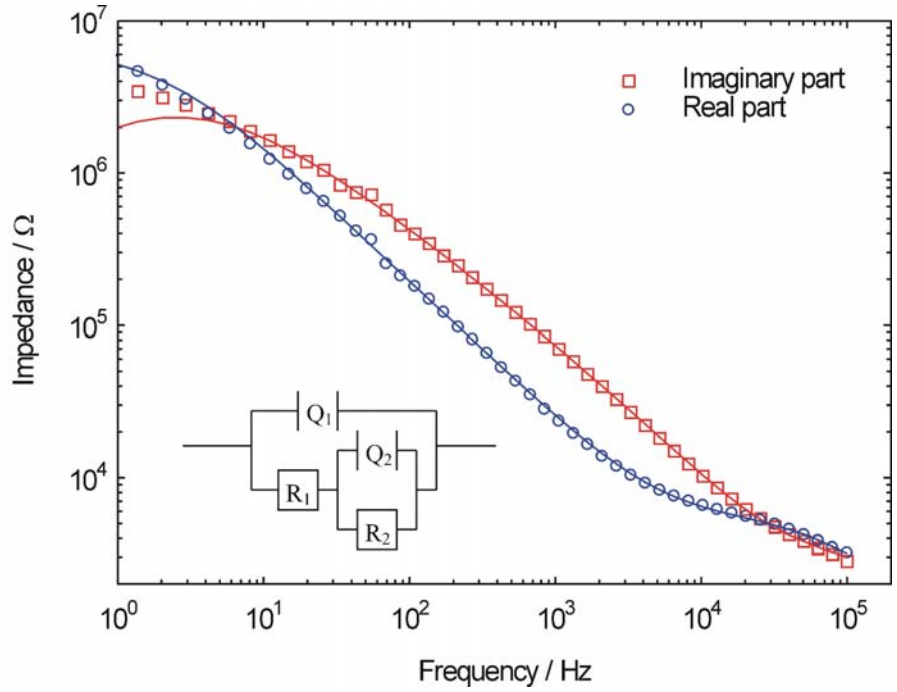

Figure 3.8: Impedance between the electrode arrays in a liquid filled pumping cell. The open symbols indicate experimental values and the filled lines are calculated values based on the equivalent circuit shown in the inset. The parameters used in the equivalent circuit are given in table 1.

polymers, and is probably associated with slow polymer chain relaxations.

Initially the current through the pump was measured in a situation when the output velocity of the pump was 150 $\mu m/s$. A 22 kΩ resistor was placed in series with the pump, and an ac voltage of 7 Vrms (20 kHz) was applied over the pump and resistor. The voltage drop over the resistor was measured to be 1.4 Vrms. Based on this measurement the power consumption of the pump could be calculated to be 0.36 mW. In order to investigate where power is dissipated in the pump, a small-signal ac impedance spectrum of the pump filled with fluid was measured using an IM6 ac potentiostat (Zahner, Kronach, Germany). The spectrum was measured from 0.1 Hz to 100 kHz with zero bias and 50 mV signal amplitude. The measured impedance was fitted to the equivalent circuit, as shown in the inset of figure 3.8, using a nonlinear least squares fitting program [26]. The fitted parameters are given

in table 1, and figure 3.6 shows the real and imaginary parts of the measured impedance as a function of frequency compared to the impedance of the equivalent circuit. It is seen that the simple equivalent circuit reproduces the measured data well down to 1 Hz. At lower frequencies, transport into the electrode (see above) and deviations from simple planar electrode geometry would require a more elaborate model to give a full description of the electric properties of the cell. The parameters of the equivalent circuit of figure 3.6 are assigned to pump properties in the following way: Q1 is the parallel geometric capacitance across the cell. The series resistance R1 is assigned to the ohmic resistance in PEDOT leads and electrolyte. The interface between electrolyte (pumping fluid) and electrodes (PEDOT) is modelled by a parallel combination of a capacitor Q2 (accounting for charge accumulation at the interface) and a resistor R2 (inversely proportional to the rate of the electrode reactions consuming charge at the interface). The capacitances are modelled by a constant phase elements $Q(ZQ = (j\omega Q)^{-n})$, as is usually done for electrochemical systems in order to model systems with non-ideal surfaces [27]. At the operating frequency (10 kHz) the real part of the impedance is totally dominated by R1, meaning that nearly all the power is dissipated in electrolyte and electrodes The characteristic frequency of the C2/R2 parallel combination is just below 20 Hz and only when this frequency is approached, an appreciable amount of the charge passed through the cell is involved in electrochemical reactions at the electrodes.

3.7 Conclusion

The construction of an all-polymer micropump was demonstrated using a blend of the conducting polymer PEDOT with PMMA for the electrical parts and a flexible thermoplastic polyurethane for the channel structure. The PEDOT/PMMA blend show good adhesion and wear resistance, and a procedure for micro patterning was developed, making this blend well suited for microfluidic applications. The properties of the all-polymer pump described here compare well with the properties of pumps produced with noble metals on glass. An analysis of the polymer electrode structure showed that this type of electrodes at low frequencies are able to deliver much larger charges than noble metal electrodes without decomposing the electrolyte. The kinetics of the charge accumulation in the polymer electrodes is, however, too slow to be in effect at the relatively high operating frequency of an electroosmotic pump, and damage to the electrodes was observed when the pump was operated at extreme conditions. It was shown that damage to

the electrodes can be avoided by applying a insulating encapsulating layer on top of the electrodes, although this reduces the pumping velocity. The ability to construct all-polymer microfluidic devices opens up to a variety of opportunities of inexpensive polymer based pumps and actuators for, e.g., disposable medical devices.

3.8 References

[1] Laser D J, Santiago J G, *J. Micromech. & Microeng.*, **2004**, 14, R35-R64

[2] Nguyen N T, Huang X, Chuan T K, *Journal of Fluid Engineering*, **2002**, 124, 382-392

[3] Peter Woias, *Sensors and Actuators B*, **2005**, 105, 28-38

[4] Squires T M, Quake S R, *Reviews of Modern Physics*, **2005**, 77, 977-1026

[5] Ajdari A, *Physical Review E*, **2000**, 61, 45

[6] Brown A B D, Smith C G, Rennie A R, *Physical Review E*, **2000**, 63, 16305

[7] Green N G, Ramos A, González A, Morgan H, Castellanos A, *Physical Review E*, **2000**, 61, 4011

[8] Green N G, Ramos A, González A, Morgan H, Castellanos A, *Physical Review E*, **2002**, 66, 26305

[9] Mpholo M, Smith C G and A. B. D. Brown A B D, *Sensors and actuators B*, **2003**, 93, 262

[10] Studer V, Pépin A, Chen T, Ajdari A, *The Analyst*, **2004**, 129, 944

[11] Green N G, Ramos A, González A, Morgan H, Castellanos A, *Physical Review E*, **2000**, 61, 4019

[12] Mortensen N A, Belmon L, Olesen L H. And Bruus H, *Physical Review E*, **2005**, 71, 56306

[13] Winther-Jensen B, West K, *Reactive & Functional Polymers*, **2006**, 66, 479-483

[14] Hansen T S, West K, Hassager O, Larsen N B, *Synthetic Metals*, **2006**, 156, 1203-1207

[15] Stoyanov I, Tewes M, Koch M, Löhndorf M, *Microelectronic Engineering*, **2006**, 83, 1681-1683

[16] Mcdonald J C et al, *Electrophoresis*, **2000**, 21, 27-40

[17] Poomalai P, Siddaramaiah, *Journal of Macromolecular Science, part B: Pure and applied chemistry*, **2005**, 10, 1399-1407

[18] Kumara H, Siddaramaiah, *Polymer*, **2005**, 46, 7140-7155

[19] Desal S, Thakore IM, Brennan A, Devi S, *J. Applied Polymer Science* **2002**, 83, 1576-1585

[20] Bhattacharya S, Datta A, Berg J M, Gangopadhyay S, *Journal of Microelectromechanical systems*, **2005**, 14, 590-597

[21] Morra M et al, *Journal of colloid and Interface Science*, **1990**, 137, 11-24

[22] Hillborg H, Gedde UV, *Polymer*, **1998**, 39, 1991-1998

[23] "Transport Phenomena", 2nd edition, R. Byron, W. E. Stewart and E. N. Lightfoot, *Wiley*, *2001*

[24] Master Thesis by Thomas Steen Hansen
(http://www.student.dtu.dk/ s991799/reporthoved)

[25] West K, Jacobsen T, Zachau-Christiansen B, Atlung S, *Electrochim. Acta*, **1983**, 28, 97

[26] B. A. Boukamp B A, *Solid State Ionics*, **1986**, 20, 31.

[27] "Impedance Spectroscopy: Theory, Experiment, and Applications ", E. Barsoukov and JR Macdonald, eds., *John Wiley*, **2005**.

Chapter 4

Highly stretchable and conductive polymer material made from poly(3,4-ethylenedioxythiophene) and polyurethane elastomers

4.1 Introduction

The stability and high conductivity of poly(3,4-ethylenedioxythiophene):p-tosylate (PEDOT) have made it an interesting material for polymer electronics and devices [1]. PEDOT does, however, have poor mechanical properties compared to nonconductive polymers [2]. Herein we present a method for making mechanically stable PEDOT, which is highly stretchable, elastic, scratch resistant, adhesive, and easy to apply to a substrate. Several applications of such a material can be suggested: electrode material in electrostatic actuators, impregnation material for making conductive fabric, and as ink for printing circuits on flexible substrates or making electronic polymer devices. There has been substantial research in making flexible conducting fabrics by impregnating fibers with conductive polymers [3-5] and in making devices from polyurethane foam impregnated with conductive polymers [6-8]. Drawbacks of both methods are low conductivity, usually below 1

[3]This chapter is based on an article published in *Advanced Functional Materials* 17, (**2007**) , 3069-3073

S/cm, and slow fabrication as the monomer and the oxidant have to diffuse into the substrate in subsequent processes typically lasting hours. Conductive polyaniline fibers can be stretched by 500% [9]. Conductive polypyrrole films immersed in suitable organic solvents may be stretched at elevated temperatures with a concomitant increase in conductivity [10-12]. Neither the stretched polyaniline nor polypyrrole exhibited elasticity, and facile ways of applying the materials to substrates were not reported. We present a fast and easy procedure of general applicability: a polymer blend solution is applied to a substrate, the coated substrate is heated to 65°C for a few minutes, and then rinsed by water. The blend solution can therefore be used for fast printing, stamping, or impregnating stretchable conductive circuits. The material used is a blend of a polyurethane elastomer (PUR) and PEDOT. It exhibits a high conductivity of 100 S/cm, even if stretched by more than 100%. Furthermore, it shows good adhesion to many types of materials, such as metal, glass, polymers, and fabric, both in dry and wet conditions.

4.2 Experimental

The EDOT monomer and oxidation agent (Baytron C; iron tosylate solution) were purchased from Bayer (Leverkusen, Germany). The polyurethane, Tecoflex EG-80A, is an aliphatic block copolymer with a hard segment consisting of polymerized 4,4'-methylenediphenyl diisocyanate and 1,4-butanediol, and a soft segment consisting of the macrodiol poly(tetramethylene oxide) [22, 23]. Tecoflex EG-80A were purchased as granulate for injection molding from Noveon (Cleveland, OH). The PEDOT/PUR blend was polymerized from a mixture of 2 ml butanol, 6.5 ml Baytron C, 0.22 ml EDOT, and varying amounts of anisole and PUR dissolved in THF. Three blend types containing 33 wt%, 40 wt%, and 50 wt% PEDOT, respectively, were made by adding 8.46 ml anisole and 8.46 ml of 10 wt% PUR/THF (for 33% PEDOT content), or by adding 6.26 ml anisole and 6.26 ml of 10 wt% PUR/THF (for 40% PEDOT content), or by adding 4.17 ml anisole and 4.17 ml of 10 wt% PUR/THF (for 50% PEDOT content). The solutions showed no signs of aging after a month of storage at 5°C, but they did become slightly green, an early sign of polymerization, when stored at room temperature (RT). The 40% PEDOT and 33% PEDOT samples became rough and inhomogeneous without added anisole, probably due to THF evaporating faster than butanol and thereby leading to precipitation of the PUR. Silicon wafers were used as planar molding substrates. Each solution was spin coated onto a wafer at 1000 rpm for 20 seconds, and placed on a hotplate

at 65°C for 5 minutes to evaporate the solvents and initiate the polymerization. The sample was then washed for 2 seconds in boiling water followed by thoroughly rinsing in water at RT. The boiling water was required to make the 33% and 40% PEDOT films homogenous. Microscopic crystals in the films were observed when only water at RT was used - probably caused by iron tosylate or iron tosylate hydrates in the polyurethane structure. All three film types were washed in boiling water to use a consistent fabrication method. This fabrication method yields films with a thickness of 500 - 700 nm. A 0.5 mm thick PUR film was placed on top of the film and heated to 70°C for 2 minutes. During the heat treatment the PEDOT/PUR layer and the PUR film are bonded together and after cooling they can carefully be peeled off the wafer. The resistance in the PEDOT/PUR blend during strain was monitored using a four-point measurement: PEDOT/PUR on PUR film was cut into a 60 mm long and 10 mm wide rectangle. Four copper wires were placed with distances of 10 mm on the film. The 2 outer copper wires serve as current electrodes and the 2 inner wires as potential electrodes. A sandwich holding the wires in place was formed by bonding a second 0.5 mm thick PEDOT/PUR rectangle of equal size on top (figure 4.1). The two inner electrodes spaced by 10 mm and the film width of 10 mm delineate a square area of measurement. The initial output is therefore the resistance per square. Furthermore, only the deformation between the potential electrodes will influence the resistance measurement. All elongations were conducted at a strain rate of 100 μm/s corresponding to approximately 0.5% strain per second. The resistance was measured using a Keithley 2400 SourceMeter (Keithley, Cleveland, US) with a constant current of 100 μA during straining by a translation stage (Physik Instrumente, Model M-410-DG). Differential Scanning Calorimetry analysis was conducted using a DSC Q1000 system from TA instruments (New Castle, US)

4.3 Results and Discussion

Three kinds of samples with 33 wt%, 40 wt%, and 50 wt%, respectively, of PEDOT blended with PUR were prepared as 500-700 nm thick film and attached to a 0.5 mm thick film of cast PUR, as described in the experimental section. The resulting homogeneous films were examined optically and showed no signs of phase separation by light microscopy at 500X magnification. The threshold concentration for conductive polymers in blends to permit substantial conductance is often given as 16 vol% although lower values have been reported [13,14]. The threshold of 16 vol% corresponds to

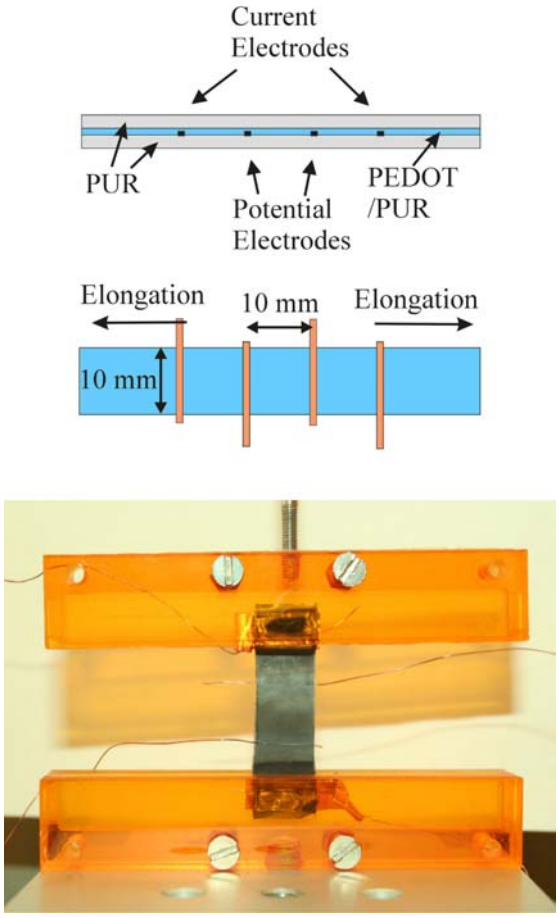

Figure 4.1: Schematic of the PEDOT/PUR / PEDOT film sandwich with crossing copper wires for establishing a four-point resistance measurement shown in side view (top) and top view (middle). A picture of the actual stretching setup is shown at the bottom.

23 wt% PEDOT in PUR. This limit was approached by preparing a 25 wt% PEDOT in PUR sample, but it was not possible to produce a smooth and homogeneous film at this lower concentration. The inhomogeneity of the 25 wt% PEDOT originates from the washing step. The necessary washing out of excess Fe(II)Tos becomes more difficult as the fraction of PUR in the blend increases, Water at room temperature is sufficient at 50 wt% PEDOT, while boiling water is required for 40 wt% and 33 wt% PEDOT samples (see ex-

perimental section). At 25 wt% PEDOT it is no longer possible to wash out the Fe(II)Tos without formation of crystals that makes the film inhomogeneous. The resistance in the elongated PEDOT/PUR blends was monitored using a four-point measurement on 10 mm wide strips of PEDOT/PUR on PUR film by sandwiching four copper wires spaced by 10 mm between the PEDOT/PUR film and a second 0.5 mm PUR film (figure 4.1). The conductivity of the PEDOT/PUR samples was calculated using Equation 4.1 (constant volume is assumed):

$$\sigma = \frac{\alpha^2 L_0}{A_0 R} \qquad \left(\alpha = \frac{L}{L_0}\right) \tag{4.1}$$

where σ is the conductivity, R the resistance, L_0 the length before elongation, L the length during elongation, and A_0 the cross sectional area of the PEDOT/PUR layer before elongation. The films were strained by 50% and relaxed to their unstrained configuration 10 times while monitoring changes in the film resistance (figure 4.2). The films show an irreversible increase in resistance during the initial elongation, but during the following cycles the development in resistance is remarkably stable and reversible. The increase in resistance during the initial elongation is not as large as would be expected for a material exhibiting isotropic conduction, e.g. a metal. The conductivity relative to the unstrained sample is therefore also shown in figure 4.2. Equation 1 shows that 50% strain should increase the initial resistance, R0, by a factor of 2.25 assuming constant conductivity, but the observed increase is only 1.6-1.9 times R0.

Another set of films were cyclically strained by 200 percent and relaxed to their unstrained state 4 times. The conductivity development during the first two cycles is presented in figure 4.3. All three samples showed an increase in conductivity during the initial strain. Before stretching, the samples show conductivity correlating to their PEDOT content, which is what could be expected. At 100% strain the conductivity of the 50% PEDOT sample decreases rapidly and ends up having the lowest conductivity. Although the 40% PEDOT sample has the highest conductivity at all elongations beyond initial 50% strain, the 33% PEDOT sample has approximately the same conductivity per PEDOT amount. Upon straining by 200 percent multiple times (only the first two cycles are shown in figure 4.3) the samples show a stable development in resistance, as was also observed for repeated straining by 50 percent (figure 4.2). The observed increase in conductivity correlates with results observed for spun micro fibers of polyaniline [9], when elongated

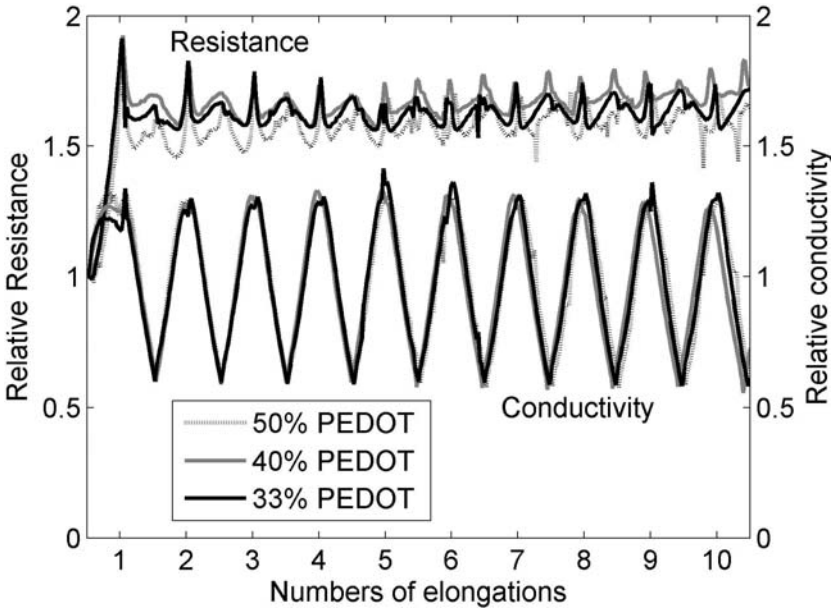

Figure 4.2: The relative resistance and conductivity of the 50 % PEDOT, 40 % PEDOT, and 33% PEDOT samples, respectively, cyclically elongated by 50% and relaxed to their unstretched state 10 times.

by 500%. Both in the case of the polyaniline fibers and the current material the conductivity is measured parallel to the elongation.

Several observations indicate that the PEDOT does not simply exist as grains in the polyurethane matrix. This is strongly suggested by the observed increase in conductivity upon straining. Previous work on carbon black particles in a silicon rubber matrix show a decrease in conductivity when the loaded matrix is strained [15,16]. Pramanik et al. [17] examined the resistivity of short carbon fibers ($\approx$ 7 mm long and $\approx$ 10 μm wide) in nitrile-rubber and found a significant decrease in conductivity at a strain up to 50%. If the PEDOT exists as fibers in a polyurethane matrix it would be expected that they exhibited a similar behavior, which is not the case. Earlier research has shown that PEDOT can be diluted with a number of non-conductive polymers and fillers, [2, 18, 19] without a change in the conductivity of the PEDOT. The conductivity of the composite/blend was at most reduced by the degree of filling and sometimes even less. A blend of 1/3 PEDOT and 2/3 PMMA shows both excellent mechanical and electrical

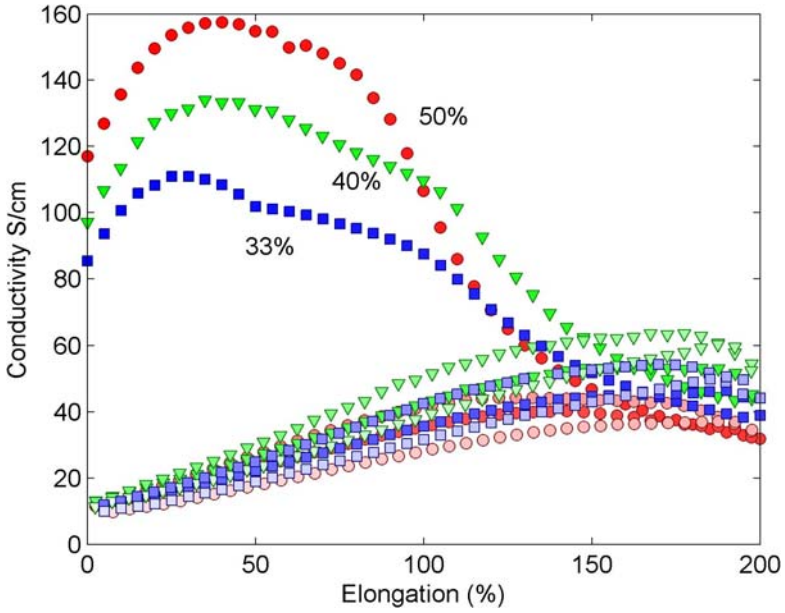

Figure 4.3: Conductivity vs. elongation of the 50 % PEDOT (circles), 40 % PEDOT (triangles) and 33 % PEDOT (squares) during repeated straining by 200%. The filling of the data points goes from dark to bright as the experiment progresses through two full cycles of elongation and relaxation.

properties [2]. This may indicate that the PEDOT exists as a network of chemically or physically crosslinked polymer chains where space can be made for filling on the molecular scale without affecting the conducting mechanism. This is in agreement with experimental results obtained for other kinds of conductive polymer blends [13, 14].

Adlayers of the 40% and 50% PEDOT/PUR blends applied to a piece of PUR (without being sandwiched) exhibited optical changes after 50% strain and relaxation with the surface layers becoming slightly opaque. This was most explicit for the 50% PEDOT samples and to some extent the 40% PEDOT samples, but not observed for the 33% PEDOT samples. Optical microscopy on the surfaces before and after elongation revealed that wrinkles had appeared perpendicular to the direction of strain. The surface structure was examined in more detail for the 33% and the 50% PEDOT/PUR samples using Atomic Force Microscopy (AFM, figure 4.4). AFM confirmed that only

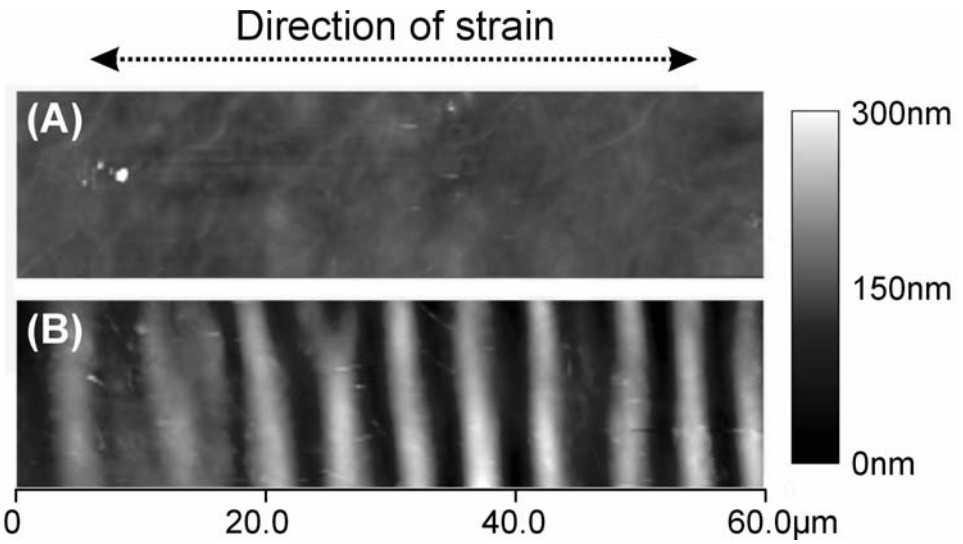

Figure 4.4: Atomic Force Microscopy performed on (A) 33% and (B) 50% PEDOT/PUR adlayers after 50% strain and relaxation to their unstrained state. The 50% PEDOT/PUR film has wrinkles oriented perpendicular to the direction of strain which is not observed on the 33% PEDOT/PUR film.

the high PEDOT content blend exhibits structural changes. It is expected that the blends lose elasticity with increasing PEDOT content. In contrast to the PUR substrate, the blend is irreversibly deformed during stretching, causing wrinkling of the surface when the strain is reduced. Figure 4.2 (B) shows that the height of the wrinkles (around 0.3 μm peak-to-valley) is small compared to their width (approximately 6 μm), indicating that the irreversible deformation is probably not a dominant factor in the conductivity changes. The AFM analysis did not reveal any signs of multiple phases. This was confirmed by Scanning Electron Microscopy (SEM) analysis of 50% and 33% PEDOT films deposited on silicon as a highly planar support. Figure 4.5 shows scanning electron micrographs as top and cross-sectional views, respectively, of the 50% PEDOT/PUR film most likely to exhibit distinct phases. No discernable ultrastructure indicative of phase separation is found in either view. Differential Scanning Calorimetry analysis was performed on samples of PUR, PEDOT, 33% PEDOT, and 50% PEDOT to examine

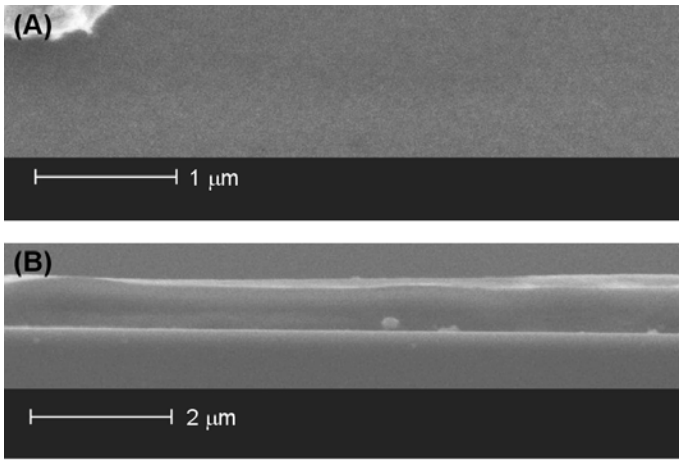

Figure 4.5: Scanning Electron Microscopy of a 50% PEDOT/PUR film on a silicon wafer as support. (A) Top view; dust particle in the top left corner to show level of contrast. (B) Cross section with the film at the center and the silicon wafer at the bottom

the crystallinity of the species (data not shown). The glass transition temperature, Tg, for the hard segment of the polyurethane was found to be approximately 80°C, in accordance with values reported in literature [20]. The same Tg was observed for the 33% PEDOT sample, but no Tg could be detected for the 50% PEDOT sample. This indicates loss in the amount of the crystalline domains acting as physical cross links in the elastomer, explaining the difference in mechanical properties of the 50% PEDOT sample compared to the 33% PEDOT sample. An exothermic phase transmission for pure PEDOT is observed around 125°C. This phase transition was shifted upwards to 135°C for the PEDOT/PUR blends, again indicating interactions at molecular scale between the PEDOT and PUR chains. It is known that blends of PUR and the conductive polymer polyaniline exhibits intermolecular hydrogen bonding between the two polymers [14]. Similar behavior could be expected between PUR and PEDOT, based on the known strong pH dependence of the conductivity of PEDOT indicative of proton excepting properties [21]. The changes in thermal and mechanical properties of the blend indicate strong molecular interactions between PEDOT and PUR, and supports our hypothesis that PEDOT does not exist as a separate phase in the PUR matrix.

It is known from literature that PEDOT experiences a decrease in con-

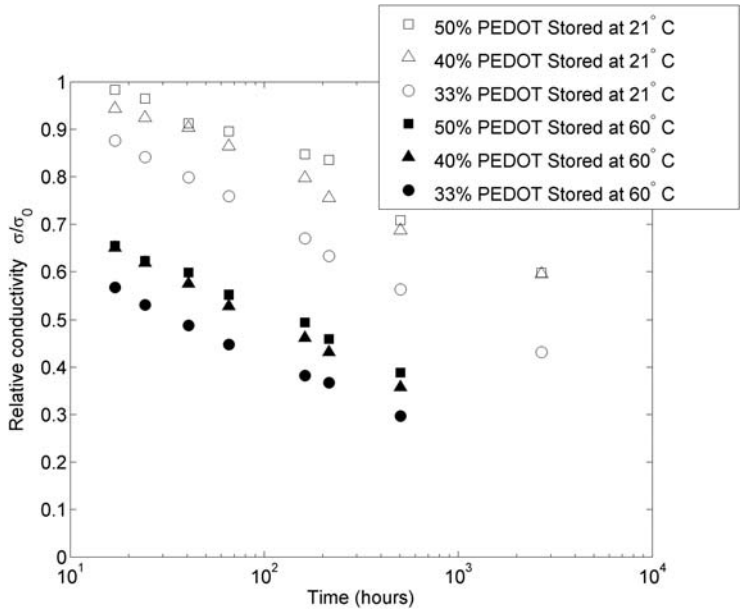

Figure 4.6: The temporal development of the conductivity (relative to time zero for the given material) for the PEDOT/PUR blends stored at 21°C and 60°C, both at a relative humidity of 50%@21°C.

ductivity to approximately 1/3 of its original conductivity due to aging [21]. This was examined for the current material by storing samples at 21°C and 60°C, see figure 4.6. The data points are normalized to the initial conductivity, which is not included due to the logarithmic x-axis. The conductivity was measured at room-temperature for all the samples including the 60°C-samples. The latter were removed from the oven, left to cool before measuring the conductivity, and immediately placed in the oven again. The samples stored at 60°C showed a significant decrease in conductivity during the first 17 hours between the first and second measurement. After the initial decrease, all the samples followed a logarithmic decay in conductivity. Interpolation of the decay showed that the samples would remain fairly conductive for at least $2\text{-}3 \cdot 10^4$ hours (2-3 years) when stored at room temperature if the conductivity continues to follow the logarithmic decay. The aged samples were stretched and the measured conductivity showed the same pattern as the new samples although starting at a lower conductivity. It is known from literature that PEDOT can regain its conductivity if the pH

is lowered [21]. We tested for a similar behavior in the PEDOT blends: A sample aged for 21 days at 60°C and with a remaining conductivity of 41 S/cm was placed in a closed chamber together with an open vial of diluted hydrochloric acid for 5 hours. Afterwards the sample showed a conductivity of 74 S/cm corresponding to 68% of its original conductivity. This indicates that the long-time conductivity can be increased by additives that adjust the pH of the material.

4.4 Conclusions

A highly stretchable conductive polymer blend material was fabricated from commercially available compounds using a facile method that can easily be utilized to make conductive layers on different types of substrates. The material showed an increase in conductivity when initially strained by up to 50% followed by an irreversible decrease in conductivity upon further elongation. The conductivity changes during repeated elongation were, however, reversible showing a fairly good conductivity of 10-50 S/cm at 200% strain. Optical, mechanical and thermal analyses of the blends suggest that the two polymers exist as a single phase. The mechanical properties of the blends resembles those of the polyurethane elastomer matrix with some changes occurring at the highest PEDOT concentrations. Aging tests of the blend materials indicated that these new materials probably will retain substantial conductivity for at least a few years, and that the decrease in conductivity is correlated to pH changes in the material.

4.5 References

[1] H. Sirringhaus, T. Kawase, R.H. Friend, T. Shimoda, M. Inbasekaran, W. Wu, E.P. Woo, *Science* **2000**, 290, 2123.

[2] T. S. Hansen, K. West, O. Hassager, N. B. Larsen, *Synth. Met.* **2006**, 156, 1203.

[3] K. Wha Oh, H. J. Park, S. H. Kim, *J. Appl. Polym. Sci.* **2003**, 88, 1225.

[4] C. L. Heisey, J. P. Wightman, E. H. Pittman, H. H. Kuhn, *Sens. Actuators B* **2005**, 109, 329.

[5] K. W. Oh, K. H. Hong, S. H. Kim, *J. Appl. Polym. Sci.* **1999**, 74, 2094-

2101.

[6] S. L. Shenoy, D. Cohen, C. Erkey, R. A. Weiss, *Ind. Eng. Chem. Res.* **2002**, 41, 1484.

[7] F. F. He, M. Omoto, T. Yamamoto, H. Kise, *J. Appl. Polym. Sci.* **1995**, 55, 283.

[8] Y. P. Fu, R. A. Weiss, P. P. Gan, M. D. Bessette, *Polym. Eng. Sci.* **1998**, 38, 857.

[9] S. J. Pomfret, P. N. Adams, N. P. Comfort, A. P. Monkman, *Polymer* **2000**, 41, 2265

[10] M. Yamaura, T. Hagiwara, M. Hirasaka, T. Demura, K. Iwata, *Synth. Met.* **1989**, 28, 157.

[11] K. Sato, M. Yamaura, T. Hagiwara, K. Murata, K. Tokumoto, *Synth. Met.* **1991**, 40, 35.

[12] J. H. Lee, I. J. Cheng, *Synth. Met.* **1993**, 53, 245.

[13] M. C. De Jesus, Y. Fu, R. A. Weiss, *Polym. Eng. Sci. 1997*, 37, 1936.

[14] J. Njuguna, K. Peilichowski, *J. Mater. Sci.* **2004**, 39, 4081.

[15] J. Kost, M. Narkis, A. Foux, *Polym. Eng. Sci.* **1983**, 23, 567.

[16] J. Kost, M. Narkis, A. Foux, *J. Appl. Polym. Sci.* **1984**, 29, 3937.

[17] P. K. Pramanik, D. Khastagir, T. N. Saha, *J. Mater. Sci.* **1993**, 23, 3539.

[18] B. Winther-Jensen, J. Chen, K. West, G. Wallace, *Polymer* **2005**, 46, 4664.

[19] G. V. A. Aben, M. J. M. Somers, P. H. C. Hanssen, L. M. Schrooten, *SID Symposium Digest of Technical Papers* **1998**, 29, 528.

[20] M. Yang, Z. Zhang, C. Hahn, G. Laroche, M. W. King, R. Guidoin, *J. Biomed. Mater. Res.* **1999**, 48, 13.

[21] B. Winther-Jensen, K. West, *React. Funct. Polym.* **2006**, 66, 479.

[22] P. A. Gunatillake, D. J. Martin, G. F. Meijs, S. J. McCarthy, R. Adhikari, *Aust. J. Chem.* **2003**, 56, 545.

[23] S. J. McCarthy, G. F. Meijs, N Mitchell, P. A. Gunatillake, G. Heath, A. Brandwood, K. Shindhelm, *Biomaterials* **1997**, 18, 1387.

Chapter 5

Direct fast patterning of conductive polymers using agarose stamping

5.1 Introduction

Conductive polymers (CP) may form the basis of new generations of active devices. Main advantages include low cost, ease of processing, and direct integration with many other polymer based functional materials. Organic thin-film transistors are of particular recent interest as enabling technology for (flexible) displays and for disposable electronics, to be employed in, e.g. disposable sensor systems. The successful realization of this potential requires methodologies for fast, inexpensive, large area, micro-patterning of CP layers [1]. Access to patterning at the micrometer length scale is important for integration of multiple active components, and to achieve acceptably fast switching in transistors based on CP of comparatively low conductivity [2]. This paper describes a new and easy patterning methodology based on spatially selective transfer of a chemical agent from a gel stamp onto a layer of CP, leading to spatially selective loss of electrical conductivity. We believe this approach is the most facile in patterning large areas of CP layers of planar or non-planar geometries at detail levels below 100s of micrometers

Patterning of conductive polymers can broadly be divided into additive and subtractive approaches [3]. Additive patterning spatially confines the deposition of a solution containing the polymer or monomer leading to for-

[4]This chapter is based on an article published in *Advanced Materials* 19, (**2007**), 3261-3265

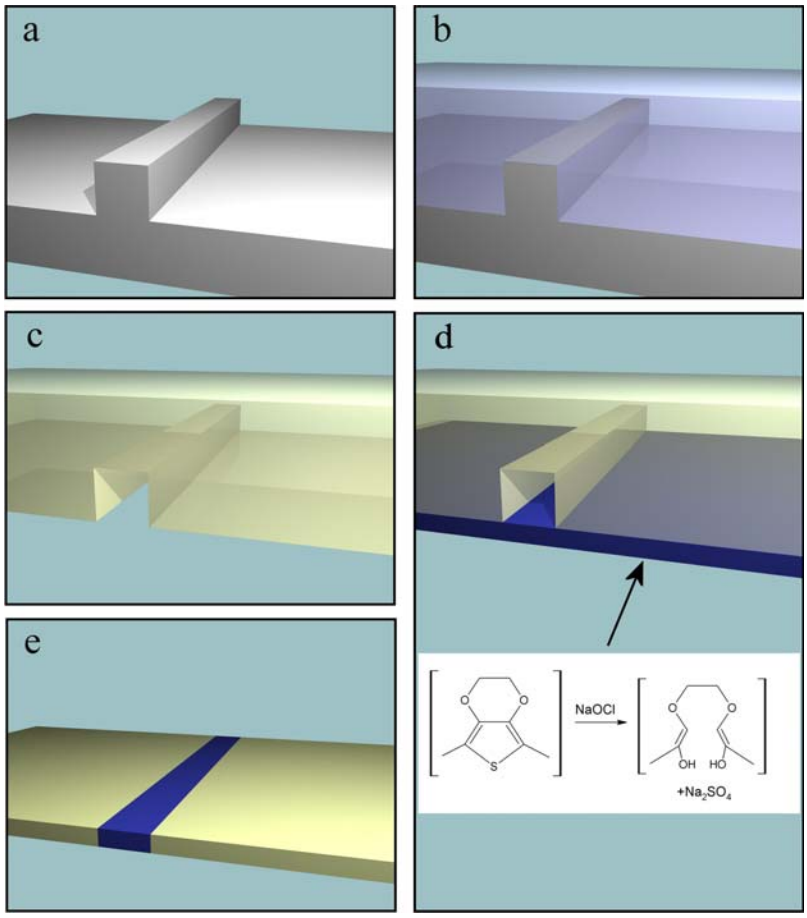

Figure 5.1: Patterning of the conductive polymer PEDOT: (a) A master surface-relief structure made of patterned SU-8 on silicon is produced using classical lithographic methods. (b) Agarose is molded against the photoresist relief structure, and (c) the resulting stamp is cooled, peeled off the master and impregnated with hypochlorite. (d) The stamp is placed on the conductive polymer where the hypochlorite reacts with the PEDOT in areas of contact. (e) The agarose stamp is removed and the patterned PEDOT is washed by water.

mation of a patterned conductive polymer. The most extensively studied additive patterning technique is ink-jet printing of either pre-polymerized CP, the oxidant, or a mixture of the monomer and the oxidant [4-6]. Ink-jet

printing has an inherent spatial resolution of approximately 25 μm unless chemical or structural prepatterning of the target surface is undertaken [7]. Laser surface modification of PET followed by the application of PEDOT was shown to yield minimum features sizes of 100 μm [8]. Screen printing has also been demonstrated but at even poorer resolution [9]. Spatially defined thermal dry transfer of CP has been accomplished over large areas for 20 μm wide lines [10]. Soft lithography, based on surface structured PDMS to guide reagents to specific surface areas, has been successfully used for the moulding of CP at micrometer length scales [11]. This approach is, however, not easily employed for the micropatterning of large areas that will require long filling times through the capillary structures. Subtractive patterning employs an initially uniform film of CP subjected to a mechanical or chemical treatment to remove the CP, or substantial reduce its electrical conductivity, in specific areas. Mechanical methodologies include lithography lift-off,[12] microcutting,[13] and laser ablation [14]. Subtractive chemical patterning has been demonstrated by ink-jet printing of deactivation agents,[15-16] and etching/over-oxidation after lithographic patterning with photoresist [3,17]. Ink-jet printing has the same resolution limits as in additive patterning, while the use of lithography requires expensive clean room processing. Laser processing and microcutting may provide the required resolution. However, laser processing is comparatively slow and expensive for processing of large areas at high resolution, while microcutting may be limited to certain combinations of CP layer thickness and type of polymer support. Our approach to fast patterning with micrometer scale resolution of CP layers on polymers is based on the spatially confined delivery of a deactivating agent from the surface of a gel stamp. The gel surface has initially been patterned in bas-relief to allow intimate contact with the CP layer in selected areas only. Smoukov et al. recently reported on a similar approach for the 2D [18] and 3D [19] etching of solids using agarose as their stamp material. Agarose has good mechanical stability combined with fast internal diffusion caused by a high water content of 85%-98%. It is therefore well suited as material for stamping of aqueous reagents. Aqueous sodium hypochlorite is well known to over-oxidize and degrade the conductive polymer poly(3,4-ethylenedioxythiophene) (PEDOT), leading to irreversible loss of electrical conductivity [15,20]. Agfa, a commercial manufacturer of PEDOT, reported that exposure of PEDOT to aqueous hypochlorite initially leads to deactivation followed by physical etching of the polymer [20]. Deactivation alone was found to be sufficient to decrease the conductivity by a factor of 107. The loss of conductivity in PEDOT is caused by oxidation of the thiophene ring to thiophene-1,1-dioxide followed by ring-opening and

splitting off of SO_4^{2-} [15,21]. Hypochlorite is also known to degrade the conductive polymer polypyrrole [22] and will generally attack double bonds of organic compounds. This property makes the methodology applicable to the patterning of a range of conductive polymers.

The individual steps of the procedure are outlined in Figure 5.1. Photoresist is patterned by conventional photolithography processing to present a surface relief corresponding to the final conductive pattern in the CP layer. Agarose is moulded against the photoresist relief structure to yield a stamp with an inverted bas-relief. The resulting stamp is incubated with aqueous sodium hypochlorite, briefly dried in a stream of nitrogen, and placed on the homogeneous layer of CP. Deactivation times range from seconds to minutes depending on the CP layer thickness and the polymer substrate used. Apart from rinsing with pure water, no further processing is required after removal of the agarose stamp. The resulting pattern in the CP layer was found to be reduced by 1-2% in both dimensions compared to the photoresist master structure. Signs of evaporation were observed from the "backside" of the stamp, which is exposed to air, but no significant evaporation was seen on the relief side, which is in contact with the PEDOT. Stamps could be reused for patterning several times after repeated incubation with the deactivation agent, and numerous agarose stamps could be moulded against each photoresist master structure.

5.2 Experimental

The EDOT monomer (Baytron M) and Fe(III) tosylate (40 % in butanol, Baytron C) were purchased from Bayer AG (Leverkusen, Germany). The PMMA substrates were purchased from Nordisk Plast A/S (Auning, Denmark). The polyurethane (Tecoflex EG-80A) was purchased from Noveon (Cleveland, USA). The sodium hypochlorite was purchased from Eigil Pedesen Aps (Rodovre, Denmark) as aqueous bleach (app. 10 wt% hypochlorite in water). The Agarose used was UltraPure Agarose from Life Technologies (Paisley, Scotland). All chemicals were used as received. Ultra-pure water with a resistivity of >18.2 MΩ cm was used. The conductivity was measured with a four-point probe (Jandel Engineering Ltd, Linslade, UK) connected to a four-point resistance meter (Keithley 2400 SourceMeter, Cleveland, US). Topographical micrographs were recorded using a PSIA XE-150 Atomic Force Microscope in tapping mode using BudgetSensor BS300 cantilevers. Fabrication of the agarose stamp was done using a master made of SU-8 photoresist. 3 ml of SU-8 2015 was mixed with 1 ml thinner and was

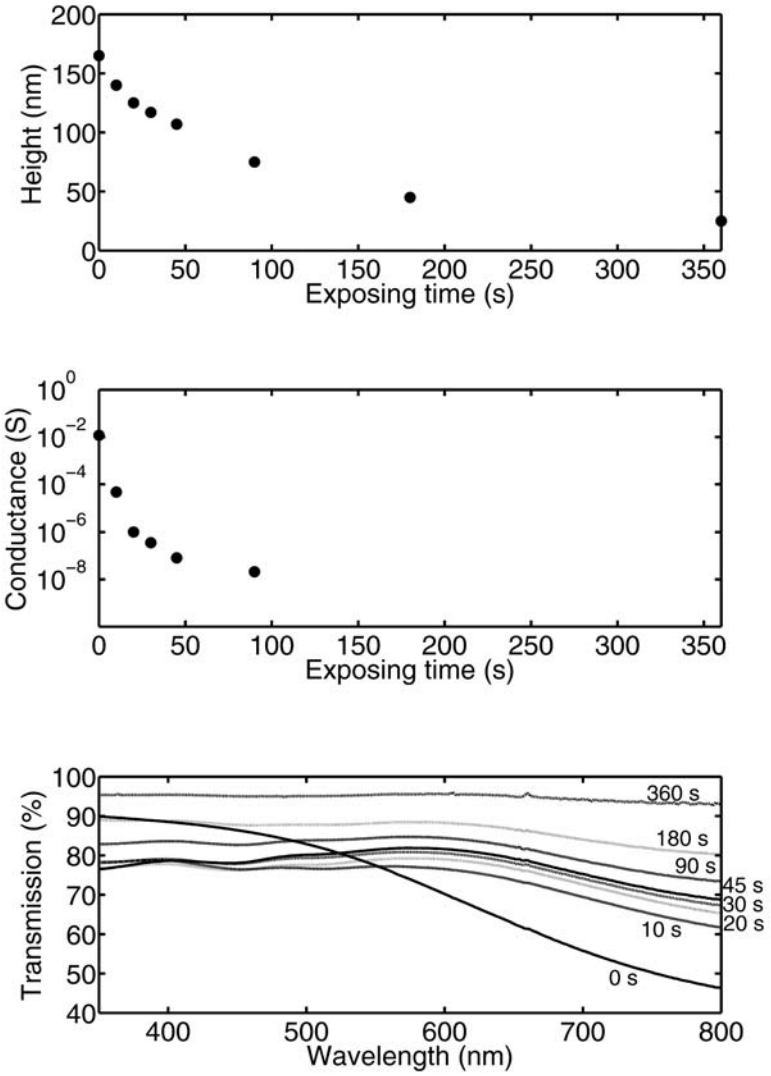

Figure 5.2: Effects of varying the exposure times of a pure PEDOT film on glass to a flat agarose stamp wet by 1 wt% hypochlorite. Top and middle: The thickness and conductance, respectively, of the exposed films. Bottom: UV/Vis absorption spectra of the exposed films for the indicated exposure times.

spun at 2000 rpm for 30 seconds on a clean silicon wafer yielding a 5 μm thick layer. The sample was prebaked at 65°C for 2 minutes and at 95°C for 2 minutes with a temperature ramp to avoid cracking of the structure. The SU-8 was exposed in Karl Suss MA4 mask aligner (365nm illumination) at a dose of 480mJ/cm^2, followed by post-baking at 65°C for 2 minutes and at 95°C for 2 minutes with a temperature ramp. The post-baked layer was developed in SU-8 Developer for 60 seconds and hard baked at 160°C for 20 minutes. The agarose stamps were made from a 12 wt% mixture of agarose in water. The mixture was heated to the boiling point in a microwave oven and thoroughly mixed. The mixture was repeatedly heated to the boiling point in the microwave oven to remove air bubbles trapped in the mixture. The master was placed on a hotplate at 80°C, and the warm mixture was poured on the master. The liquid agarose was covered with aluminium foil to avoid evaporation of water. The stamp and agarose were left on the hot plate for 5 minutes - giving remaining air bubbles time to rise to the surface of the agarose. The sample was removed from the hotplate, and after a few minutes at room temperature the stamp had solidified. The stamp was removed from the master and placed in a solution of hypochlorite for 10 minutes. The required hypochlorite concentration depended on the PEDOT configuration being patterned. The samples were dried in a stream of N2 for 15 seconds and placed on the PEDOT sample. The deactivation time varied from 30 seconds to 5 minutes depending on the polymer configuration being exposed. The hypochlorite concentrations and deactivation times are presented in table 5.1. The stamping was immediately followed by a rinse in ultra-pure water to remove excess hypochlorite and reaction products.

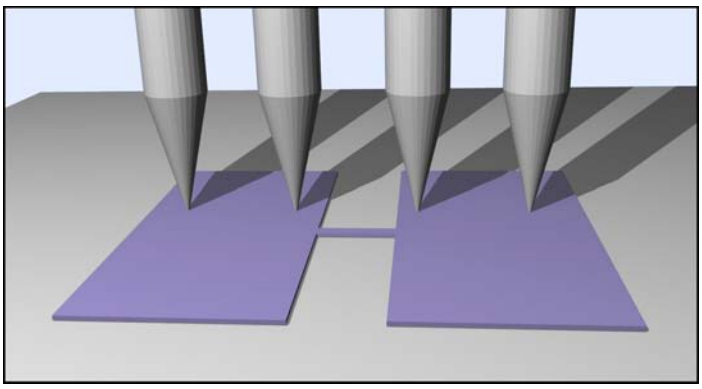

Figure 5.3: Sketch of the electrode geometry fabricated for 4-point probe analysis.

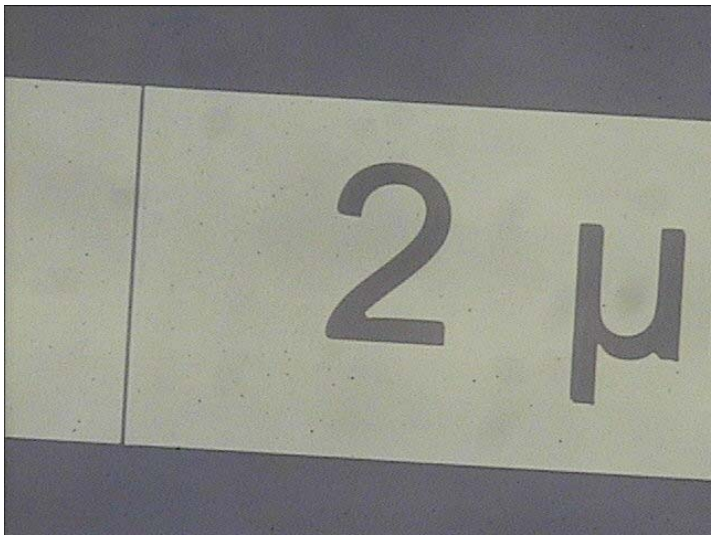

Figure 5.4: Optical microscope image of a 2 μm wide wire in a 150nm thick PEDOT layer on glass, resulting from deactivation and partial removal of material. The height difference between native PEDOT and deactivated/etched areas is approximately 60nm.

5.3 Results

We have recently demonstrated that conductive polymer layers may be blended with their polymer support material to give CP layers of much improved mechanical properties. PEDOT blended into the surface of poly(methyl methacrylate) (PMMA) yielded mechanically very stable CP layers [23]. Deformable conductive layers resulted from blending PEDOT into polyurethane (PUR) elastomers [24]. The proposed methodology should ideally be capable of micropatterning pure adlayers of CP as well as layers of CP blended into the polymer support. This capability was explored by agarose stamping on three different configurations of PEDOT: 1) a layer of pure PEDOT on glass (PEDOT/glass) fabricated as described in [22], 2) PEDOT blended with PMMA (PEDOT/PMMA) produced as reported in [23], and 3) PEDOT blended with PUR (PEDOT/PUR) made according to [24]. The PEDOT/PMMA blend was produced by partially dissolving ("washing") the PEDOT into the PMMA surface while removing the excess oxidation ions from the polymerization process. The PEDOT/PUR blend was made by the

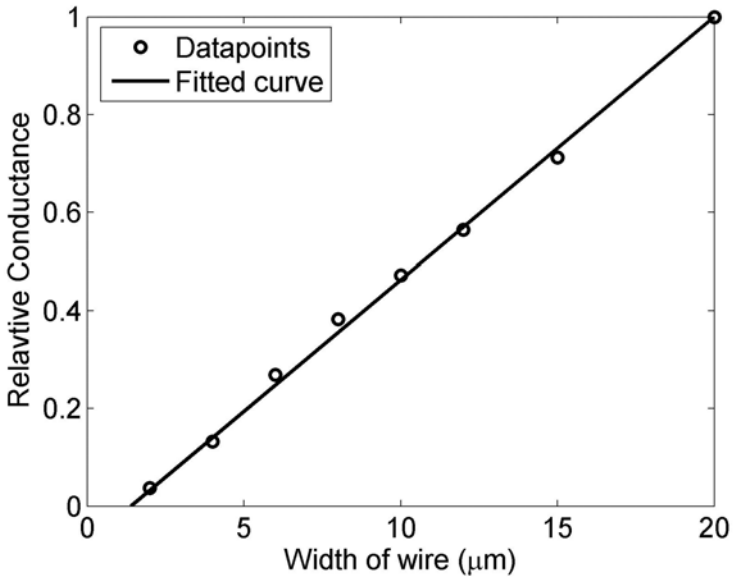

Figure 5.5: Relative conductance of the pure PEDOT wires on glass. Extrapolation of a linear fit to the measurements predicts zero conductance at a line width of 1.5 μm.

presence of polyurethane during the in situ polymerization of PEDOT. The over-oxidation/etching process was examined by varying the exposure time of pure PEDOT on glass to a flat stamp impregnated with 1 wt% sodium hypochlorite. The samples were washed with water immediately after the treatment to remove excess hypochlorite. The conductivity, UV/Vis absorbance, and the layer height of the resulting films were subsequently measured. The results are presented in figure 5.2. The film thickness is found to decrease by less than 25% within 30s of exposure. In contrast, the relative conductance is below 1% after 10s and decreases to less than 10^{-4} of the original film conductance after 30s of contact. The relative conductance after 180 and 360 seconds was less than 10^{-6} which was the sensitivity limit of the detection setup. The UV/Vis spectrum shows a significant change in chemical composition of the film already after 10 seconds. This change most likely reflects the oxidation of the thiophene ring with an associated reduction in the electrical conductivity as reported previously [15,21]. Continued deactivation/etching causes an ever decreasing absorbance, and a gradual reduction in height as the layer is physically etched away. This is probably caused by

the PEDOT splitting into smaller fragments, which can then diffuse into the agarose stamp or be removed by the washing step following the treatment. A PEDOT sample was exposed to a hypochlorite stamp, but not washed after the exposure, to test whether the over-oxidation/etching would continue after the removal of the stamp. No significant over-oxidation/etching was observed, indicating that a continuous diffusion of hypochlorite from the stamp is necessary to retain the deactivation process. The hypochlorite concentrations were chosen to give exposure times of tens of seconds to minutes. These timescales are suitable for development work in the laboratory, but it is noted that the exposure time can be reduced to a few seconds or below if a higher hypochlorite concentration is used. This might be an advantage if the process is to be implemented in an automated process, e.g. large area pad printing.

A pattern consisting of two contact pads connected by a thin wire was used to explore the minimum feature size exhibiting electrical conductivity (figure 5.3). The 5.0 mm x 1.5 mm rectangular contact pads, separated by 500 μm, were sized to allow two pins of a 4-point probe to contact each rectangle when using a four point probe with an electrode distance of 1 mm. In this geometry, one current electrode and one potential electrode contacted each rectangle. The pattern was then reproduced with wire widths of 2, 4, 6, 8, 10, 12, 15, and 20 μm, respectively. The much larger width of the contact pads in comparison to the wire widths ensured that the measured resistance was totally dominated by the resistance of the investigated wire. An optical microscope picture of a 2 μm wide wire resulting from the stamping process on PEDOT/glass is presented in figure 5.4. Surface areas contacted by the hypochlorite-loaded agarose stamp became visually transparent and showed a very large decrease in conductivity. In the geometry used here, conductivity through the deactivated areas could.

PEDOT areas not in direct contact with the hypochlorite-loaded agarose also showed changes in electrical properties. Two phenomena were observed: a decrease in overall conductivity of the bulk material, and edge effects near the boundaries of the agarose stamp protrusions. The decrease in overall bulk conductivity depended on the material patterned, but varied from 30 to 70 percent. The pure PEDOT/glass layer had the largest decrease in conductivity from 700 S/cm to 250 S/cm. The conductivity could, however, be partially recovered to a level of 400 S/cm by treatment with HCl gas. The decrease in bulk conductivity was independent on the wire width. The reduction in conductivity may be caused by chlorine gas diffusing from the stamp, or by long range over-oxidation resulting from hole-injection at the contact areas, although no direct evidence is accessible to validate or

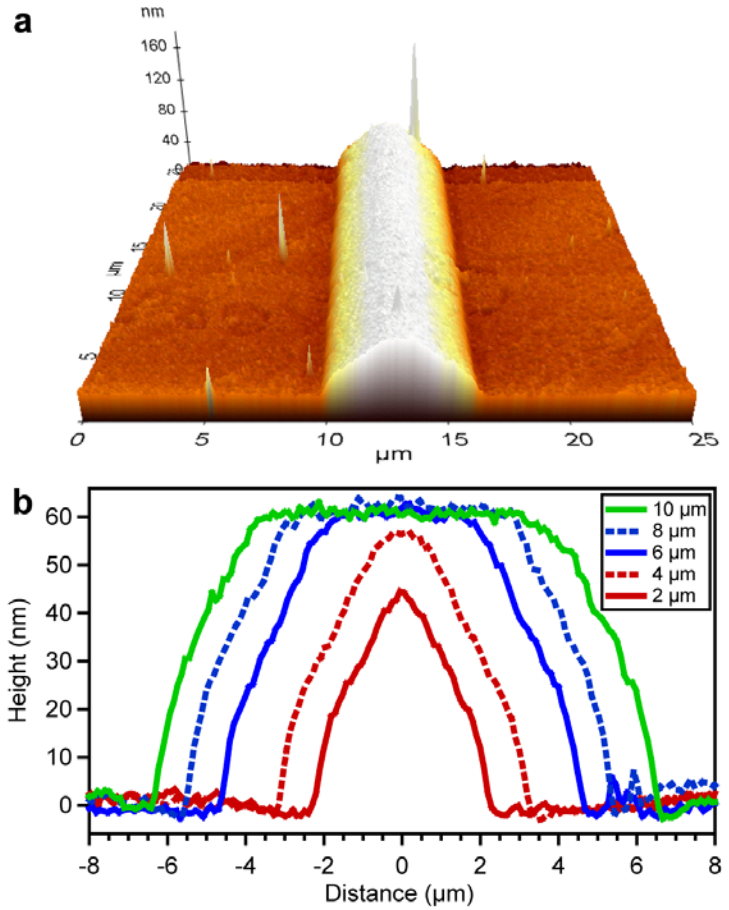

Figure 5.6: (a) Atomic Force Micrograph of a 4 μmm wire. (b) Typical cross-sectional profiles of 2, 4, 6, 8, and 10 μmm wide wires in pure PEDOT as measured by AFM.

reject either explanation. The conductance of neither the deactivated nor the non-deactivated areas showed any significant change over time (weeks). The conductance of the wires should scale with their width, assuming reproducible microfabrication. This is however not the case using this patterning technique due to edge effects near the boundaries of material contacted by the agarose surface relief structures. The edge effects can be quantified by extrapolating the conductance of wires having different widths to nominal zero conductance. This is shown in figure 5.5 for the PEDOT/glass configuration using the conductance of the widest (20 μm) as reference. The edge

effects are found to be approximately 0.75μm on either side of the wire for the processing conditions used. The same analysis was applied to samples of PEDOT/PUR and PEDOT/PMMA. The results are summarized in table 1. The pure PEDOT/glass configuration clearly yields the smallest edge effects. This is probably due to reduced isotropic diffusion in the thin pure PEDOT layer, as the ratios of the edge effect to the thickness of the PEDOT layer are found to be 3-5 for all three configurations investigated. Campbell et al. [19] report on feature sizes etched in glass with HF impregnated agarose down to 1 μm with 500 nm separation. However, their etched structures have a depth of only 34 nm and are therefore expected to exhibit much less pronounced edge effects. The underlying patterning mechanism is also fundamentally different in being a true etch and remove process for HF on glass, while the hypochlorite gradually diffuses into the PEDOT layer and deactivates the CP on its way. The consequence is that during the time it requires to completely deactivate the desired areas, the surrounding PEDOT has been exposed to the deactivation agent and therefore have a reduced conductivity. An evidence of the reduced conductivity zone is that some of the thin wires usually was optical visible, but with no or very low conductivity. This was especially pronounced for the PEDOT/PUR blend, where the 2 μm wire often looked well reproduced optically but had very low conductance. It is known from literature that the conductivity gradually decreases with over-oxidation [3]. This indicates that the PEDOT has been affected by the deactivation agent, but that the fraction of broken conjugated double bonds was not large enough to affect the visual appearance of the polymer but sufficiently high to reduce its conductivity. Distortion of the pattern due to stamping defects or deformation of the agarose was not observed when the stamp was carefully placed on the PEDOT. This corresponds to results presented by Campbell et al [19]. Removal of material from the pure PEDOT layer (PEDOT/glass) was examined by Atomic Force Microscopy. Typical cross-sectional profiles of the wires are overlayed in figure 5.6. There is good agreement between the targeted geometries and the physical thickness of the wires, although the wires seem to be a bit wider than the photoresist masters. This indicates that less material is removed near the edges of the agarose, which is most likely caused by diffusion from the areas of contact into areas of non-contact. This leaves the PEDOT just below the edge less exposed than contact areas far away from the agarose edges. The PEDOT can be deactivated without being physically removed [20], as mentioned earlier, and the cross-sectional area of a wire is therefore not proportional to its conductance.

Material	Hypochlorite Conc.	Deactivation time	Thickness	Edge Effect	Edge/Thickness Ratio
PEDOT	1 wt%	30 sec	150 nm	0.75	5
PEDOT/PUR	10 wt%	30 sec	535 nm	1.5-2	3-4
PEDOT/PMMA	10 wt%	150 sec	800 nm	3	3.5-4.5

Table 5.1: The patterning conditions and width of the edge-effects for the three PEDOT configurations examined.

5.4 Conclusion

In conclusion, a new simple and versatile method for fast micropatterning of conductive polymer has been demonstrated. The methodology applies to adlayers of PEDOT as well as PEDOT layers blended into supporting bulk polymer materials. The underlying chemical process is shown to pattern PEDOT and is most likely equally applicable to a range of other conducting polymers, including polypyrrole. The process involves deactivation of the conductivity and partial removal of material in the PEDOT layer. High-resolution micropatterning (details <2 μm) is found to be limited by isotropic diffusion of the oxidant in the CP layer. Furthermore, substantial loss of conductivity is found for smaller oxidation levels than required for loss of colour or polymer etching. Both observations suggest minimum contact time and minimum CP layer thickness to attain the highest spatial resolution. The method was shown to produce features down to 2 μm in width on PEDOT. Optimization of the process conditions and reduction in layer thickness should easily allow access to sub-micron length scale patterning in a simple process suitable for scaling to fast patterning of large areas of conducting polymers.

5.5 References

[1] C. D. Dimitrakopoulos, P. R. L. Malenfant, *Adv.Mater.*, **2002**, 14, 99

[2] T.W. Kelley, P.F. Baude, C. Gerlach, D.E. Ender, D. Muyres, M.A. Haase, D.E. Vogel, S.D. Theiss, *Chem. Mater.*, **2004**, 16, 4413

[3] P. Tehrani, N. D. Robinson, T. Kugler, T. Remonen, L-O. Hennerdal, J. Häll, A. Malmström, L. Leenders, M. Berggren, *Smart Mater. Struct.*, **2005**, 14, N21

[4] H. Sirringhaus, T. Kawase, R. H. Friend, T. Shimoda, M. Inbasekaran, W.

Wu, E. P. Woo, *Science*, **2000**, 290, 2123

[5] T. Kawase, T. Shimoda, C. Newsome, H. Sirringhaus, R. H. Friend, *Thin Solid Films*, **2003**, 438, 279

[6] B. Chen, T. Cui, Y. Liu, K. Varahrmanyan, *Solid-State Electron.*, **2003**, 47, 841

[7] J. Z. Wang, Z. H. Zheng, H. W. Li, W. T. S. Huck, H. Sirringhaus, *Nat. Mater.*, **2004**, 3, 171

[8] D. Hohnholz, H. Okuzaki, A. G. MacDiarmid, *Adv. Funct. Mater.*, **2005**, 15, 51

[9] Z. Bao, Y. Feng, A. Dodabalapur, V.R. Raju, A.J. Lovinger, *Chem. Mater.*, **1997**, 9, 1299

[10] G. B. Blanchet, Y.-L. Loo, J. A. Rogers, F. Gao, C.R. Fincher, *Appl. Phys. Lett.*, **2003**, 82, 463

[11] W. S. Beh, I. T. Kim, D. Qin, Y. Xia, G. M. Whitesides, *Adv. Mater.*, **1999**, 11, 1038-1041

[12] J. R. Chan, X.Q. Huang, A.M. Song, *J. Appl. Phys.*, **2006**, 99, Art. No. 023710

[13] N. Stutzmann, T. A. Tervoort, D. J. Broer, H. Sirringhaus, R. H. Friend, P. Smith, *Adv. Funct. Mater.*, **2002**, 12, 105

[14] M. Schrödner, R.-I. Stohn, K. Schultheis, S. Sensfuss, H.-K. Roth, *Org. Electron.*, **2005**, 6, 161.

[15] Y. Yoshioka, P. D. Calvert, G. E. Jabbour, *Macromol. Rapid Commun.*, **2005**, 26, 238

[16] Y. Yoshioka, G. E. Jabbour, *Adv. Mater.*, **2006**, 18, 1307

[17] T.S. Hansen, K. West, O. Hassager, N.B. Larsen, *Journal of Micromechanics and Microengineering* 17 (**2007**) 860-866.

[18] S. K. Smoukov, K. J. M. Bishop, R. Klajn, C. J. Campbell, B. A. Crzybowski,

Adv. Mater., **2005**, 17, 1361

[19] C. J. Campbell, S. K. Smoukow, K. J. M. Bishop, E. Baker, B. A. Grzybowski, *Adv. Mater.*, **2006**, 18, 2004

[20] Information provided by the manufacturer of PEDOT, available on: http://www.agfa.com/docs/sp/sfc/jul05_application_PatterningUVlithografie.pdf

[21] B. Winther-Jensen, D. W. Breiby, K. West, *Synth. Met.*, **2005**, 152, 1

[22] C. C. Chen, K. Rajeshwar, *J. Electrochem. Soc.*, **1994**, 11, 2942

[23] T. S. Hansen, K. West, O. Hassager, N. B. Larsen, *Synth. Met.*, **2006**, 156, 1203

[24] T.S. Hansen, K. West, O. Hassager, N.B. Larsen, *Advanced Functional Materials* 17, (**2007**) , 3069-3073.

[25] G. V. A. Aben, M. J. M. Somers, P. H. C. Hanssen, L. M. Schrooten, *SID 98 DIGEST*, **1998**, P-21, 528

Chapter 6

Micropatterning of a stretchable conductive polymer using inkjet printing and agarose stamping

6.1 Introduction

A new kind of stretchable conductive material (SCM) consisting of polyurethane (PUR) and poly(3,4-ethylenedioxythiophene) (PEDOT) has recently been described [1]. The SCM is fabricated by adding an elastomeric polyurethane to the solution from which the PEDOT is polymerised. The resulting blend of PEDOT and PUR was found to be without detectable micro- or nanometer scale structure, thus suggesting their mixing in an interpenetrating network. The result is a highly stretchable material with conductivity around 100 S/cm. The SCM can be repeatedly elongated by up to 50% without significant decrease in conductivity.

A range of applications of conducting polymers have been developed, including antistatic films and electronics [2], displays [3], and sensors for biomedical and military use [4]. The combination of stretchability with conductivity makes the SCM suitable for many additional applications, such as electrodes in flat electrostatic speakers [5] and membranes in microfluidics [6]. Further, products based around the concept of wearable electronics require the application of conducting inks to textiles and other forms of apparel [7],

[5]Based on an article published in **Synthetic Metals** 157, **2007**, 961-967

and flexible conducting polymers could be suitable for this market. Finally, smart packaging products, where conducting inks are applied to flexible substrates such as papers and films, are another potential market for SCMs, provided low cost is possible [8].

Development of methodologies for inexpensive micropatterning of SCMs is essentiel for their use in these applications. In previous work we have micro-patterned blends of PEDOT and poly(methyl methacrylate) (PMMA) [9] using classical clean room techniques involving photoresist, masked UV-exposure and reactive ion etching [10]. However, the new SCM is incompatible with most organic solvents, which prevents the use of conventional photoresists and therefore most clean room techniques. Furthermore, the high cost of conventional clean room processing would strongly reduce the number of viable applications.

In this paper, two different techniques were studied to assess their potential for micro-patterning the SCM. The first application method was subtractive patterning using an agarose gel stamp impregnated with hypochlorite solution, an oxidant that deactivates some conductive polymers by over-oxidation [11]. The patterning of conductive polymers using agarose stamps has been described previously [12] but the effects on the conductivity and stretchability of the SCM were not investigated.

The second application method was inkjet printing. Inkjet printing of PEDOT dispersions has been reported previously [13]. In our work, a solution containing the monomer, oxidant and polyurethane was printed, producing patterned SCM structures by in-situ polymerisation on selected substrates. Alternatively, a mixture of oxidant solution and polyurethane was printed, with the monomer subsequently applied in vapour phase polymerisation.

Both stamping and inkjet printing have advantages and disadvantages. Inkjet printing is an additive method, hence the SCM can be patterned on many kinds of substrates. In contrast, stamping is a subtractive method that requires a uniform film of conductive polymer, possibly integrated with its underlying substrate. Stamping also requires a master structure to be produced, which is time-consuming and typically involves expensive clean room processes. Stamping does have the advantage that once the master is made the patterning is fast and multiple copies can be easily produced with high resolution; 2 μm wide features have been demonstrated in pristine PEDOT [12]. The prime advantage of inkjet printing is the speed with which a range of different prototype patterns can be produced. Disadvantages of inkjet printing are the low speed at which large-scale continouous production can be conducted, and the lower resolution attainable (generally in the hundreds

of micrometers).

Previous work on the stretching of the PEDOT/PUR blend material only considered strain-induced changes in resistance parallel to the direction of strain. In this study, stamping and inkjet patterning techniques were used to prepare SCM structures that allowed the measurement of conductivity parallel and perpendicular to the direction of elongation.

6.2 Experimental

Graphic patterns were designed so that the electrical resistance would be mainly through an electrode oriented either parallel or perpendicular to the direction of elongation. SCM was patterned to these designs by the hypochlorite stamping and inkjet printing methods detailed below. Four electrodes were "sandwiched" between two layers of polyurethane to make a four-point measurement. For the stamped samples, the resistance measurements were made with a Keithley 2400 SourceMeter (Keithley, Cleveland, USA) at a constant current of 10 μA. For the inkjet printed pattern, resistance measurements were made with a Fluke 741 Documenting Process Calibrator and a Fluke 23 multimeter (Fluke, Sydney, Australia). Changes in resistance were observed in former work when the unpatterned SCM was elongated by 100-200% [1]. The same strain range was chosen for exploring strain/conductivity relations of SCM patterned by stamping and inkjet printing, respectively. Viscosity was measured using a DV II+ viscometer (Brookfield, Middleboro, USA) and surface tension was measured using the rod pull method [14]. The molecular weight of polyurethane was determined using a Waters 410 Differential Refractometer with a Waters 590 programmable HPLC pump.

6.2.1 Stamping

Patterning of PEDOT/PUR by stamping is described in detail in references [1] and [12]. Briefly, a PEDOT/PUR base solution was made from EDOT monomer, Baytron C (both from Bayer, Leverkusen, Germany) and Tecoflex 80A (Noveon, Cleveland, OH) dissolved in a mixture of n-butanol, anisole, and tetrahydrofuran. A base solution with 33 wt% PEDOT was spun at 500 rpm on a Hexamethyldisilazane (HMDS)-treated silicon wafer and heated to 65°C for 5 minutes. Reaction side products in the film were removed by washing in boiling water for 2 seconds followed by rinsing with water at room temperature. As reported in [1], it is not possible to fabricate polymers with lower PEDOT contents due to crystallisation in the washing

step. In future studies this issue might be avoided by using an oxidant with a lower crystallisation tendency [15], but for simplicity in the current work the commercially available and well-studied iron(III)p-toluenesulfonate (Fe(III)Tos) [2] was used. A surface relief master structure of the targeted design was made in SU-8 2015 using photolithography. Agarose in water (12 wt%) was heated and thoroughly mixed. The master was heated to 80°C and the agarose solution was poured onto the master and left on a hot plate for 5 minutes. The master and stamp were removed and allowed to cool to room temperature. The gel stamp was carefully peeled off the master and placed in a 10 wt% sodium hypochlorite solution for 10 minutes. The stamp was then removed, blown dry in a stream of nitrogen and brought into contact with the PEDOT/PUR film for 30 seconds. The result was spatially confined delivery of deactivation agent to the areas of contact between the film and stamp. The stamp was removed and the film was washed with water. An approximately 0.5-mm thick polyurethane (Tecoflex 80A) film was cut into a 10 x 70 mm rectangle and placed on the sample pattern. After being heated to 70°C for 2 minutes the pattern adhered to the polyurethane rectangle more strongly than the HMDS-treated wafer and could be easily peeled off. Two electrodes were placed on both ends of the sample to facilitate four-point resistance measurements. A second rectangle of polyurethane of equal dimensions was added on top of the sample, holding the electrodes in a sandwich configuration.

6.2.2 Inkjet printing

Printing was performed with a Dimatix DMP-2800 inkjet printer (FujiFilm Dimatix Inc., Santa Clara, USA). The most important parameters in formulating a fluid for inkjet printing are viscosity, surface tension and vapour pressure. The optimum fluid properties recommended by the manufacturer were a viscosity of 10-12 cps, surface tension of 28-33 dynes/cm, and a boiling point above 100°C. In addition to these specifications, the solvent had to be capable of dissolving both the Fe(III)Tos and polyurethane, and have good film-forming properties. The solvent used in our previous stretching studies [1] was a mixture of n-butanol, tetrahydrofuran, and anisole. However, tetrahydrofuran has a boiling point of only 66°C which makes it unsuitable as co-solvent in inkjet printing, as rapid evaporation can lead to solute precipitation and blockage of the nozzles of the inkjet head [16]. Various alternative solvents or co-solvents with 1-butanol, anisole, toluene, dodecane, decane, nonane, 2-methyl-2-propanol, 1,4-dioxane, 1,2-propanediol or cyclopentanol were considered. The simplest and most effective solvent mixture was found

to be a mixture of anisole and cyclopentanol, taking into account boiling point, surface tension, dissolving power and film forming properties.

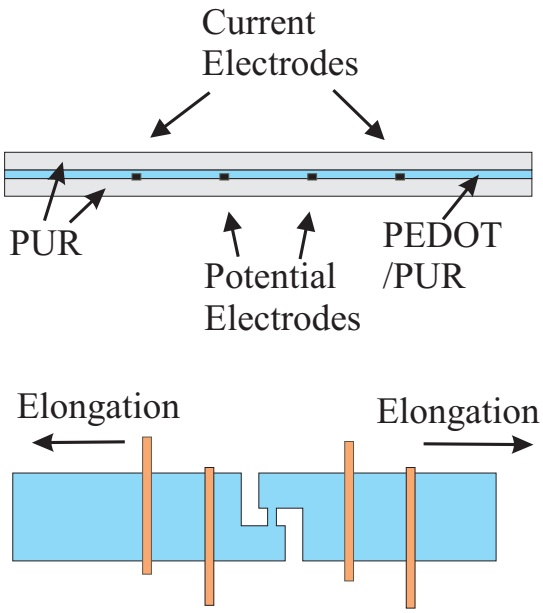

Figure 6.1: Schematic (side view and top view at top and bottom, respectively) of the sample layout to measure resistance perpendicular to the direction of elongation. The longer dimension of the probing line electrode in the centre of the layout, designed to have the largest resistance in the system, is perpendicular to the direction of elongation.

6.3 Results

6.3.1 Stamping

Two different designs, with a 1000 μm x 50 μm electrode either parallel or perpendicular (see Figure 6.1) to the elongation direction, were fabricated using the agarose stamping technique. An optical microscope image of the device produced by stamping is shown in Figure 6.2.

For comparison, the resistance of an unpatterned sample was measured (as in Figure 6.1 but with no constriction to the conductive pathway between the potential electrodes). Previous work has shown that the conductivity of

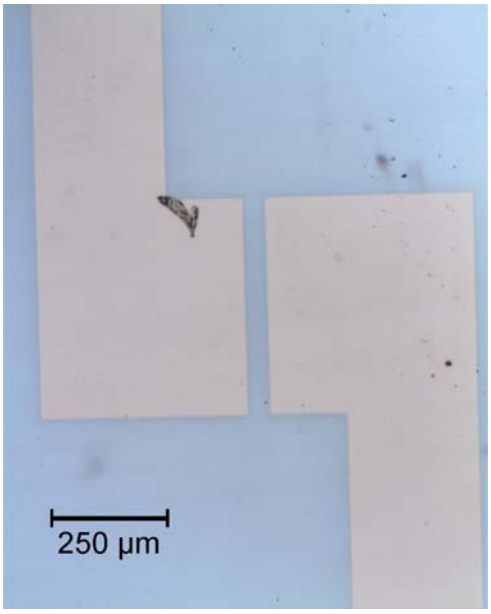

Figure 6.2: Central section of a device patterned by agarose stamping. The light areas are deactivated PEDOT/PUR. The longer dimensions of the line electrode is perpendicular to the horizontal stretching direction.

the non-deactivated parts of a stamped PEDOT film may be reduced (from approx. 700 S/cm to approx. 300 S/cm) in the vicinity of the deactivated pattern [12]. This indicates that the hypochlorite oxidant diffuses laterally in the conducting polymer film.

The resulting strain/resistance behaviours of the three electrode configurations are presented in Figure 6.3, each normalised to the resistance of the respective unstrained configuration. The unpatterned SCM and the SCM with an electrode parallel to the direction of strain did not correlate, suggesting that the patterning itself changed the structure of the PEDOT in the SCM, and therefore influenced the way it behaved when elongated. The cause of this behaviour could be traces of hypochlorite diffusing into the conductive polymer and disrupting the conjugated structure of the PEDOT. Even a few disrupted double bonds would reduce the effective length of the chain of conjugation in the PEDOT and therefore change its conductive properties. The resistance perpendicular to the stretching direction did not increase as much as the resistance parallel to the elongation, as may be ex-

pected. In summary, the presence of hypochlorite during stamping affected conductivity during stretching, but even with these altered conductivities observed, the SCM is still a relative good conductor.

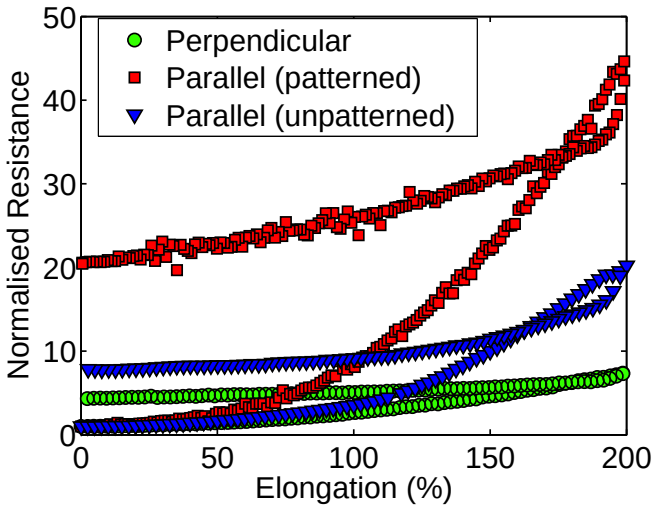

Figure 6.3: The relative resistance of an untreated SCM and two agarose stamped samples. The two parallel samples do not follow the same curve, which indicates that the patterning itself changes the properties of SCM.

6.3.2 Inkjet printing

Some polymer solutions may cause problems in inkjet printing. When a drop of fluid is expelled from a print head nozzle, the neck of the drop is stretched, causing rapid strain-hardening [15]. This may cause the drop to be either pulled back to the nozzle, or to result in the formation of an uncontrollable string of fluid instead of a drop. An example of this phenomenon is shown in Figure 6.4 (left). In the current study, inkjet printing was initially attempted with the commercially available polyurethane Tecoflex 80A (Noveon, Cleveland, USA), which has a molecular weight of approximately Mn 160,000. To avoid strain-hardening and consequent malfunction of the printer, the concentration of polyurethane had to be lowered to 0.25 wt%, which then required a large number of passes to generate an adequate film thickness. Since strain-hardening is highly dependent on the molecular weight of the polymer [15], a polyurethane with a lower molecular weight was needed.

A low molecular weight polyurethane was synthesized from a commercially available, two-component polyurethane (Erapol OC80A - Era Polymer Inc., Sydney, Australia), which contained a diisocyanate component and a diol component. It was established that mixing the two components at a 5:4 molar ratio instead of the 1:1 ratio prescribed by the manufacturer, incomplete polymerisation occurred, producing a short chained polymer (SCP). The two components were added in the 5:4 ratio to anisole, heated to 100°C and stirred for 4 hours. The molecular weight was measured as Mn $50.5 \cdot 10^3$ and the polydispersity to 3.5. Using this SCP, it was found that a loading of 1.5 wt% could be inkjet printed succesfully. Figure 6.4 (right) shows a drop of 1.5% SCP compared with a drop of 0.5% Tecoflex (left). It can be seen that the 0.5% Tecoflex solution creates a string behind the drop, which results in poorly-defined patterns. In contrast, the SCP solution formed well-defined drops that resulted in much better resolution, even at three times the concentration of the tecoflex. The optimal printing solution was found to be a mixture comprising 5 mL cyclopentanol, 1 mL Baytron C (40% Fe(III)tosylate in butanol), 0.7g of 25 wt% polyurethane in cyclopentanol and 5 mL anisole. This solution had a viscosity of 7.0 cps and a surface tension of 32.7 dynes/cm and yielded an SCM blend comprising 25 wt% PEDOT. The substrate was heated to 60°C during printing and evaporation of the solvent.

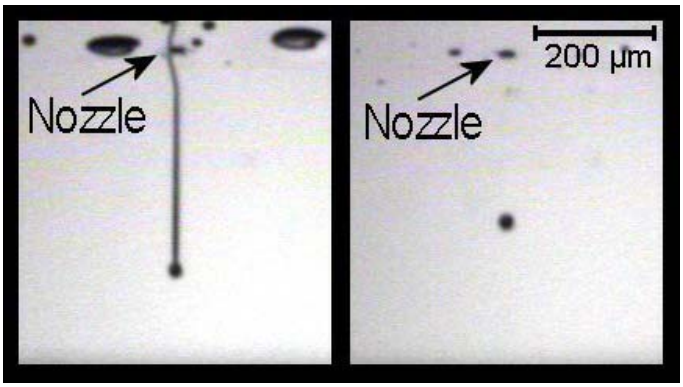

Figure 6.4: Left: Inkjet printing a 0.5 wt% Tecoflex 80A in anisole/cyclopentanole produces a long uncontrollable tail after the drop. Right: Printing with 1.5 wt% SCP yields well-defined drops.

When EDOT monomer was added to this solution for in situ polymerisation, a film was produced that was lighter in colour than similar films

produced by vapour phase polymerisation. This was most probably caused by evaporation of the monomer. The main solvents used in the printing solution (cyclopentanol and anisole) have higher boiling points (140°C and 154°C respectively) than the 1-butanol (118°C) normally used for in situ polymerisation, and are much closer in boiling point to the monomer 3,4 ethylenedioxythiophene (193°C, Sigma Aldrich). The higher boiling points of the solvents imply that relatively more EDOT will evaporate with the solvents before the concentration of EDOT necessary of polymerisation is reached. Although the monomer was added in excess, the amount of PEDOT in the final film varied when the printing parameters were varied. Drop size and drop spacing influence the thickness of the printed film and hence monomer evaporation rate. The monomer-to-oxidant ratio should therefore be optimised each time the printing parameters are changed. For consistency it was decided to use vapour phase polymerisation (VPP) [17], so that the amount of PEDOT in the SCM depended only on the amount of oxidant in the film. For industrial purposes, printing a "one-pot" solution that includes the monomer would probably be a better alternative and should give similar results once the parameters and monomer content are optimised. Both VPP and in situ polymerised blends showed conductivity around 80 S/cm, comparable with the values observed when using the Tecoflex polymer. A pattern corresponding to the one prepared by agarose stamping was printed four times on a PET overhead transparency and a polyurethane sandwich was made in the same way as described for the pattern formed by stamping above. An image of the perpendicular electrode is shown in Figure 6.5.

The inkjet printer was well suited for patterning conductive polymers. There was, however, some difficulty obtaining straight edges on the patterns when printed on non-porous substrates like glass or polymer sheets, as shown in Figure 6.5. The non-linearity of the edges is possibly caused by surface tension effects and could perhaps be prevented by adding surfactants or by changing the surface chemistry of the substrate. Alternatively, microroughness in the surfaces of the sheets may be responsible. Characterisation of the microroughness of the films and its effects on edge perimeter of printed patterns will be the subject of a separate study. No difficulty was encountered when printing on porous substrates like paper and the non-linear features of the edges were smaller in magnitude than those seen on smooth substrates. In for the current study the conductive polymer had to be printed on a flat, non-porous substrate, from which it could be transferred to a polyurethane film. The manufacture of the inkjet printer states that drops with a diameter of approximately 40 μm can be printed with an increment of 5 μm [18]. It was not possible to reach satisfactory results with this resolution

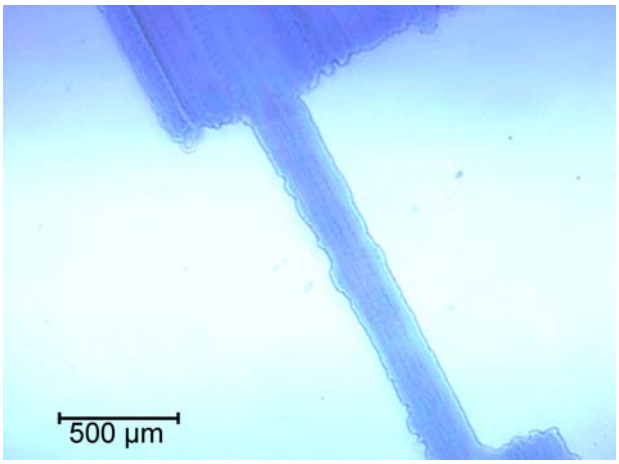

Figure 6.5: The central area of the inkjet printed electrode. The electrode was printed on a flat PET transparency that made well-defined edges difficult to achieve.

on none-porous substrates, probably due the effects mentioned above. The structure shown in figure 6.5 represents the best resolution achieved with the setup. Attempts to make the electrode thinner than 200 μm resulted in an incoherent or none well-defined line. Clearly, whether or not the resolution of an inkjet printer will be adequate will depend on the requirements of the application that is contemplated.

Replacing the long chain polyurethane with a short chain polymer for improved printability reduced the degree of elongation to which the SCM could be subjected prior to failure. When stretched about 150%, small cracks appeared in the PEDOT/SCP films, followed by an abrupt drop in conductivity at around 200% elongation. Images obtained with an optical microscope at 100%, 150%, 200%, and 300% elongation are presented in Figure 6.6, with the elongation direction being parallel to the scale bar shown on Figure 6.6A. The shorter chain length of the polyurethane apparently led to early mechanical failure of the SCM. In contrast, the blend containing the long chain Tecoflex could be stretched more than 400% without any signs of mechanical failure, although this result could also be influenced by differences in the chemical composition of the two polymers. In subsequent elongation versus resistance measurements, the SCP samples were only stretched 100% to ensure no mechanical cracking of the film occured. As indicated in Figure 6.7, there is an irreversible increase in resistance both parallel and perpen-

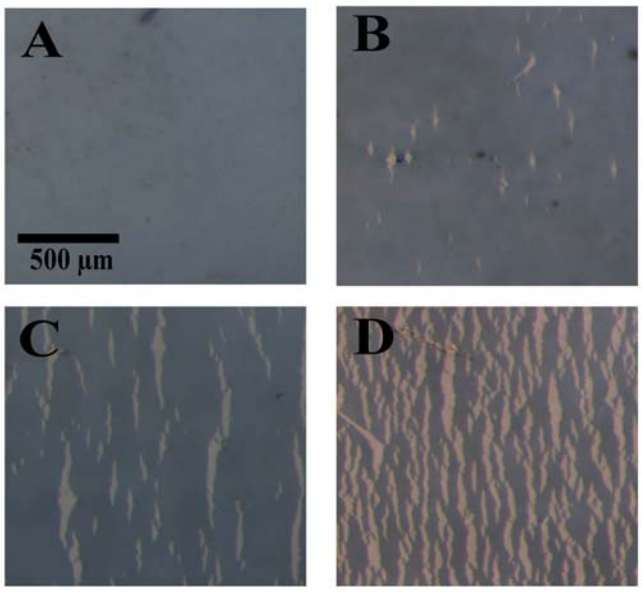

Figure 6.6: PEDOT with short chain length polyurethane at different degrees of elongation. A) 100% elongation, B) 150% elongation, C) 200% elongation and D) 300% elongation. At elongations above 150%, cracks begins to appear, leading to complete failure of the film at around 300%.

dicular to the stretching direction. Whether or not these increases and their irreversibility will be of practical utility will depend on the intended application. It was not possible to find a strong correlation between the resistance perpendicular and parallel to the stretching direction for either of the two patterning methods, other than a tendency for the parallel resistance to be proportional to the squared perpendicular resistance. No theoretical explanation for why such a relationship might exist can be advanced at this stage.

The surface of the inkjet printed sample was examined using Scanning Electron Microscopy. See Figure 6.8. The SEM microscopy revealed that the surface is not as smooth and homogeneous as the spin coated samples (see [1]). The craters on the surface (seen on the top image in Figure 6.8) may be impact features from printing. The sample was inkjet printed several times to build up film thickness and spattering of droplets on existing film could be responsible for the observed appearance.

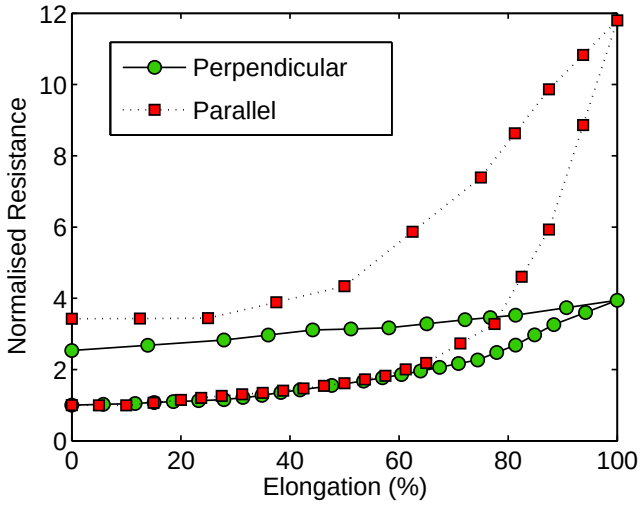

Figure 6.7: Relative resistance of the inkjet printed PEDOT/SCP films parallel and perpendicular to the stretching direction. The lower curve shows values obtained during extension and the upper curves shows values measured during relaxation. It is evident that there is an irreversible loss of electric conductivity both parallel and perpendicular to the direction of elongation.

6.4 Conclusion

Two methods for patterning of the stretchable conductive material have been tested. The agarose stamping of the SCM showed that the deactivation agent affects the conductivity during elongation, but not to a degree that would prevent the patterning method being useful in practical applications. The agarose stamping proved to be a good solution in application where well-defined structures of SCM on the micrometer scale are required. For the SCM to be printable with an inkjet printer, a short chain polyurethane was required. However, this formulation reduced the elongation of the SCM achievable to below 150%, a level still adequate for many applications. Inkjet printing was shown to be a fast iterative method for making prototypes. Print quality was affected by substrate-formulation interactions but acceptable results could be obtained for both porous and non-porous substrates. Both patterning methods were used to make SCM measuring devices in which the resistance perpendicular to the stretching direction could be measured.

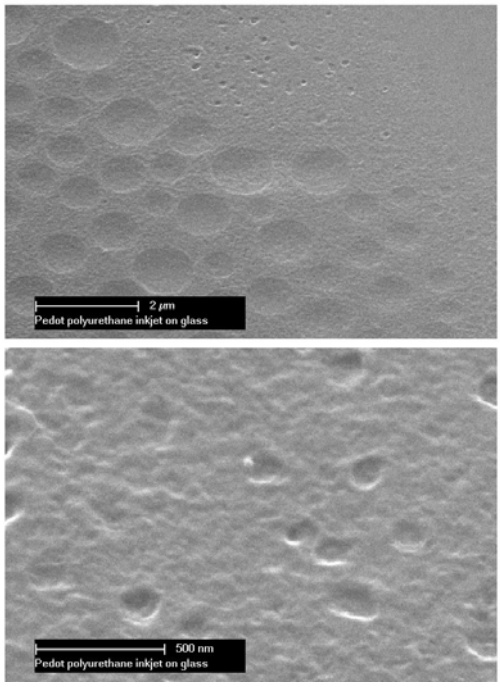

Figure 6.8: SEM images of the surface of the inkjet printed stretchable conductive polymer.

6.5 References

[1] T.S. Hansen, K. West, O. Hassager, N.B. Larsen, *Advanced Functional Materials* 17, (**2007**) , 3069-3073.

[2] L. Groenendaal, F. Jonas, D. Freitag, H. Pielartzik, J.R. Reynolds, *Advanced Materials* 12, (**2000**) 481-494.

[3] J. Bharathan, Y. Yang, *Appl. Phys. Lett.* 72 (**1998**) 2660.

[4] A. G. MacDiarmid, *Synthetic Metals* 84 (**1997**) 27-34.

[5] R.D. Billson, A.D. Hutchins, *International Patent*, WO200219764-A1 (**2002**).

[6] R. Zengerle, J. Ulrich, S. Kluge, M. Richter, A. Richter, *Sensors & Actuators* A 50 (**1995**) 81-86.

[7] D. Marculescu, R. Marculescu, Zamora, Stanley-Marbell, Khosla, Park, Jayaraman, Jung, Lauterbach, Weber, Kirstein, Cottet, Grzyb, Tröster, Jones, Martin, and Nakad, *Proc. IEEE. 91* (**2003**) 1995-2018.

[8] B. Winther-Jensen, N.B., Clark, P. Subramanian, R.J.N Helmer, S. Ashraf, G.G. Wallace, L. Spiccia, D. MacFarlane. *J. App. Polym. Sci.* 104 (**2007**) 3938-3947.

[9] T.S. Hansen, K. West, O. Hassager, N.B. Larsen, *Synthetic Metals* 156 (**2006**) 1203-1207.

[10] T.S. Hansen, K. West, O. Hassager, N.B. Larsen, *Journal of Micromechanics and Microengineering* 17 (**2007**) 860-866.

[11] Y. Yoshioka, , P.D. Calvert, G.E. Jabbour, *Macromol. Rapid Commun.* 26 (**2005**) 238-246.

[12] T.S. Hansen, K. West, O. Hassager, N.B. Larsen, *Advanced Materials* 19, (**2007**), 3261-3265.

[13] H. Sirringhaus, T. Kawase, R.H Friend, T. Shimoda,. M. Inbasekaran. W. Wu, E. P. Woo, *Science* 290 (**2000**) 2123.

[14] S.D. Christian, A.R. Slagle, E.E Tucker, J.F. Scamehorn, *Langmuir* 14 (**199**8) 3126-3128

[15] P. Subramanian, N.B. Clark, L. Spiccia, B. Winther-Jensen D. R. MacFarlane. *Advanced Materials* to appear (**2007**).

[16] B. de Gans, P.C. Duineveld, U.S. Schubert, *Advanced Materials* 15 (**2004**) 203-213.

[17] B. Winther-Jensen, J. Chen, K. West, G. Wallace, *Macromolecules* 37 (**2004**) 5930-5935.

[18] Please see the manufacture homepage: www.dimatix.com

Chapter 7

Summary

This chapter is a summary of the results presented in the previous chapters.

7.1 Integration of conducting polymers in non-conductive polymer substrates

The conducting polymer PEDOT has poor mechanical properties compared to most non-conductive polymers and its adhesion to glass and polar polymers with hydrophilic to medium hydrophobic surfaces is poor. Delamination of the PEDOT film from the substrate has been experienced numerous times during this project. This is obviously a problem, if the film is intended to be utilised in a microfluidic system containing water. The problem was solved by integrating the PEDOT in a non-conductive polymer substrate. While polymerising the conducting polymer, a large amount of oxidant is required, which remains in the film after polymerisation (see reaction scheme in figure 1.3). The excess oxidant is subsequently removed in a washing step. During the washing step the film collapses from a rough film to a thin homogeneous film with approximately 10% of its original thickness. Water or ethanol is normally used as washing solvents. A former PhD student at DTU/Risø has shown that it is possible to trap macromolecules in the PEDOT matrix, by adding the macromolecules to the washing solvent [1]. The macromolecules are trapped in the structure as it collapses and an apparently homogeneous film is formed. This method was utilised to fabricate a blend of PEDOT and a non-conductive polymer. PEDOT was polymerised on a PMMA substrate, followed by a washing step, using a solvent that both removes the excess salt and dissolves the PMMA. It is believed that the top part of the PMMA is dissolved and trapped in the collapsing PEDOT, re-

sulting in a blend of PMMA and PEDOT. The three washing methods are sketched in figure 7.1. The blend exhibited very good mechanical properties, a good integration into the PMMA substrate, and an electrical conductivity higher than pristine PEDOT. The blend was therefore well suited for applications in microfluidic devices. The blend was examined with Atomic Force Microscopy and it was not possible to identify different phases on the surface of the blend, indicating that the film is homogeneous down to length scales of ∼20 nm (The approximately tip diameter of the AFM). A piece of the blend was stepwise etched using a reactive ion etcher and the composition of the blend down through the sample was examined using UV/Vis and resistance measurements. Both techniques showed a PEDOT and PMMA content of approximately 1/3 and 2/3, respectively, in the entire film.

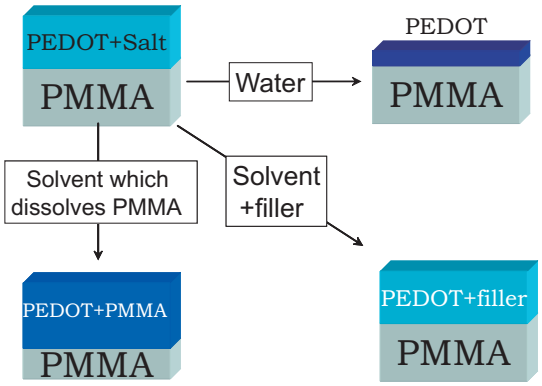

Figure 7.1: A sketch of the different results obtained by changing the washing solution.

The method was reproduced with a number of conducting polymers and non-conductive substrates to test whether the fabrication method was specific for only PMMA and PEDOT or generic for other combinations of polymers. The conducting polymer Polypyrrole was successfully integrated into PMMA and PEDOT was successfully integrated into Polycarbonate, Polystyrene, Polyurethane and Cyclic olefin copolymer using various solvents. Hence it could be concluded that the method is generic. It is known from classical polymer physics [2] that most polymers are not mixable with other polymers due to the unfavourable thermodynamics of polymer-polymer mixes. This correlates very poorly with the observed results and leaves one with the question: how can a very hydrophilic and otherwise completely insoluble conducting polymer make an apparently homogeneous blend with a

number of hydrophobic polymers? The reason might be that the time required for the polymer chains to disentangle is longer than the time it takes for the solvent to evaporate, and that the blend therefore is trapped in a metastable state. Another paradox is that the conductance of the blend is higher than the pristine PEDOT, although diluted with a non-conductive polymer. So while the work yielded a mechanical resistant polymer blend with high conductivity it also left some unanswered theoretical questions regarding the thermodynamics and conductivity of conducting polymers.

7.2 All polymer AC electroosmotic micropump

The integrated PEDOT in PMMA was utilised to make an all polymer AC electroosmotic (ACEO) micropump. The ACEO pumping mechanism was chosen due to its simple design and absence of movable parts. The pump consists of an array of small and large interdigitated microelectrodes with an AC electric potential applied between each set of asymmetric microelectrodes. An asymmetric field is generated in the pumping fluid, resulting in an asymmetric force applied on the charged ions in the pumping fluid. The movement of the ions generates the fluid flow. A more detailed description of the ACEO pump can be found in section 3.2. According to theory, the propulsion generated by the pump scales with the inverse of the geometric dimensions, hence the smaller electrodes the better pump. The pumps reported in literature were constructed with electrode dimensions of 4 μm and the intent was to construct PEDOT/PMMA electrodes with similar dimensions. A patterning method was developed, using clean room techniques, and the resolution was found to be satisfactory for producing electrodes with dimensions down to 4 μm. The method for micropatterning the PEDOT/PMMA is sketched in figure 7.2. Some variations of the patterning mechanisms were tested, with the purpose of eliminating the RIE process. These are described in appendix A.

To control the fluid and encapsulate the pump it was necessary to apply a channel system on top of the ACEO micropump. PDMS, which is extensively used for microfluidics channels by other research groups, could not be used, because it only bonds to glass and other PDMS parts and not to PMMA or PEDOT. The polyurethane, Tecoflex 80A, possesses some properties advantageously for a channel-material: it is transparent, flexible and bonds to PMMA. Compared to PDMS it has two other advantages: It has a contact angle below 90° and is therefore wetting, and it bonds thermally to PMMA. PDMS on the other hand requires plasma treatment for bonding and for re-

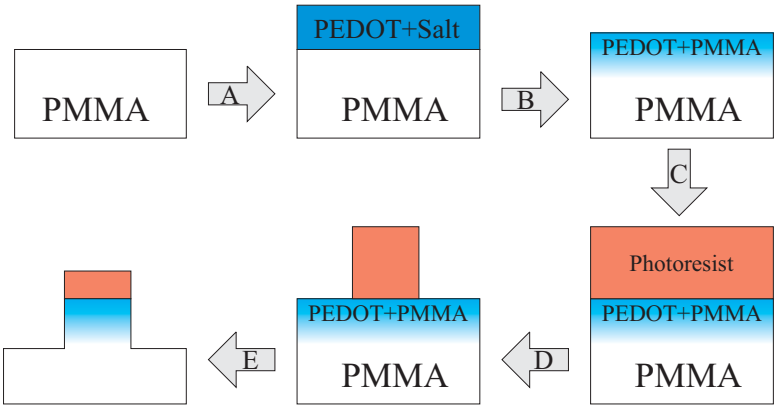

Figure 7.2: The fabrication method for micropatterning of conducting polymers: PEDOT is polymerised on a plain PMMA substrate (A) followed by integration of the PEDOT into the PMMA (B) as described in chapter 3. The PEDOT/PMMA is spin coated with photoresist (C), exposed in a mask aligner and developed (D). Finally the sample is etched in a reactive ion etcher (E) and the remaining photoresist is removed by ethanol (not shown).

ducing the contact angle to below 90°. The polyurethane pellets were heated and pressed to a uniform disc. The disc was heated and pressed against a bas-relief SU-8 photoresist master, cooled, and peeled off the master. The patterned PUR was placed on the patterned PEDOT/PMMA, constituting the micropump electrodes. The sample was then heated to bond the PUR to the PMMA and the pump was complete. Testing of the micropump was conducted with fluorescent microbeads with a diameter of 0.5 μm. The beads were added to the pumping solution and tracked using a confocal microscope. The generated images were analysed with a MatLab program, yielding the average fluid velocity as a function of frequency and voltage. The results showed that the pump-characteristics resembled pumps described in literature, made with noble metal electrodes. The PEDOT-pump did however show a tendency to be damaged at a slightly lower voltage than the metal-pumps. The damage could be prevented by coating the electrodes with a thin layer of non-conductive polymer, like PMMA or COC. The thin layer of non-conductive polymer prevented damage to the electrodes and extended the lifetime of the pump, but reduced the maximum pumping velocity of the pump.

7.3 Stretchable Conducting Polymer

The stretchable conducting polymer was developed in the search for a material suited as a membrane material. The optimal material should have a fairly good electrical conductivity and should withstand elongation up to at least 50%. The combination of PEDOT and polyurethane turned out to possess these properties. Polyurethane (Tecoflex 80A) can be dissolved in the PEDOT casting solution if a number of co-solvents are added. The original non-polyurethane casting solution used in chapter 2 and 3 contained 6.5 ml Baytron C (40 wt% Fe(III)Tos in butanol), 2 ml butanol, 0.15 ml pyridine and 0.22 ml EDOT. THF was added to this solution to ensure solubility of the polyurethane and anisole was added, in order to gain a satisfactory film smoothness when spin coated. Furthermore it was also necessary to remove the pyridine, as it prevented the polymerisation of PEDOT. The polymerisation of PEDOT is proton-catalysed [3], and the presence of the basic pyridine slows down the polymerisation rate, which enhances the electrical conductivity of the final polymer. Apparently the polyurethane possesses the same kind of inhibiting effect on the polymerisation as the pyridine, and the presence of both pyridine and polyurethane in the casting solution completely prevented the initiation of the polymerisation. This property of polyurethane could arise from complex bonding between the Fe^{3+} ion and the urethane link, or be caused by residual tertiary amines used as catalyst in the polymerisation of the polyurethane. The optimal solution for a 50 wt% PEDOT in PUR film was 6.5 ml Baytron C, 2 ml butanol, 0.22 ml EDOT, 8.46 ml Anisole, 8.46 ml 10 wt% PUR in THF. The solution containing polyurethane showed a remarkable long pot life of several months, compared to the non-polyurethane pot that polymerised within hours. The solution was spin coated on a rigid surface and heated to 65° degrees for 5 minutes, washed in boiling water, and transferred to a polyurethane film. Three film types were made with a PEDOT concentration of 33 wt%, 40 wt%, and 50 wt%. All three films showed relative good conductivity around 100 S/cm. The films were elongated 50 % and relaxed ten times, while the resistance was monitored. All three films exhibited the same kind of pattern: A small increase in resistance during the first elongation, followed by a stable resistance during the next 9 elongations. The films were also elongated 200 % and relaxed 4 times. The resistance increased significantly when elongated more than 100 %, and a large irreversible change in the conductivity was observed. The material did however remain fairly conductive. The combination of elasticity and electrical conductance for a homogeneous organic film is quite remarkable, and has not previously been reported in literature.

The film could be used in a number of applications, such as strain gauges, artificial muscles, or for impregnation of conductive fabric.

Aging of the PEDOT/PUR material was examined by storing a number of films at 21°C and 60°C for 3000 hours. The conductivity of the films was measured during the period. The experiment revealed a logarithmic decay in conductivity and the material would probably remain fairly conductive for at least a few years, if stored at room temperature. Furthermore the conductivity could be partially regained if the aged samples were exposed to HCl vapour, indicating that the decay in conductivity is pH dependent.

The polyurethane swells easily in most polar organic solvents, and the solvent resistance of the PEDOT/PUR blend is therefore very poor. The film is only resistance to water and very unpolar solvents like heptane.

7.4 Agarose Stamping

The motivation for developing a new patterning method was the poor solvent resistance of the stretchable conductive polymer described above. A method where a homogenous film of PEDOT/PUR could be patterned without the use of polar solvents was desired. The fabrication method described in section 7.2 involves photoresist containing several polar solvents. Another approach was therefore developed. The idea of using agarose stamping came from two excellent articles by S. K. Smoukov et al [4] and C. J. Campbell et al [5] in which glass was etched using HF impregnated agarose. The same concept was applied to conducting polymers using the deactivation agent hypochlorite instead of HF. A 12 wt% agarose solution is heated and cast against a photoresist master patterned in a bas-relief. The agarose stamp is cooled, and after solidification removed from the master and impregnated with sodium hypochlorite. After impregnation the agarose stamp, shaped as an inverse of the bas-relief master structure, is placed on a homogenous film of conducting polymer. The agarose stamp delivers the hypochlorite to the conducting polymer surface in the areas of contact, hence the conducting polymers contact with hypochlorite is spatially confined to the relief-structure of the stamp. The result is a patterned conducting polymer film, where the conductive areas of the film correspond to the elevated areas of the original master relief.

The deactivation agent, hypochlorite, deactivates the conducting polymer followed by chemical etching of the film. During the first few seconds of exposure of a pristine PEDOT film to hypochlorite, the conductance is reduced two orders of magnitude and a significant change in colour is ob-

served. In the following tens of seconds the deactivation continues, but is now accompanied by a chemical etching, removing the PEDOT. The ability of small amounts of hypochlorite to significantly reduce the conductivity of PEDOT leads to edge effects near the edge? of the agarose stamp, caused by hypochlorite diffusion from the stamped areas into the non-stamped areas. This edge effect was the limiting factor for the resolution. The resolution of the patterning method on pristine PEDOT was examined and found to be around 2 μm with an edge effect around 750 nm. Pure PEDOT, PEDOT/PMMA, and PEDOT/PUR samples were etched with satisfactory results. The experiments showed good coherence correlation? between the film thickness and edge effect, with width of the edge effect being approximately 3-5 times the film thickness.

7.5 Ink-jet printing of PEDOT/PUR

A patterning method, complimentary to the agarose stamping, was developed using a scientific inkjet printer. The agarose stamping is a subtractive method, hence it deactivates or removes conducting polymer from a uniform CP film. That implies that the surface has to be highly homogeneous. Inkjet printing is an additive method and complete surface homogeneity is not a necessity, e.g. CP can be applied to structured substrates like paper or fabric. Patterning of conducting polymers using inkjet printing has been extensively studied in literature, and many positive results have been reported. It was therefore decided to print the PUR/PEDOT using a scientific inkjet printer with a fitted camera and controllable expelling velocity and frequency. The restrictions to the viscosity and surface tension of the printing fluid in an inkjet printer are fairly narrow. The addition of a polymer to a solution causes the viscosity to become non-newtonian. This is mainly seen by strain hardening, where the viscosity of the polymer solution rapidly increases, if the solution is strained. In the printing head, a microdrop is expelled through a narrow nozzle and the neck of the drop is stretched until it breaks and the drop is released. By adding the polyurethane to the solution, it was observed that the neck did not break. The drop was either sucked back into the nozzle or an uncontrollable string was expelled instead of a drop. This phenomenon was ascribed to strain hardening in the drop neck. To avoid the strain-hardening, the solution had to be very diluted and the pattern had to be printed tens of times to achieve a satisfactory film thickness. The first polyurethane used was the commercially available Tecoflex 80A with a molecular weight (Mn) of 160,000. Since strain hardening increases with increasing

molecular weight of the polymer, a polyurethane with a shorter molecular weight was necessary to decrease the required number of prints. This was synthesised from a two component commercially available polyurethane. The new polyurethane had a molecular weight (Mn) of 50,000 and solutions with much higher polyurethane loading could be printed using this polymer. The resolution of the inkjet printer was around 200 μm, compared to approximately 5 μm for the agarose stamping of the PEDOT/PUR. The advantage of the inkjet printer is, besides the low restrictions to the substrate surface, the possibility for fast prototyping.

The electrical properties of the stretchable conducting polymer PEDOT-/PUR were examined during stretching in chapter 4, but only in the elongation direction. Using both agarose stamping and inkjet printing, a pattern in PEDOT/PUR was made with an electrode placed perpendicular to the stretching direction. The conductivity perpendicular to the stretching direction could therefore be monitored during elongation of the sample. The result showed that the agarose stamping affected the stretchability of the PEDOT/PUR material. Both tests showed a decrease in conductivity when elongated, but it was not possible to find a meaningful correlation between the conductivity perpendicular and parallel to stretching direction.

7.6 Conclusion

The objective of the project was to construct an all polymer micropump. It quickly became clear that to reach this objective, a number of fabrication and processing methods had to be developed. A major part of this thesis does therefore concern the handling and patterning of PEDOT rather than microfluidics devices. The methods developed are however all intended to be applicable in an all polymer microsystem. The integration of PEDOT in non-conductive substrates and the PEDUT/PUR material both aim at optimising the mechanical properties of the conducting polymer to the microfluidic system. The micropatterning using agarose stamping and inkjet printing is necessary to generate the structures required for gaining functionality in a microsystem. Two micropumps were however developed and constructed, one functional (chapter 3) and one not functional (appendix B). Especially the fabrication of the ACEO micropump confirmed that an all polymer micropump could be realised and that conductive polymers could be utilised to gain functionality in all polymer devices. It can therefore be concluded that PEDOT is suitable for applications where all polymer devices are required or profitable.

References

[1] Bjørn Winther-Jensen, Jun Chen, Keld West, and Gordon Wallace. Stuffed conductive polymer. *Polymer*, 46:4664–4669, 2005.

[2] Masao Doi. *Introduction to Polymer Physics*. Oxford Science Publications, 1 edition, 1996.

[3] S. Kirchmeyer and K. Reuther. Scientific importance, properties and growing applications of poly(3,4-ethylenedioxythiophene). *Journal of Materials Chemistry*, 15:2077–2088, 2005.

[4] Stoyan K. Smoukov, Kyle J. M. Bishop, Rafal Klajn, Christopher J. Campbell, and Bartosz A. Grzybowski. Cutting into solids with micropatterned gels. *Advanced Materials*, 17:1361–1365, 2005.

[5] Christopher J. Campbell, Stoyan K. Smoukov, Kyle J. M. Bishop, Eric Baker, and Bartosz A. Grzybowski. Direct printing of 3d and curvilinear micrometer-sized architectures into solid substrates with sub-micrometer resolution. *Advanced Materials*, 18:2004–2008, 2006.

Appendix A

A.1 Unsuccessful patterning mechanisms

Several attempts were made to develop a patterning method without the use of clean room techniques. Generally, clean room techniques are not well suited for cheap mass production of disposable devices due to the expenses involved in operating the equipment. Two clean room techniques, a mask aligner and Reactive Ion Etcher (RIE), are employed in the fabrication of the PEDOT/PMMA patterns used in chapter 3. Several etching mechanisms were tested in an attempt to eliminate the last step, the RIE. A pattern in photoresist on a PEDOT film was fabricated using spin coating and the mask aligner as described in section 3.4. The pattern was then immersed in NaOCl which is known to rapidly deactivate conducting polymers. The intend was that the NaOCl should deactivate the uncovered PEDOT and not affect the PEDOT protected by the photoresist, hence replace step E in figure 7.2. It was however observed that the photoresist used (Microposit S-1813) was slightly soluble in the basic NaOCl solution. It was therefore not possible to deactivate the PEDOT/PMMA before the photoresist was dissolved. The solubility in basic solutions is used to develop this kind of photoresists and most of the available photoresists exhibited therefore the same kind of behaviour. The epoxy based photoresist SU-8 is patterned by cross-linking and could therefore withstand the NaOCl, but it could not be removed after the deactivation, leaving the sample useless.

It was attempted to etch the PEDOT/PMMA chemically with a dilute solution of H_2SO_4 and $KMnO_4$. The attempt was somewhat more successful than the NaOCl etching, but the photoresist was still dissolved although slow enough for a pattern to be fabricated. An example of a structure fabricated with this method is presented in figure A.1. Some problems did however render the method unsuitable. On figure A.1 a $\sim$15 μm dark edge can

be observed near the edge of the PEDOT indicating a distinct edge effect. The etching also generated a thin layer of the insoluble mineral MnO_2 that covered the sample. The H_2SO_4 was added to avoid the precipitation of MnO_2 and the precipitation could be avoid if the solution was stirred during etching, but this led to uneven etching of the surface and faster dissolving of the photoresist. The conclusion was that the combination of photoresist and chemical deactivation/etching did not led to the wanted resolution and it still required clean room techniques (mask aligner). The method was therefore abandoned.

Figure A.1: Optical microscopy images of 4 μm and 20 μm electrodes fabricated with $H_2SO_4/KMnO_4$ etching.

A.2 Combination of PEDOT and other polymers

After successfully polymerising PEDOT in a PUR matrix, a number of experiments were conducted where other polymers were added to the polymerisation solution. These were PDMS, SEBS (Poly(styrene-ethylene-co-butylene-styrene)) and PVDF (polyvinylidene flouride). The PDMS used, was a two component Sylgard 184. The two components were added to the polymerisation solution together with THF to ensure solubility. The idea was that the PDMS would cross link within the PEDOT and generate a cross linked stretchable conductive polymer. The concept did not work for two reasons. The PDMS components and the PEDOT solution phase-separated when the THF evaporated and the PDMS did not polymerise. The lacking

polymerisation was probably due to incompatibility between the PDMS catalyst (Pt-complex) and the Fe(III)Tos or the polymerising PEDOT might have reacted with the ethylene groups on the PDMS chains required for crosslinking. Further attempts with PDMS was abandoned. The SEBS used was a hardness shore 80A. SEBS is much more hydrophobic than PUR, and could only be dissolved in the polymerisation fluid if a high amount of toluene and THF was added. When heated, the SEBS precipitated before the polymerisation initiated, leaving a very inhomogeneous film. The third polymer that was attempted added to the polymerisation fluid was a co-polymer PVDF (Kynar). PVDF is a piezoelectric polymer used in e.g. thinfilm speakers. The PVDF could be dissolved in the polymerisation solution if excess amounts of N-methyl-2-pyrrolidone (NMP) were added. The drawback of using this solvent is its high boiling point of 202°C, compared to the boiling point of the EDOT monomer, 193°C. A high amount of EDOT monomer is therefore lost before all the solvent has evaporated and the polymerisation initiates. This could be compensated for by adding 3-4 times the required amount of monomer and increasing the polymerisation temperature to 100°C. A conductive polymer film consisting of approximately 50 wt% PEDOT in PVDF was fabricated using this method. The film showed conductivity corresponding to the PEDOT/PUR film, but it did not have the same homogenous surface structure.

Appendix B

Fabrication of an all polymer electrostatic micropump

B.1 Introduction

The developed materials and fabrication methods described in chapter 4 and 5 were utilised to fabricate an electrostatic microvalve. Unfortunately it was not possible to construct a fully functional microvalve. The concept and principles of the microvalve are described in the following chapter along with the difficulties encountered during development.

B.2 Theory

The force exerted by electrostatic attraction between two planar equally sized planes is described by equation B.1 [1]

$$F_{el} = \frac{1}{2}\epsilon A\frac{V^2}{d^2} \tag{B.1}$$

where F is the force, ϵ is the permittivity of the material between the electrodes, A is the area of the planes, V is the voltage, and d is the distance between the electrodes. Equation B.1 is only valid if d is significantly smaller than the diameter/width of the planes. For a valve, the electrostatic pressure is a more convenient measure than the electrostatic force. The pressure generated on the electrodes can be found by division by the area, yielding equation B.2.

$$p_{el} = \frac{F_{el}}{A} = \frac{1}{2}\epsilon\frac{V^2}{d^2} \tag{B.2}$$

As can be seen from equation B.2, the electrostatic pressure (and force) is highly depending on both voltage and distance between the electrodes. It is therefore important to have a short distance, if the device is restricted to using moderate potentials, as would be expected in a microfluidic device. For a distance of 5 μm and a potential of 100 V the electrostatic pressure is 1770 Pa (for an air gap), but if the distance is increased to 50 μm, a potential of 10000 V is required to reach the same electrostatic pressure. Another method to increase the electrostatic pressure is by choosing a gap-material with a high permittivity.

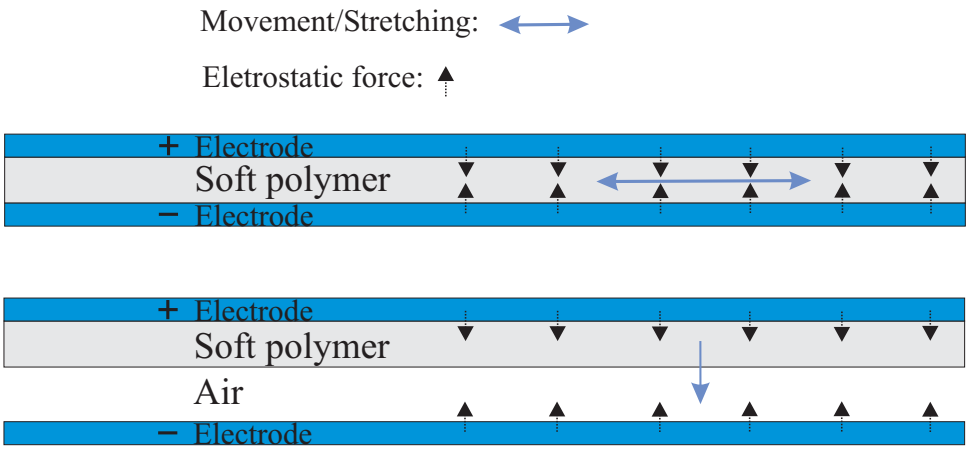

Figure B.1: The electrostatic pressure can be used to elongate a soft polymer film (A) or to close an air gap between two electrodes (B)

The electrostatic pressure can be used to "'squeeze"' a soft polymer film which is then elongated or the electrostatic pressure can be used to close an air gap between the electrodes. Both examples are illustrated in figure B.1. Using electrostatic pressure to elongate polymer membranes has been exploited for artificial muscles and has been thoroughly described in literature [2–4]. Using electrostatic pressure to close a valve has also been reported in litterature [5]. This type of microvalves has however been limited by the lack of stretchable electrodes. T. Bansal et al [5] report of a method where gold electrodes are implemented in stretchable PDMS, generating an electrode which can sustain minor deformations and elongations. The gold/PDMS membrane was used to fabricate an electrostatic microvalve operated by an AC potential. They used water filled channels and an AC

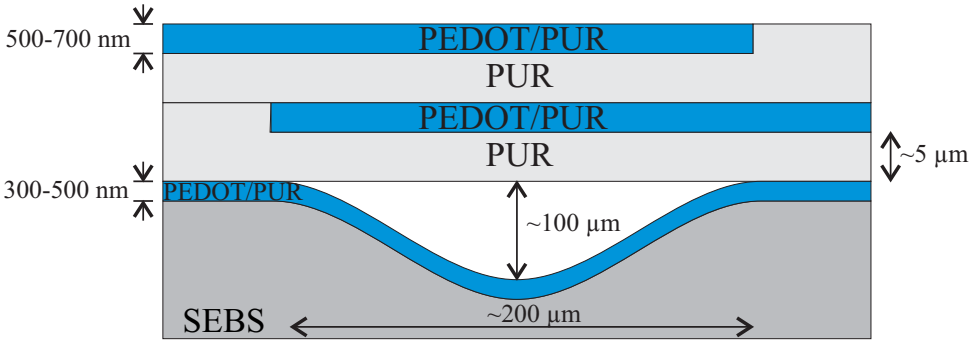

Figure B.2: A sketch of the electrostatic valve with approximated dimensions. The bottom of the fluid channel is covered with an electrode and the top is covered with a membrane consisting of 2 layers of non-conductive polyurethane and 2 layers of conductive PEDOT/PUR.

potential with a frequency of 5 MHz. The AC potential was required to prevent screening from ionic species in the fluid. The high frequency implies a relative high power consumption when the valve is closed. Replacing the gold/PDMS membrane with a conducting polymer membrane would lead to an even higher power consumption and significant joule heating, due to lower conductivity of PEDOT than gold. Another design was therefore devised.

B.3 Design

The design was based on both the squeezing and valve principle. A channel was fabricated using laser ablation (see section 1.4.4) yielding a channel with an approximately gaussian shape. The channel system was then spin coated with a thin layer of electrical conducting polymer. On top of the channel, two layers of stretchable conducting polymer separated by non-conductive polyurethane were added. A sketch of the design and the approximate dimensions are shown in figure B.2. The concept of the electrostatic valve is presented in figure B.3 showing the electrostatic forces near the corner of the valve. The electrostatic attraction between the top and middle layers ensures an elongation of the membrane and the electrostatic attraction between the middle and bottom electrodes ensures the membrane deflects downwards.

Since the electrostatic pressure is highly depending on the electrode distance the valve would close from the corner where the distance between the middle and bottom electrode is shortest. The point of contact would then move down the wall and finally close the channel. One could argue that the top electrode is redundant, but as the valve closes the middle part of the membrane is stretched and without the top electrode, the electrostatic force between the bottom and middle electrode would have to overcome the forces from both the stretched membrane and the fluid in the channel. By using a top electrode the membrane is immediately elongated when the potential is applied, and thereby easing the closing of the valve. The polymer used as membrane material was a two-component cross-linkable polyurethane named OC25A, purchased from Erapol (Sydney, Australia) with a hardness of shore 25A. This is an extremely soft polymer with a tensile strength of only 1 mPa [6]. The force required to deform the polymer film is depending on the hardness, and it is therefore beneficial to choose as soft a polymer as possible. The OC25A polymer is an optically clear aliphatic polyurethane, but the manufacture could not reveal the exact structure of the polymer or the electrical properties. The permittivity of polyurethanes in general is however between 4.4-5.1 [6] and the dielectric strength is 17-29 kV/mm [6]. Equation B.2 can be used to calculate the electrostatic pressure between the middle and bottom electrode. The electrodes are separated by a 5 μm polyurethane film and the permittivity is assumed to be 5. The maximum voltage is around 100 V (corresponding to 20 kV/mm). The electrostatic pressure according to equation B.2 is 8850 Pa or approximately 0.1 atm. This value represents the maximum theoretical counter pressure the valve can withstand.

B.4 Fabrication and testing

The fabrication method is sketched in figure B.4. A 10 nm layer of COC (Topas 8007, Ticona, Frankfurt, Germany) was spin coated on a silicon wafer from a solution of 5 wt% COC in Toluene at 30 sec@4000 rpm. The COC layer served as an adhesion inhibitor. On top of the COC an 600 nm layer of PEDOT/PUR was spun as described in chapter 4. The PEDOT/PUR was patterned using agarose stamping as described in chapter 5. Finally, a 5 μm layer of the curable two component polyurethane was spun on top. The two components were mixed with heptane, filtered through a 0.45 μm PTFE-filter and spun at 2000 rpm for 30 seconds and left to cure for 48 hours. The heptane was added to reduce viscosity and therefore film thickness. The

[6] Please see the manufactures homepage: www.erapol.com.au

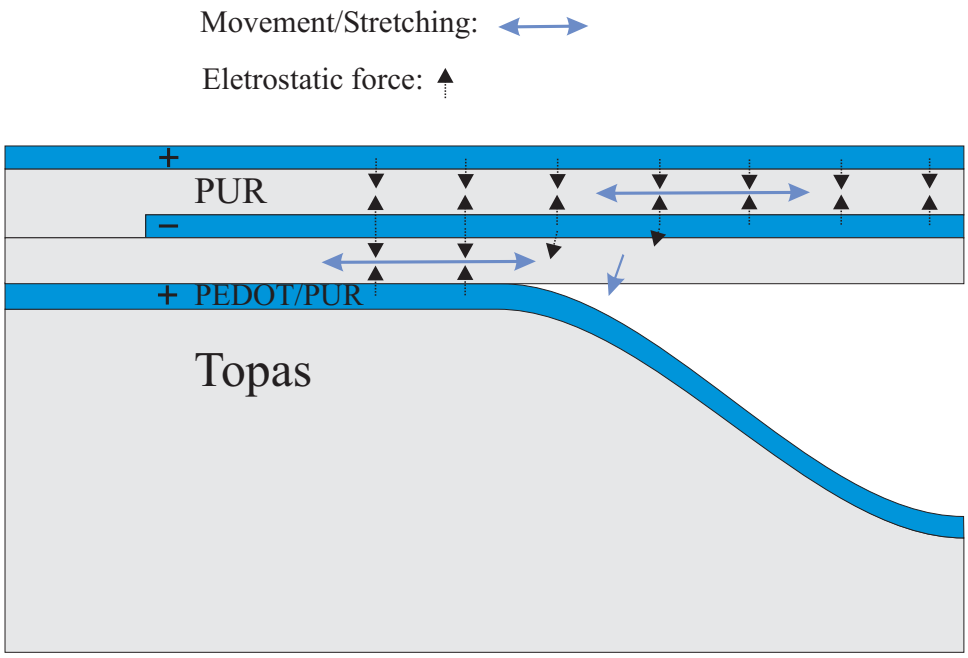

Figure B.3: The electrostatic forces near the corner of the channel. The electrostatic attraction between the top and middle electrode elongates the membrane and the electrostatic attraction between the middle and bottom electode closes the valve.

channel was fabricated in the elastomeric block co-polymer poly(Styrene-Ethylene-Butylene-Styrene) (SEBS) with a hardness of shore 80A. The channels were constructed using a CO_2 laser manufactured by Synrad (FH Series marking head 2, Washington, USA). The channels were subsequently spin-coated with a 400 nm layer of PEDOT/PUR. The SEBS ensured a flexibility of the channel system, which made it easier to bond it to the membranes that were spin-coated on the rigid silicon wafer. Attempts were made with a rigid material (PMMA) for the channel system, but it was impossible to transfer the membrane from the wafer to the channel system.

The voltage was generated using a USB function generator (TiePie, HS3) and a potential amplifiere. Contacts were made with conductive ink.

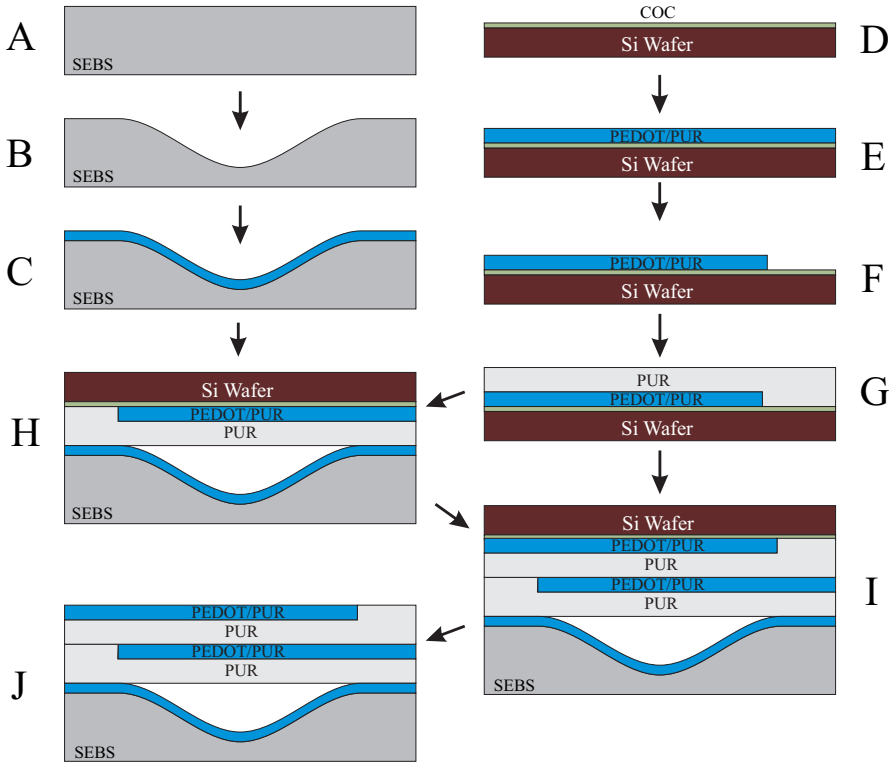

Figure B.4: The fabrication of the electrostatic pump. A) A disc of SEBS is molded and B) channels are made using laser ablation. C) a layer of PEDOT/PUR is spin-coated on the SEBS sample. D) A COC coated wafer is E) spin-coated with a layer of PEDOT/PUR. F) The PEDOT layer is patterned using agarose stamping, G) followed by spin-coating of a layer of two component curable polyurethane. H) When the polyurethane is cured, the two layers are transferred to the SEBS channel. I) The Si wafer is carefully removed and another patterned layer of PEDOT/PUR and PUR is transferred to the sample. J) The final setup.

B.5 Difficulties

Two problems were encountered during the fabrication and testing of the micropump: handling of the thin membranes and internal short-circuiting. Handling of the thin membranes was made difficult by the soft and sticky

nature of both the cross-linked OC25A polyurethane and the PEDOT/PUR electrode. As mentioned above, the channel system constructed was in elastomeric SEBS, which made it possible to bond the channel system directly to the membrane, while the membrane was still on the silicon wafer. The problem arose when the channel system and membrane had to be released from the wafer. The areas of contact between the SEBS and membrane were not a problem, but where the SEBS had been removed (to generate channels) it was difficult to release the membrane without damaging it. Several defect valves were constructed where membranes were broken or stretched to a point where the membrane was irreversibly elongated and therefore slacking.

The second and most severe problem encountered was short-circuiting internally in the membrane structure. This was probably caused by inhomogeneities in the polyurethane membrane, lowering the dielectric strength locally in the membrane. The dielectric strength of polyurethane is, as mentioned above, around 20 kV/mm, compared to only 3 kV/mm for air [7]. Hence a small air bubble or air containing dust particle would cause a penetrating current at a much lower voltage than expected. Once the membrane has been penetrated, the resulting spark probably lowers the threshold voltage even more. The two-component polyurethane was filtered through a 0.45 μm filter and the fabrication was performed in a clean room to eliminate impurities, but the presence of air-bubbles could not be excluded. Furthermore, the fabrication of the channel system was done using a CO_2-laser in a non-clean environment and particles from the channel system could have damaged the membrane during bonding. The internal short-circuiting was revealed because it was difficult to maintain the applied potentials on the electrodes. It was not possible to construct a fully functional valve due to problems with short-circuiting.

References

[1] Philip M. Morse and Herman Feshbach. *Methods of Theoretical Physics*. McGraw-Hill Book Company, 1 edition, 1953.

[2] Ron Pelrine, Roy Kornbluh, and Guggi Kofod. High-strain actuator materials based on dielectric elastomers. *Advanced Materials*, 12:1223–1225, 2000.

[3] M Zhenyi, J. I. Scheinbeim, J. W. Lee, and B. A. Newman. High-field electrostrictive response of polymer. *Journal of Polymer Science - B*, 32:2721–2731, 1994.

[4] G. Kofod, P. Sommer-Larsen, R. Kornbluh, and R. Pelrine. Actuation response of polyacrylate dielectric elastomers. *Journal of intelligent material systems and structures*, 14:787–793, 2003.

[5] Tushar Bansal, Meng-Ping Chang, and Michel M. Maharbiz. A class of low voltage, elastomer-metal "'wet"' actuators for use in high-density microfluidics. *Lab on a Chip*, 7:164–166, 2007.

[6] Loctite. *The Design guide for bonding Plastics*, volume 3. Henkel, 2005.

[7] David R. Lide. *Handbook of Chemistry and Physics*. CRC, 84 edition, 2003.